

IMPLEMENTATION OF CMS HIGH RESOLUTION MODEL TO STUDY  
MORPHOLOGY CHANGE IN A GROIN FIELD DURING HURRICANE SANDY

by

Omar L. Lopez-Feliciano

A THESIS

Submitted to the Faculty of the Stevens Institute of Technology  
in partial fulfillment of the requirements for the degree of

MASTER OF ENGINEERING – OCEAN ENGINEERING

---

Omar L. Lopez-Feliciano, Master in Science

ADVISORY COMMITTEE

---

Dr. Thomas Herrington, Advisor	Date
--------------------------------	------

---

Dr. Jon K. Miller, Reader	Date
---------------------------	------

STEVENS INSTITUTE OF TECHNOLOGY  
Castle Point on Hudson  
Hoboken, NJ 07030  
2014



IMPLEMENTATION OF CMS HIGH RESOLUTION MODEL TO STUDY  
MORPHOLOGY CHANGE IN A GROIN FIELD DURING HURRICANE SANDY

## **ABSTRACT**

The Borough of Bay Head is a coastal community located northern oceanfront shoreline of the Barnegat Bay in Ocean County New Jersey. Its beach is protected by a groin field and a seawall covered with a dune system. The timber groin field was rebuilt in the early 1960's to delay the net longshore sediment transport to the north, but nowadays it is very weathered and ineffective. Superstorm Sandy hit the coast of New Jersey during the fall of 2012 leaving billions of dollars in losses and severe erosion to the famous Jersey Shore beaches including Bay Head. The Coastal Modeling System (CMS) is a numerical model developed by the U.S. Army Corps of Engineers that was used to closely study the morphology change and the sediment transport that took place during the storm at Bay Head beach. The final elevation dataset of the model was compared with a post-storm RTK GPS surveying performed by The Center of Maritime System at Stevens and post-storm LiDAR data collected by the Joint Airborne Lidar Bathymetry Technical Center of eXpertise (JALBTCX) under the United States Army Corps of Engineers National Coastal Mapping Program. The beach erosion calculated by the computer model was  $107,930 \text{ m}^3$  and was within 15% of the erosion calculated from the surveys. Total sediment loss from the system, past the depth of closure, was  $115,600 \text{ m}^3$ ; and the net

sediment transport calculated at the middle of the groin field using spatial integration of the total load transport within an established feature arc was found to be 61,540 m<sup>3</sup>/day northward, greater than the published yearly net transport.

Author: Omar L. Lopez-Feliciano

Advisor: Thomas O. Herrington, PhD

Date: May 5, 2014

Department: Civil, Environmental & Ocean Engineering

Degree: Master of Science

## **Acknowledgments**

I would like to thank my advisors Dr. Thomas O. Herrington and Dr. John K. Miller for sharing their knowledge and experience with me. In addition, I wish to express my gratitude to two crucial persons which greatly helped on my research advancement; Lihwa Lin, developer of CMS, for the technical support regarding the numerical model and Coast & Harbor Engineering, Inc. for the David P. Simpson Coastal Engineering Scholarship award which made possible to acquire a workstation computer needed to perform the simulations.

I would also thank my coworkers and friends from the Davidson Laboratory for their help on the data collection process and their guidance and encouragement. Finally, I want to thank my family for the unconditional support and love.

# Table of Contents

ABSTRACT .....	iii
Acknowledgments .....	vi
List of Tables .....	xi
List of Figures .....	xii
List of Symbols .....	xiv
List of Acronyms .....	xv
CHAPTER 1 .....	17
INTRODUCTION .....	17
1.1 Overview .....	17
1.1.1 Project Site Background .....	17
1.1.2 Bay Head Groin Field History .....	23
1.1.3 Hurricane Sandy .....	29
1.1.4 Reasons for Using Sediment Transport Models .....	31
1.2 Objectives .....	32
1.3 Thesis Organization .....	33
CHAPTER 2 .....	34
LITERATURE REVIEW .....	34
2.1 Sediment Transport .....	34
2.1.1 Field Conditions .....	34

2.1.2 Laboratory Experiments .....	35
2.1.3 Boundary Layer .....	37
2.1.4 Transport Modes .....	39
2.1.5 Cross-shore Sediment Transport .....	41
2.1.6 Longshore Sediment Transport .....	42
2.1.7 Sediment Transport Models .....	43
2.2 Groins .....	45
2.3 Tidal Inlets.....	48
CHAPTER 3 .....	51
Computational Procedures .....	51
3.1 CMS Model Development .....	51
3.1.1 CMS-Wave .....	52
3.1.2 CMS-Flow.....	53
3.1.3 Coupling Models.....	54
3.1.4 Limitations and Assumptions.....	55
3.2 Input Data .....	57
3.2.1 National Geophysical Data Center (NGDC) .....	57
3.2.2 LiDAR.....	57
3.2.3 Dynamic Underwater and Coastal Kinematic Surveying (DUCKS) System .....	58
3.2.4 US Army Corp of Engineers .....	60



3.2.5 Orthoimagery.....	61
3.2.6 Meteorological data .....	63
3.3 Grid Generation .....	64
3.4 Calibration.....	67
3.5 Hurricane Sandy Simulation.....	70
3.5.1 CMS-Flow Parameters .....	70
3.5.2 Sediment Transport.....	71
3.5.3 Wind Velocity and Direction.....	74
3.5.4 CMS-Wave Parameters.....	76
3.6 Validation .....	77
CHAPTER 4 .....	79
MODEL RESULTS .....	79
4.1 Water Surface Elevation .....	79
4.1.1 Storm Surge .....	79
4.1.2 Seawall Overtopping .....	81
4.2 Significant Wave Height.....	83
4.3 Wave-Induced Currents .....	84
4.4 Morphology Change.....	85
4.5 Shoreline Position Change.....	87
4.6 Beach Profiles.....	89
4.7 Sediment Transport .....	92

4.7.1 Observation Cells .....	92
4.7.2 Feature Arc.....	94
4.7.3 Polygon .....	96
CHAPTER 5 .....	97
Conclusions.....	97
5.1 Conclusion .....	97
5.2 Future Work .....	98
Vocabulary.....	99
Appendix A .....	108
Appendix B .....	121
References .....	125

## List of Tables

Table 1: Available Shoreline Data. ....	19
Table 2: Water Parameters.....	70
Table 3: Sediment parameters used in the model. ....	74
Table 4: Average percent of error for each profile. ....	90
Table 5: Sediment bypassing the groins.....	93

## List of Figures

Figure 1: Location of borough of Bay Head, NJ. (Source: Google Earth, 2012) .	20
Figure 2: Shoreline variability at Howe St. Groin. ....	21
Figure 3: Bay Head streets and groin locations. ....	22
Figure 4: Seawall and dune system.....	25
Figure 5: Groin at Karge St.....	26
Figure 6: Groin at Howe St. ....	26
Figure 7: Google Earth historical imagery for groin field at Bay Head. ....	28
Figure 8: Hurricane Sandy trajectory. (Source: NOAA, 2012) .....	30
Figure 9: Beach profile before and after storm Nor'lda at Long Branch, New Jersey.....	35
Figure 10: Bedforms under a wave. (Source: Alex Mustard, 2012) .....	39
Figure 11: Total sediment transport calculation. ....	40
Figure 12: Groin field impact to the shoreline. ....	47
Figure 13: Manasquan Inlet in 2010; Sediment transport directed southward. ....	50
Figure 14: Schematic of steering process. (Source: CMS User Manual).....	55
Figure 15: DUCKS System Survey (9/22/2011).....	60
Figure 16: Final Bathymetry for High Resolution Model. ....	61
Figure 17: Manasquan Inlet bathymetry. ....	62
Figure 18: Karge groin recreated in the bathymetry. ....	63
Figure 19: Parent grid.....	66
Figure 20: High resolution grid.....	67

Figure 21: Manasquan River tide gauge location. ....	69
Figure 22: Water level comparison. ....	69
Figure 23: Wind velocity during Hurricane Sandy. ....	75
Figure 24: Wind direction during Hurricane Sandy. ....	75
Figure 25: Wave spectra used in the model. ....	76
Figure 26: Beach profile comparison at Howe St. ....	78
Figure 27: Hurricane Sandy surge left: at $t=0$ ; right: max surge. ....	81
Figure 28: Seawall overtopping discharge. ....	82
Figure 29: Significant wave height at the peak of the storm. ....	83
Figure 30: Wave-induced currents near the groin field. ....	84
Figure 31: Morphology change at groin field. ....	86
Figure 32: Bay Head aerial on Nov 3, 2012 (4 days after Hurricane Sandy). ....	87
Figure 33: Shoreline position change. ....	88
Figure 34: Beach profile locations. ....	90
Figure 35: Updrift profile for the Howe St. groin. ....	91
Figure 36: Downtide profile for the Howe St. groin. ....	91
Figure 37: Observation cells location. ....	93
Figure 38: Feature Arc used to calculate sediment transport. ....	95
Figure 39: Beach Profile under Feature Arc. ....	95
Figure 40: Polygons for sediment calculations. ....	96

## List of Symbols

<i>Variable</i>	<i>Meaning</i>	<i>Units</i>
$\theta$	Shield's Number.	N/A
$\tau$	Shear stress.	F/A
$\rho$	Density of the sediment.	Kg/m <sup>3</sup>
$S$	Specific Gravity of the sediment.	N/A
$g$	Gravity force.	m/s <sup>2</sup>
$D$	Diameter of the sediment.	m
$U^*$	Shear velocity.	m/s
$C$	Sediment concentration	m <sup>2</sup>
$Q$	Sediment transport	m <sup>3</sup> /s
$k$	Von Karman constant.	N/A
$z$	Water depth.	m
$z_0$	Reference depth.	m
$h$	Still water depth.	m
$y$	Horizontal distance from the shoreline.	m
$A$	Sediment characteristics.	N/A

## List of Acronyms

CIRP	Coastal Inlets Research Program
CMS	Coastal Modeling System
CRM	U.S. Coastal Relief Model
DEMs	Digital Elevation Models
DUCKS	Dynamic Underwater Coastal Kinematic Surveying System
EST	Eastern Standard Time
GMT	Greenwich Mean Time
GPS	Global Position System
JALBTCX	Joint Airborne Lidar Bathymetry Technical Center of eXpertise
LiDAR	Light Detection and Ranging
NAVD 88	North American Vertical Datum of 1988
NDBC	National Data Buoy Center
NGDC	National Geophysical Data Center
NJGIN	New Jersey Geographic Information Network
NOAA	National Oceanic Atmospheric Administration
NYHOOPS	New York Harbor Observing and Prediction System
MHW	Mean High Water
MLW	Mean Low Water
MSL	Mean Sea Level
RTK	Real Time Kinematics
SIT	Stevens Institute of Technology

SMS	Surface-water Modeling System
SPM	Shore Protection Manual
USACE	United States Army Corp of Engineers
USGS	U.S. Geological Survey
XBEACH	Storm-induced BEAch Change Model



# CHAPTER 1

## INTRODUCTION

### ***1.1 Overview***

The intent of this research work was to study the sediment transport during a major storm on the Bay Head, NJ groin field. Hurricane Sandy was chosen as the storm of interest because it has been determined to be the most significant storm to hit the coast of New Jersey in the past decade, severely eroding beaches and destroying several coastal structures.

#### ***1.1.1 Project Site Background***

The Borough of Bay Head is a small coastal community located in northeastern Ocean County, New Jersey. The town was incorporated on June 15, 1886 with a land area of 0.58 square miles and, according to the US Census Bureau estimate of July 1, 2009, its population density is around 1,800 people per square mile. Part of the land in Bay Head is a barrier island which occupies the narrow Barnegat Peninsula facing the Atlantic Ocean to the east as shown in Figure 1. Bay Head is bounded to the west and north by the Borough of Point Pleasant and Point Pleasant Beach and to the south by the Borough of Mantoloking. Like many other oceanfront towns in New Jersey, Bay Head beach has experienced

significant erosion since the 1800s due to a combination of natural and anthropogenic causes. A combined construction of a seawall and groin field has been used in this particular town to control the erosion since 1920. However, due to frequent wave action from storms and an extended period of low maintenance, the groins have deteriorated.

The shoreline varies seasonally in this location, which is close to the nodal point where the net sediment transport changes direction in New Jersey, making the study more challenging. Figure 2 depicts the shoreline variability at the Howe Street groin, the most prominent groin located in the middle of the groin field (Figure 3). The groin at the end of Howe St lines up with the “x” axis of this graph. Note that for most of the years the sand is impounded to the south of the groin and erosion occurs north of it. This behavior reveals a dominant sediment transport directed to the north. The distance of the shoreline was measured from East Avenue, which runs parallel to the shoreline, to the wet/dry location of the beach, which is approximately the Mean High Water (MHW) elevation.

Historical shoreline data was obtained from several sources. A total of 7 images of the site, spanning from 1995 to 2012, were gathered from Google Earth. [Historicaerials.com](http://Historicaerials.com) has images dating back to 1920. These aerial images helped estimate when the structures were initially built. In addition, the State of New Jersey maintains a database of historical shorelines accessible as a shapefile

within its Geographic Information System (GIS) data repository ([www.state.nj.us/dep/gis](http://www.state.nj.us/dep/gis)). The data contained in the GIS file dates back to the mid 1800's, with the earlier shorelines being digitalized from historic maps. A list of all of the available aerals is given in Table 1.

Year	Source	Quality
2012	Google Earth	High
2010	Google Earth	High
2008	Google Earth	High
2007	Google Earth	High
2006	Google Earth	High
2002	Google Earth	High
1995	Google Earth	High
1977	GIS	Low
1970	Historicaerials.com	Medium
1963	Historicaerials.com	Medium
1957	Historicaerials.com	Medium
1956	Historicaerials.com	Medium
1953	GIS	Low
1947	Historicaerials.com	Medium
1940	Historicaerials.com	Medium
1936	GIS	Low
1933	Historicaerials.com	Medium
1920	Historicaerials.com	Medium
1899	GIS	Low
1868	GIS	Low
1842	GIS	Low

**Table 1: Available Shoreline Data.**

When different data sources are used, inaccuracies are introduced. Also, making use of aerial photographs to determine the shoreline location for a site on a given year can also be somewhat inaccurate as a photograph depicts a single instance

in time. Factors such as tide stage, time of the year, and weather conditions influence the perception of the shoreline location from aerial imageries. However, historic photograph and map database remain as useful tools for studying shoreline changes.

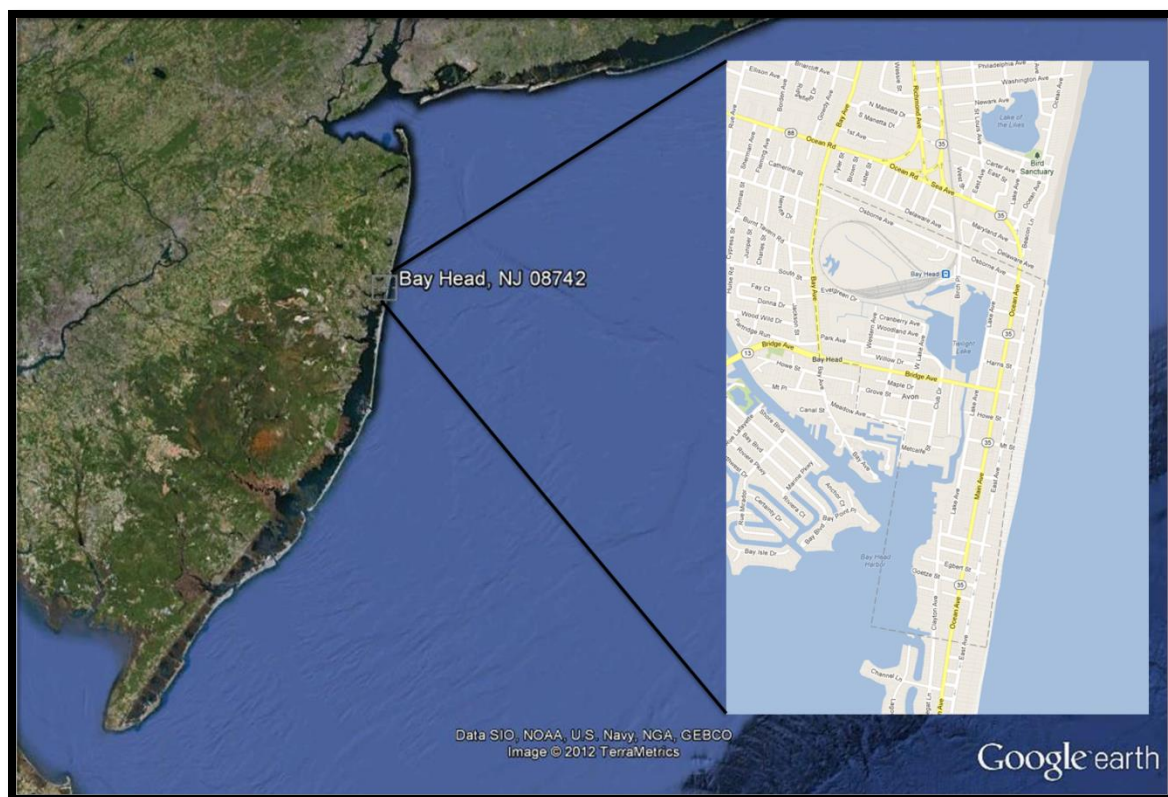


**Figure 1: Location of borough of Bay Head, NJ. (Source: Google Earth, 2012)**

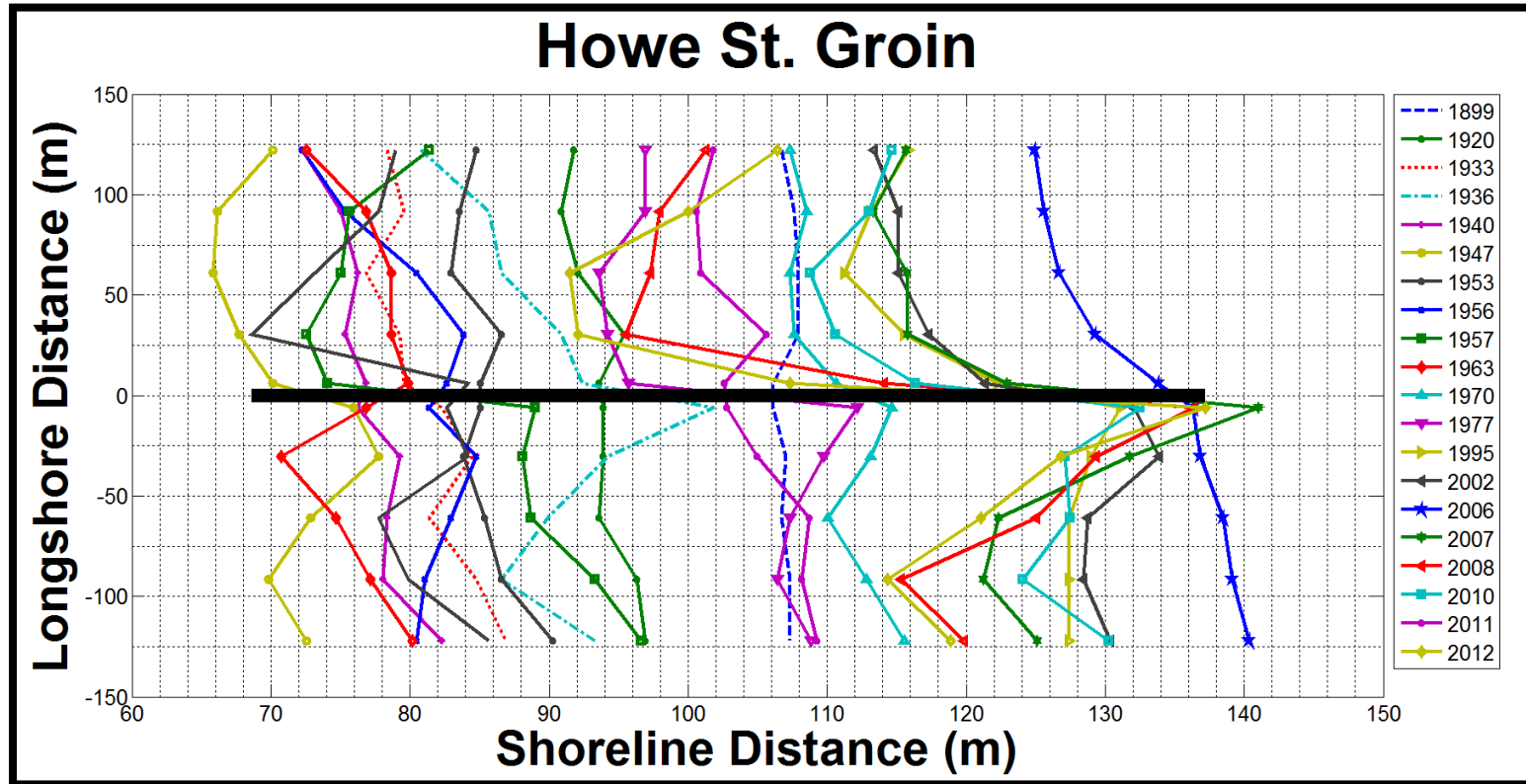


Figure 2: Shoreline variability at Howe St. Groin.

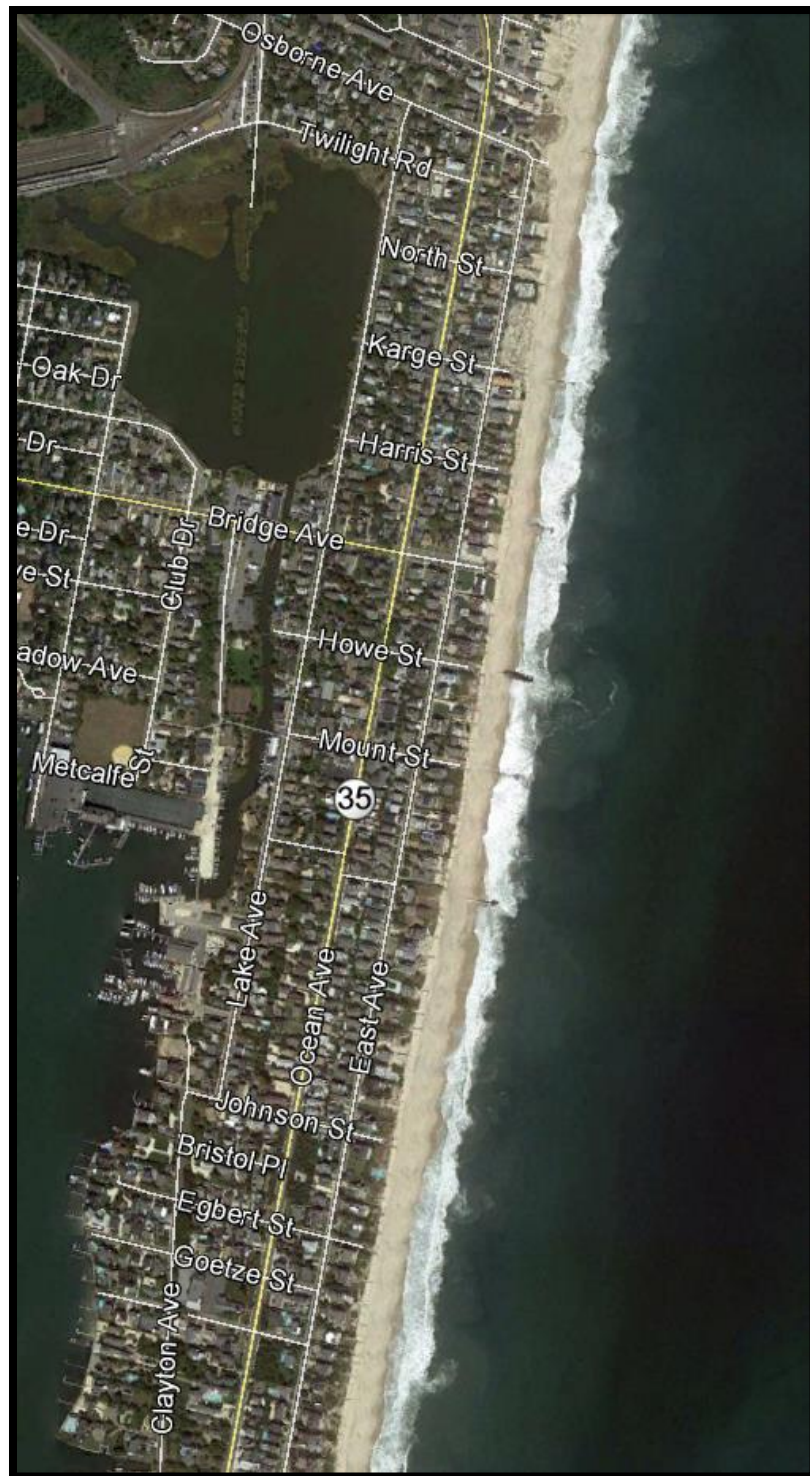


Figure 3: Bay Head streets and groin locations.

### ***1.1.2 Bay Head Groin Field History***

A little before 1920, the first groin field was built in Bay Head to prevent the coastline from eroding. Six timber groins with an average spacing of 200 meters were installed in about 1.0 kilometer of coastline, from Osborne Avenue to Chadwick Street. The groins were built with a low profile approximate to MHW and about 33 meters long. A low elevation timber bulkhead was built parallel to the shore, along the groins and extending 500 meters southward, to protect the houses from wave action. After the construction of these coastal structures, the coast experienced both erosion and accretion throughout the years. However, the beach was usually narrow. Due to this fact, and due to the low elevation of the bulkhead, even during small storm events, state agencies would send a mandatory evacuation alert as there was a high probability of waves overtopping the bulkhead. In various occasions, the town was completely flooded.

After significant storms in the early 1960s, the mayor of Bay Head decided to rebuild the deteriorated groins and replace the timber bulkhead with a higher elevation stone seawall (5 meters NAVD 88) and a slope of 3:2 facing the ocean and 1:1 in the back of the structure. With community efforts, a dune system was developed over time, covering the seawall. Figure 4 shows the buried seawall under the dune that protects the houses of the town. These are the structures present today at Bay Head beach. The restored groins were made longer in order to increase the beach width. They are made out of timber utility posts that

were vertically embedded into the sand, bolt connected to each other with horizontal timber planks and reinforced with rock tips. This is an impermeable design that it is easier to install than the common groins found in New Jersey, which are made out of boulders and a core. Figure 5 shows the state of the timber groin at the foot of Karge Street as of 2012. Note the deterioration at the seaward end where horizontal wood is missing, making the structure inefficient in trapping sediment at this location. All of the groins reveal a certain degree of damage. Some of them are falling apart and present dangerous and unsafe conditions for bathers and swimmers in the area. In the 1970's, the groin at the foot of Howe Street, located in the middle of the groin field, was much deteriorated, leaving only some vertical piles visible. It was then reinforced with rock on both sides making it the widest and tallest of all the groins in the field. Figure 6 shows how the groin at the end of Howe Street looked in November 2012.





**Figure 4: Seawall and dune system.**



**Figure 5: Groin at Karge St.**

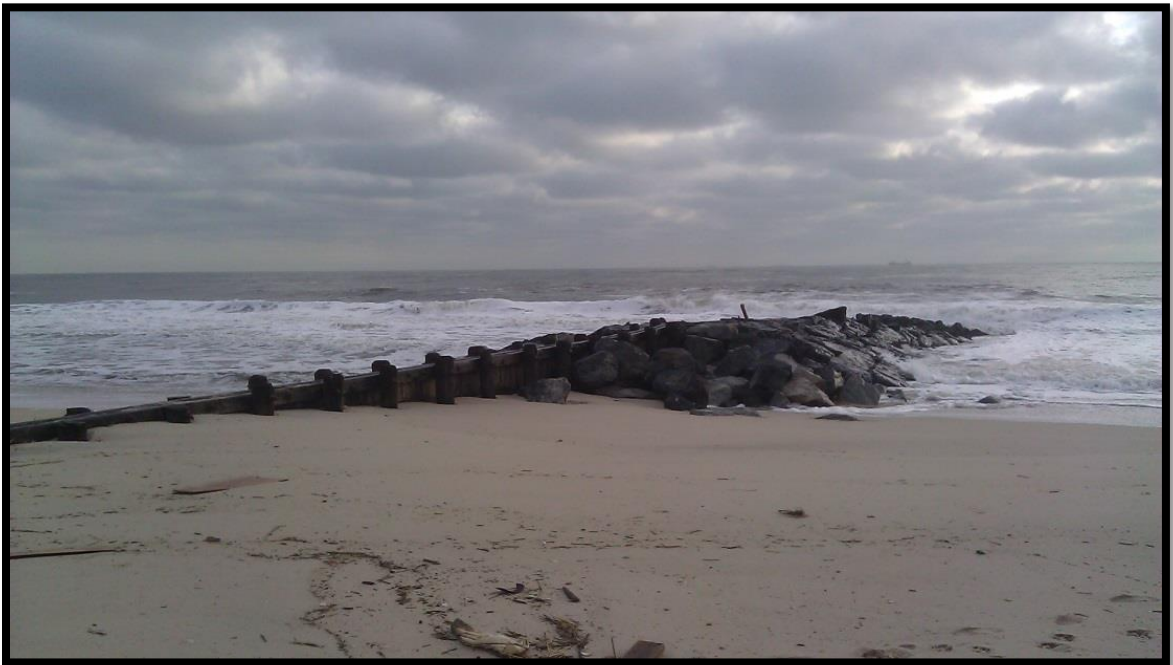


**Figure 6: Groin at Howe St.**

Throughout the years, these groins have been effective in stabilizing the shoreline and preserving the beach at Bay Head. Visually, the beach seems narrower after each winter and beachgoers complain that the groins are accelerating the beach erosion. Certainly, beaches try to find their equilibrium profile to accommodate the incident wave, which changes over time. Hence, the beach is constantly experiencing change.

Figure 7 shows a set of aerial imageries of Bay Head, obtained from Google Earth, which depict the change in morphology of the Bay Head Beach. Although the pictures were not captured during the same time of the year, in general, the net sediment transport is predominantly to the north since, for most of the years, the sand accumulates to the south of each groin. The sand that moves out of the groin field in the longshore direction is deposited in the downdrift (north) beaches of Point Pleasant Beach. At the north end of the system, the sand is blocked by the southern jetty of the Manasquan Inlet that allows only a small amount of sand bypassing. The last picture in Figure 7 was taken immediately after Hurricane Sandy. Note the severe erosion caused by this storm which completely exposed all the groins. A couple of weeks after the storm, the beach started to recover both naturally and with the help of heavy equipment that sieved and deposited sand that overwashed onto the streets back onto the beach.



Figure 7: Google Earth historical imagery for groin field at Bay Head.



### ***1.1.3 Hurricane Sandy***

Hurricane Sandy was the second costliest hurricane of the United States history with a total of 68 billion dollars in property damage. It made landfall on October 29, 2012 at 8:00 pm EST during spring tide (amplified astronomical high tide) near Atlantic City and generated the highest storm surge ever recorded at most water level gauges in the New York Bight region. Figure 8 shows the storm trajectory. NOAA buoy 44025, located 40 nautical miles offshore of the area of interest, recorded a peak wave height of 9.65 meter at 15 seconds. Inland anemometers measured 80 mile per hour wind at the time of landfall. President Obama signed an emergency declaration for New Jersey before Sandy's landfall and immediate action was taken from authorities. Coastal and inland towns were out of power for weeks, coastal inundation removed houses from their foundations, and wave action severely eroded the beaches. Beaches and boardwalks were inaccessible, part of the Seaside Pier collapsed, and boats in marinas were piled upon streets. There were 148 direct deaths and many lost their houses and valuables during this historic storm.

After the storm, structural assessments were performed at Bay Head by Stevens Institute of Technology (SIT) Center for Maritime Systems' Coastal Group. The mayor made special arrangements granting the group with access to the Bay Head community to gather data. Teams of students assessed the structural damages and measured watermark elevations throughout the town. Ground

elevations were surveyed through the use of RTK GPS at the same locations. It was found that most of the damage was caused by back-bay flooding, demonstrated by watermarks with elevation as high as 2.5 meters (NAVD 88). Overall, minimal structural damage was observed in the town and only a few of the oceanfront buildings were severely impacted. However, the beach was significantly narrower and the dunes that used to cover the seawall were gone. A beach survey was performed to later compare the erosion output of the computer model to the erosion computed from pre- and post-Sandy survey data for this specific beach.

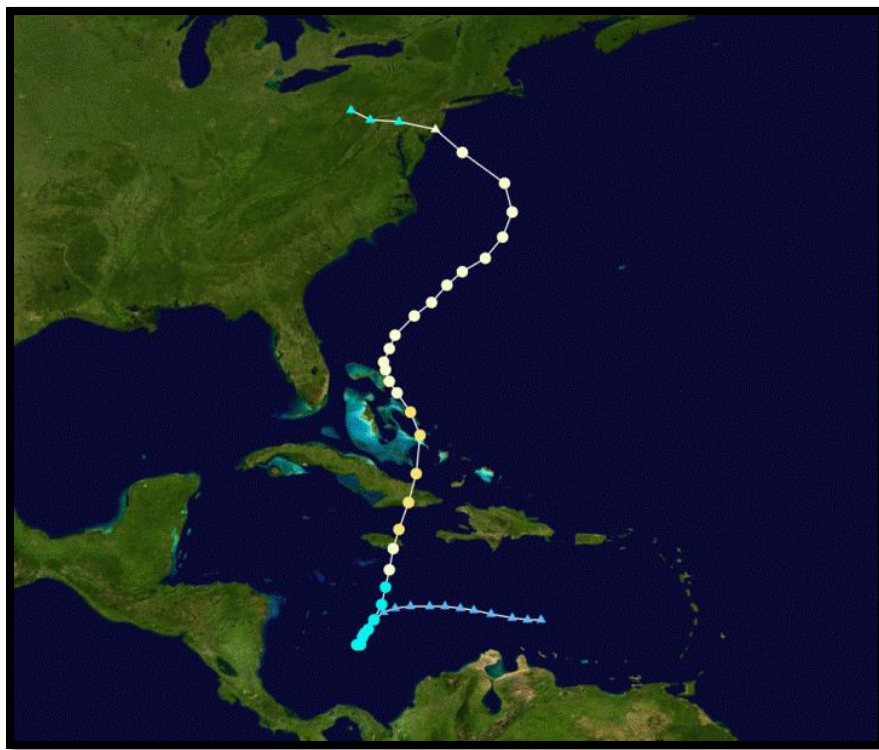


Figure 8: Hurricane Sandy trajectory. (Source: NOAA, 2012)

#### ***1.1.4 Reasons for Using Sediment Transport Models***

Studying the sediment transport of a specific beach is a complex task that involves many uncertainties due to the continuously changing environment. Usually, sediment transport rates are estimated by using dredging records of inlets. However, dredging is not performed regularly and only gives an idea of how much material shoals in a given time at that location.

Simple methods of field data collection to estimate sediment transport rates, such as streamer traps, can be hard to implement as well as to estimate the real values since data is collected only over a small portion of the beach. In contrast, with available input data, calibrated and verified sediment transport computer models are useful tools to understand the overall sediment behavior of the coastal zone.

Several simple computer models have been developed to study sediment transport and others are still under development, in an effort to capture all the physics that occurs in the coastal zone. Usually, coastal morphodynamics models examine the behavior of the bathymetry by calculating the sediment transport locally and using the conservation of sand to determine the local depth change over some unit of time (Dean and Dalrymple 2002). One would like to use the best three dimensional wave and sediment transport model available for a project. However, all have computational limitations and assumptions as well

as time consuming internal calculations. The decision of which model to use depends on project needs, established timeframe, available data, and desired output.

## **1.2 Objectives**

The intent of this project is to study the morphology change and sediment transport that occurred in the groin field located in Bay Head, New Jersey during one of the most destructive hurricanes of the history of the East Coast of the United States. These extreme conditions were modeled making use of an integrated numerical model, high resolution bathymetry and meteorological data from different ocean sensors. The model applied in this study was the Coastal Modeling System (CMS), developed and maintained by the US Army Corp of Engineers (USACE) under the Coastal Inlets Research Program (CIRP). CMS is an integrated numerical modeling system for simulating nearshore waves, currents, water levels, sediment transport, and morphology change (Militello et al. 2004; Buttolph et al. 2006; Lin et al. 2008; Reed et al. 2011). Herein, the modeling system was used to calculate the following at Bay Head beach:

- Storm-induced beach erosion.
- Sediment transport during the storm.
- Total sediment loss (out of the system).



### ***1.3 Thesis Organization***

This thesis is organized as follows:

The overview of the study, including project site background, storm description, objectives and thesis organization are discussed in Chapter 1. Chapter 2 presents a literature review related to the present research. Chapter 3 details the process of the model development. Chapter 4 discussed the model results and Chapter 5 gives the conclusions and thoughts about future work.

## **CHAPTER 2**

# **LITERATURE REVIEW**

### ***2.1 Sediment Transport***

#### ***2.1.1 Field Conditions***

Sediment transport has been studied for decades but it is still not well understood. In the coastal field, sediment transport is referred to as littoral transport. Waves and currents are the principal mechanisms by which the sediment moves in the surfzone within limited boundaries. This area is defined as the region between the swash zone and the depth of closure. The swash zone is where the water washes up on the beach and depth of closure is the offshore depth where changes in bathymetry are negligible. In New Jersey, this depth is typically estimated at 8 meters since no changes in seabed elevation are observed past this depth. Over time, on beaches where finer material is predominant, sediment moves fast and tends to create a mild slope on the beach face. The opposite occurs on beaches with coarser material, where the sediment moves slowly and, therefore, steep beach faces are common. The beach profile is in constant change but significant differences can be noticed after storms. Typical beach profiles, before and after a storm scenarios, are shown in Figure 9.

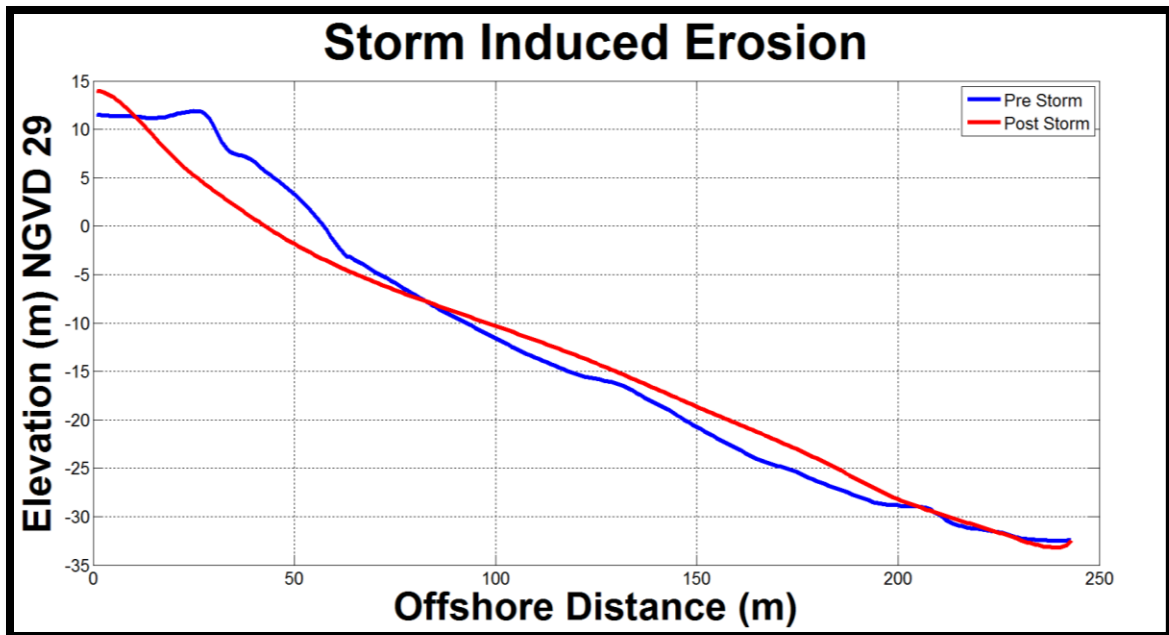


**Figure 9: Beach profile before and after storm Nor'Ida at Long Branch, New Jersey.**

It is difficult to measure sediment transport in the field due to many external factors acting at the same time, such as different wave heights, wave periods, wave directions, currents, temperature changes in the water column, salinity variations, and local bathymetry, among other variables. Hence, several laboratory experiments have been performed under specific conditions to develop empirical relations that help scientists better understand the behavior of sediment in a moving flow.

### ***2.1.2 Laboratory Experiments***

Several empirical theories were developed to describe the various factors that affect the sediment behavior in a moving flow. For example, the theory of

incipient motion for steady flow (Shields, 1936) entails an empirical relationship based on laboratory results (equation 1). It is based on equilibrium where destructive forces and stabilization forces are applied. The theory establishes that, when the Shield's critical number,  $\theta_{cr}$ , is larger than 0.05, sediment is likely to start moving under steady flow conditions. However, in field conditions, turbulent flow dominates which would lead to more complicated formulas.

$$\theta = \frac{\tau}{\rho(S-1)gD} \quad (1)$$

where

$\theta$  = Shield's Number.

$\tau$  = Shear stress.

$\rho$  = Density of the sediment.

$S$  = Specific Gravity of the sediment.

$g$  = Gravity force.

$D$  = Diameter of the sediment.

Typical forces experienced by a sediment particle are: lift, buoyancy, gravity, drag, seepage, and pressure gradient forces. Several theories and pick-up functions have been developed to describe the initiation of motion of sediment under oscillating flow and bed forms for small Reynolds numbers. Laboratory experiments to study oscillating flow have been performed using flumes with oscillatory plates and later improved using oscillating water tunnels, or U-tubes, with high Reynolds number (Soerensen, 1956). In these experiments, oscillatory

movement simulates the turbulence that the seabed experiences during traveling waves. However, the turbulence injected into the water column by a breaking wave in the surfzone creates very different physical forcing. Therefore, making use of the aforementioned analysis approaches yields inaccurate results and makes the sediment transport extremely difficult to predict in the nearshore. The results of any one of the sediment transport formulations in a given area may significantly vary. Also, sediment characteristics like size, density and shape play an important role in sediment transport calculation, making every project site unique.

### ***2.1.3 Boundary Layer***

Under steady conditions, total sediment transport “ $Q$ ” is calculated by vertically integrating the product of the sediment velocity ( $U$ ) and the sediment concentration ( $C$ ) through the water column over time (equation 2).

$$Q_{(t)} = \int_0^h U_{(z,t)} C_{(z,t)} dz \quad (2)$$

It is assumed that the sediment moves at the same velocity of the flow and the boundary layer can be represented with the log law, also called law of the wall, shown in equation 3

$$U_{(z)} = \frac{U^*}{k} \ln \frac{z}{z_0} \quad (3)$$

where

$U^*$  = Shear velocity.

$k$  = Von Karman constant.

$z$  = Water depth.

$z_0$  = Reference depth where the law of the wall profile approaches zero.

Determining the concentration profile is not straightforward. The maximum sediment concentration occurs at the sea bottom and it decreases as it approaches the top of the boundary layer, where the concentration is zero. Also, sediment concentration is influenced by nature via diffusion flux, convective flux and settling flux which are highly dependent on water temperature, density and salinity. In an oscillating flow scenario, however, additional influencing factors need to be considered.

In a breaking wave environment, the boundary layer shrinks and expands as the wave passes and the seabed is not flat, making the nearshore sediment transport calculation more difficult. Due to the influence of waves in shallow water, bedforms, also known as ripples are developed and calculation of shear forces based on steady flow conditions is no longer applicable. Figure 10 shows

migrating bedforms under a wave. Note that the bottom is disturbed from left to right, where the sediment is suspended.

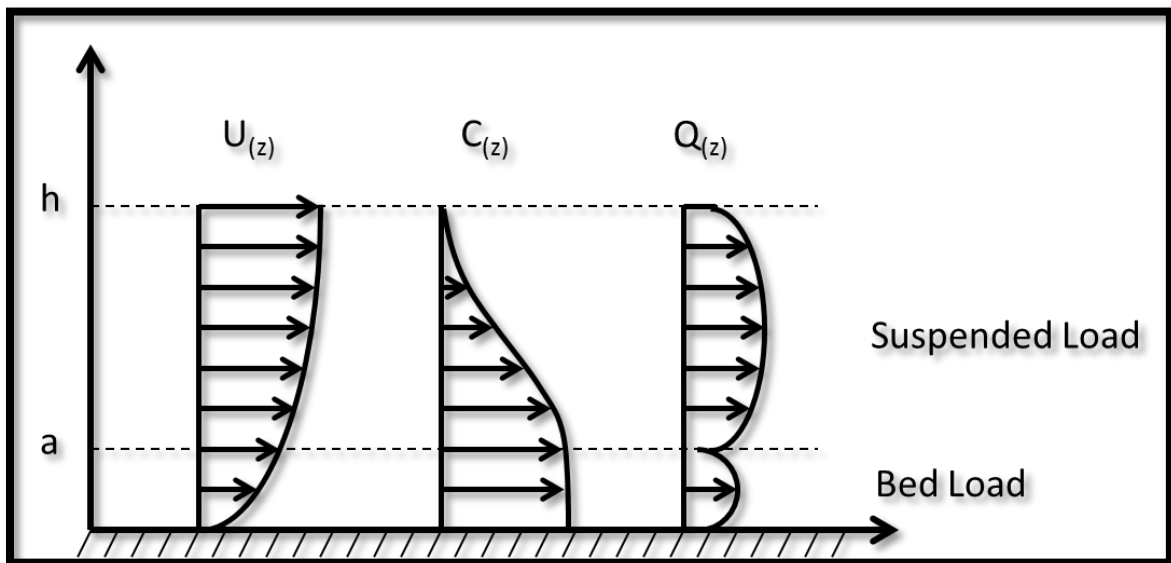


Figure 10: Bedforms under a wave. (Source: Alex Mustard, 2012)

#### ***2.1.4 Transport Modes***

The sediments are carried by means of different modes in the surfzone. The first mode of sediment transport is the bed load which occurs when the material starts to move via particle collision or by rolling motion at the bottom. Then, after some time, a thin layer of sediment slides, known as sheet load. The second mode is called suspended loads. This mode takes place when sand particles get suspended on the water column and move freely with the flow. Most of the

sediment is carried by suspended load and the sum of bed and suspended loads is called the total sediment transport (Figure 11). The last mode is the wash load where sediment is located outside the boundary layer of the concentration profile and is always suspended. Therefore, it is not considered in the total sediment transport calculation.



**Figure 11: Total sediment transport calculation.**

Another way by which sand is transported to the beach is the wind. This sediment transport mechanism is known as aeolian transport. It applies to the subaerial part of the beach where, usually, the waves do not reach under normal conditions. This is also the natural mechanism by which dunes are formed. Shoreline changes are typically the result of a combination of all of these



processes but they are mostly influenced by the waves that move the sediment in a cross-shore and longshore direction.

### **2.1.5 Cross-shore Sediment Transport**

The mechanism by which sand moves perpendicular to the shoreline is referred to as cross-shore transport and is driven by waves and the undertow currents. During a storm, the cross-shore process is responsible for depositing the material eroded from the subaerial portion of the beach into sandbars. Then, during the recovery period, small and long period swells slowly move the material shoreward. This process can take a long time and in some locations, depending on the wave climate and local conditions, the beach will never recover. The Equilibrium Beach Profiles theory (Bruun 1954 and Dean 1977) proposes that a natural beach profile will change its elevation to dissipate the incoming wave energy. In other words, if the wave conditions change, the beach will also change its profile in order to withstand the new incident wave. This theory is based on data collected from over 500 beach profiles along the United States East Coast, starting on Long Island, New York up to Texas. The following still water depth to shoreline distance relationship is based on the aforementioned theory,

$$h = A y^{2/3} \quad (4)$$

where

$h$  = Still water depth.

$y$  = Horizontal distance from the shoreline.

$A$  = Dimensional parameter related to sediment characteristics.

This methodology is useful to study beach nourishment spreading and storm induced erosion in computer models applications. Usually, cross-shore processes tend to dominate the shoreline evolution at time scales in the order of hours, such as during large storms. Over longer periods of time (several years to decades), however, morphological change is generally governed by longshore processes.

#### **2.1.6 Longshore Sediment Transport**

The mechanism by which sand moves along the shoreline is referred to as longshore sediment transport. It is produced by longshore wave-induced currents which are generated by waves breaking at an angle to the coastline. Hence, the direction of the longshore sediment transport varies with the direction of the approaching waves. Most coastlines have a dominant direction of transport which is related to both the frequency and the size of the waves. Waves approaching from the southeast are the most common in New Jersey during the summer months; however, waves approaching from the northeast generated by Nor'easters are typically the largest. In the southern half of the state, the net longshore transport is directed to the south as the larger waves from the northeast push more sand to the south. In contrast, Long Island protects much of the northern New Jersey coastline from the northeast approaching waves. As a

result, the sediment transport along the northern coast is mainly influenced by the southeast approaching waves, and is therefore directed to the north. Bay Head is located just north of the average location of the New Jersey coast nodal point (the point at which the net transport switches direction) and experiences a net northerly transport. Depending on the wave climate, in any given year the nodal point may shift to the north and cause a temporary reversal. Various studies have computed the net sediment transport rate in the vicinity of Bay Head to be between 26,800 and 279,000 cubic meters per year to the north (Beck and Kraus, 2010). The gross transport is believed to be in the order of a million cubic yards per year. Various studies using different techniques have determined sediment transport rates at the Manasquan Inlet and that it is directed toward north. Caldwell (1966) found this transport to be 57,000 m<sup>3</sup> using historical shoreline surveys. Farrell (1980) and Bruno (1988) calculated from 23,000 to 57,000 m<sup>3</sup> using inlet dredging records and aerial photos.

### ***2.1.7 Sediment Transport Models***

Making use of wave tank data and field experiments, researchers were able to develop useful numerical models for engineering applications. The early versions of the USACE simple cross-shore and longshore models are described below.

The **S**torm-induced **B**each **C**hange Model (SBEACH) is a two dimensional, purely cross-shore model developed by Larson and Kraus (1987) for simulating

short term storm-induced beach change. It is a geomorphic-based model founded on extensive analysis of beach profiles, generated in large wave tanks and in the field. Empirical relations were derived for four regions in the surfzone based on sediment mass conservation. It uses the water level and wave climate as the model forcing and assumes shore normal incident waves, natural beach system, and linear wave theory up to the point of breaking. After breaking, an energy dissipation model is used to simulate the breaker decay. Wave setup and set down, as well as bottom friction, is incorporated in the calculation of wave height distribution. Later, the surfzone is divided in four regions and sediment transport rate and direction is derived base on empirical equations valid for each region. Since the model can be used to study only the cross-shore behavior of the beach, other models called one-line models were developed to account for longshore processes.

The **Generalized Model for Simulating Shoreline Change** (GENESIS) is a one-line shoreline change numerical model developed by Hanson (1989). The model was intended for engineering use and incorporates coastal structures. The shoreline change is driven by the long-term wave climate at the site which generates a net longshore transport rate. This rate is assumed to have uniform cross-shore distribution. The model includes wave refraction and diffraction and the sediment transport is calculated using a modified version of the CERC equation (SPM, 1984) combined with mass conservation of sand.

The models presented here were the base for other models that evolved into the three dimensional Coastal Modeling System currently available.

## **2.2 Groins**

An effective shoreline stabilization technique that reduces longshore sediment transport is groins. These structures capture sand which helps widen beaches. Groins are used in beaches where longshore drift is predominant and are the most common beach stabilization technique employed in the East and Gulf Coasts of the United States. They extend perpendicular to the coast and are typically found in groups, called groin fields. Usually, groins are combined with other shore protection structures such as bulkheads, seawalls, and beach nourishment. An asymmetric beach shape typically results in groin fields as sediments accrete updrift and erodes downdrift of the structures. This phenomenon occurs because the flow velocity intensifies around the structure's updrift due to the obstruction caused by the groin itself. This in turn creates eddies downdrift that severely erode the sediment at this location and later deposits this sediment in the updrift fillet of the next groin (Figure 12). The amount of sand eroded on the downdrift of a groin is almost the same as the amount of sand deposited in the following groin's updrift fillet due to conservation of mass.

Groin permeability design is site specific, ranging from 50% to 80%, and plays an important role in sediment capture, downdrift effects, currents, and scour around the structure. More permeable structures decrease or eliminate the downdrift erosion problem. As an example, a case study that was conducted by the University of Florida where field measurements, wave tank laboratory experiment data, and computer modeling were used to study pile cluster and slotted timber groins (Poff et al. 2004). It was observed that updrift and downdrift beach profiles experienced sediment deposition, bar formation, and seaward shoreline advance. Depending on the project site, groins can be designed to have different shapes such as I, L, T or Y shapes to better trap the sediment. Spacing, length, and elevation are also very important. Short or very low profile groins will not capture enough sand making them ineffective. However, very long or high profile groins are not recommended because will completely cut off the sediment transport and result in severe erosion of the downdrift beach.

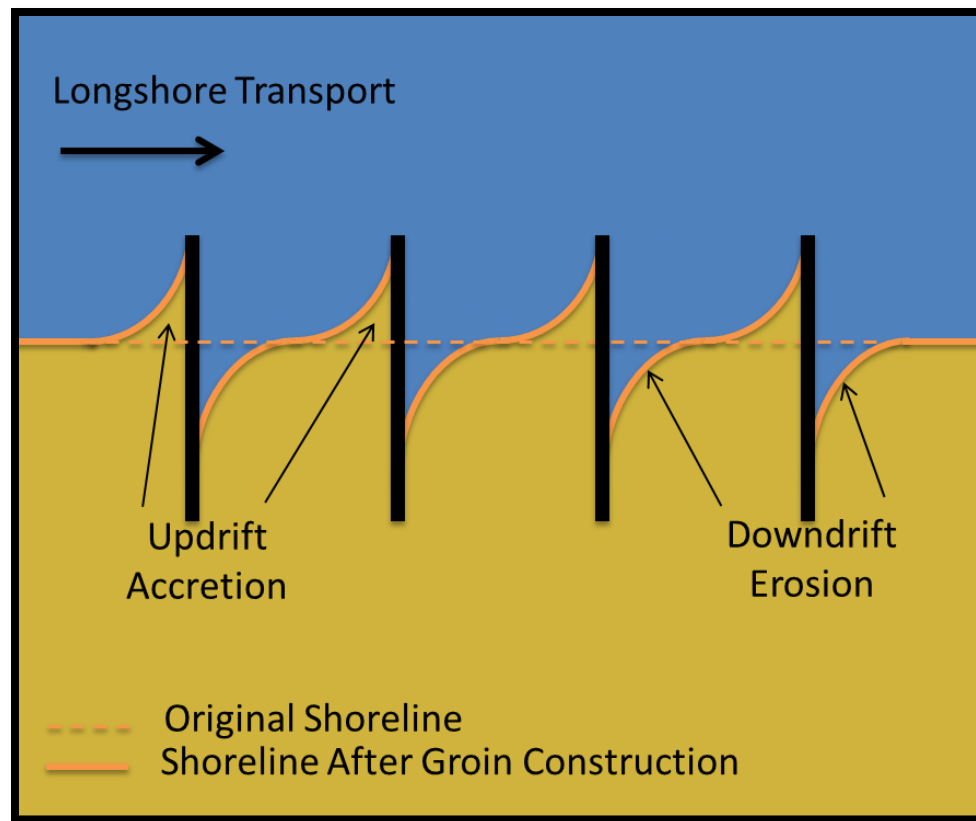


**Figure 12: Groin field impact to the shoreline.**

Common materials used to construct coastal groins are timber, steel sheet pile, geotextile fabric, and stone. The life span of groins typically ranges from 25 to 50 years, depending on the material used for its construction. Structure deterioration creates gaps, affecting its permeability, and leads to ineffectiveness of trapping sand. On places where severe downdrift erosion occurs, however, it is necessary to create gaps on the structure, commonly within the swash zone, to let the sand move longshore. This technique is called groin notching and is more cost effective than removing the groin. This helps the longshore drift to create a more symmetrical beach, but also raises other concerns such as rip currents and

beachgoers safety. The longshore sediment transport is affected by additional factors if the site is located close to an inlet since bypass transport is affected by the tidal prism.

### ***2.3 Tidal Inlets***

A natural inlet connects a bay with the ocean and its position, width, depth and shape can drastically change over time. Highly navigated inlets have been stabilized with jetties. Updrift and downdrift behavior of a jettied inlet are similar to groins. However, because these structures are usually longer than groins, the jetties completely block the longshore sediment transport, worsening the downdrift beach erosion. Sand that bypasses the inlet is deposited either offshore on the ebb shoal or in the channel, and never making it to the downdrift beach (FitzGerald et al. 2000). Some bypassing techniques, such as the combination of lowering the updrift jetty's profile near the swash zone and then using hydraulic pumps to pump the sediment accumulated in the updrift into the downdrift beach, have been implemented in some inlets but such technique involves high costs.

Sediment budget around tidal inlets is one of the most difficult systems to quantify. Strong currents from the river discharge naturally deposit sediment at the entrance of the inlet, creating an ebb shoal. During high tide and storms, waves push the sediment to a flood shoal located in the bay side of the inlet. This



mechanism is also responsible for channel shoaling. Coastal Engineers design inlets to be hydraulically efficient by specifying strategic dimensions. The width and depth of the channel should be such that the tidal prism is capable of flushing the sediment out the channel. The goal is to maintain the depth needed for navigation while minimizing maintenance requirements. However, strong storms rapidly shoal the entrance and dredging is required to remove the sediment which is usually deposited in the downdrift beach.

Bay Head is located approximately 2 miles south of the Manasquan Inlet. Therefore, it was necessary to incorporate the Manasquan Inlet in our analysis as it contributes to the sediment budget. By inspection of the historical aeriels available in Google Earth (dating back to 1995), the net sediment transport of this area is predominant to the north. However, an aerial from 2010 (Figure 13) depicts the suspended sediment moving south, bypassing the northern jetty. This confirms that the sediment transport direction is indeed reversed at some points during the year.

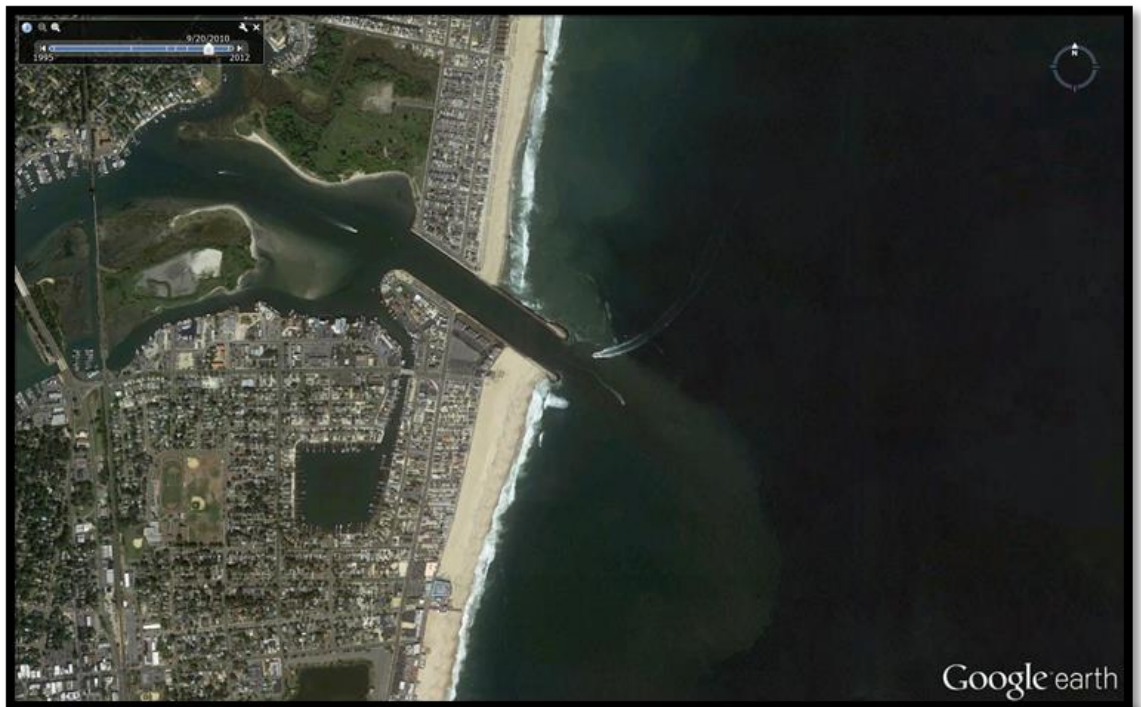


**Figure 13: Manasquan Inlet in 2010; Sediment transport directed southward.**

## **CHAPTER 3**

### **Computational Procedures**

#### ***3.1 CMS Model Development***

The storm was modeled using the Coastal Modeling System (CMS) to estimate the beach erosion volume and sediment transport that took place in the coast of Bay Head, NJ during Hurricane Sandy. CMS is a numerical model developed and maintained by the U.S. Army Corps of Engineers (USACE) under the Coastal Inlets Research Program (CIRP). This model was chosen because it has the capability of integrating a hydrodynamics numerical model with a wave spectra model. Therefore, it was possible to combine wave, wind, and tide forcing simultaneously. The Surface-water Modeling System (SMS) serves as the model interface and its major use in practice is maintenance of coastal inlet structures in navigation projects. Although the model is a beta version, it may be useful in determining the sediment transport direction, estimate transport rates, and understand the local coastal processes to better design coastal structures that stabilize the shoreline. The presented research seeks to evaluate the performance of the CMS in simulating the measured shoreline change during a significant coastal storm event.

A Modeling Process must be followed in order to obtain accurate results. First, in the planning stage, modeling objectives are discussed. Site visits to become familiar with field conditions and coastal features is encouraged. Second, relevant data is gathered to then assemble on the SMS interface. Following, a grid is generated and the model forcing and parameters are established. Using a low resolution model is recommended to conduct initial test runs. Then, the model resolution is gradually increased until the desired level of detail is achieved. The model is calibrated by comparing the obtained results with field measurements over a specified timeframe. Usually, tide gauges and current meters are used for this step. After calibration, the model is ready to be validated by applying it on a different time period and comparing the results to field data. The validation process proves that the model can be applied at the project area for different case studies and provide accurate results. Once validated, the model is revised to account for existing coastal structures and final runs are performed. Finally, analysis of the model output is conducted and documented.

### **3.1.1 CMS-Wave**

CMS-Wave is a phase-averaged spectra model for propagation and transformation of directional irregular waves that simulates wave refraction, diffraction, reflection, shoaling and breaking over complicated bathymetry by solving the wave-action balance equation using a forward marching Finite Difference Method (Mase et al.2005). It also calculates wave transmission, wave

runup, and overtopping as special features on selected cells. The model was developed to support the operation and maintenance of coastal inlet structures in navigation projects as well as in risk and reliability assessment of shipping in inlets and harbors (Lin et al. 2008). The input spectra can be generated from an external source such as the National Data Buoy Center (NDBC) or the Coastal Data Information Program (CDIP).

### **3.1.2 CMS-Flow**

CMS-Flow is a finite-volume depth average numerical model which includes the capabilities to compute both hydrodynamics sediment transport and morphology change. It calculates the water levels, currents, and sediment transport considering the boundary forcing and the influence of coastal structures (Buttolph et al. 2006; Wu et al. 2011). Its major contribution is that it can be used to calculate sediment exchange between inlets and adjacent beaches. This model has explicit and implicit solution schemes options. The explicit solver is designed for dynamic problems that require small time steps as is the case for scenarios where conditions vary quickly, such as a storm. The implicit solver is intended for simulating long term wave-induced circulation and tidal flow at inlets, navigation channels, and adjacent beaches.

### **3.1.3 Coupling Models**

CMS-Wave and CMS-Flow make the CMS one of the most complete 3D modeling tools currently available. In this study the two were combined into the steering module. Hence, the solutions are shared between the models throughout the simulation. The way CMS performs this process is as follows:

1. CMS-Wave runs two time steps and transfers the wave information to CMS-Flow (Figure 14).
2. Wave height, period, direction, breaking wave energy dissipation, radiation stress gradients, and wave unit vectors are spatially interpolated from the wave grid to the flow grid.
3. CMS-Flow runs until the next steering interval and, during the steering interval, wave variables are linearly interpolated in time. Wavelength and bottom orbital velocities are updated at each flow time step for wave-current interaction.
4. Water levels, current velocities, and bed elevations are estimated for the next wave time step and are interpolated from the flow grid to the wave grid.
5. CMS-Wave runs the next time step.
6. Step 2-5 are repeated until the end of the simulation.

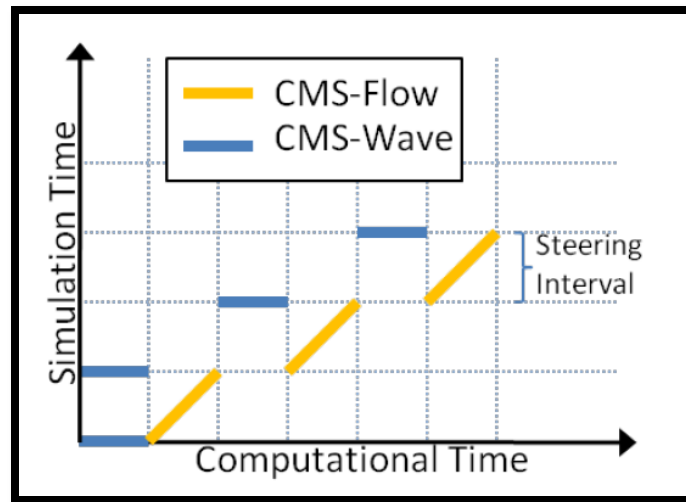


Figure 14: Schematic of steering process. (Source: CMS User Manual)

### 3.1.4 Limitations and Assumptions

The following are some of CMS limitations and assumptions which are relevant to this research work.

1. The CMS model is depth-averaged and does not calculate the vertical profile of current velocities and suspended sediments. It assumes a depth-uniform current in the presence of oscillatory waves.
2. The model assumes non-cohesive sediments with a constant mean diameter ( $D_{50}$ ), density, and porosity.
3. The wet and dry cells are defined at a depth of 0.05m.
4. Shallow water equations can be violated if cell sizes are significantly smaller compared to the flow depth used.
5. It is recommended to use the explicit solution for high Froude numbers flows.

6. Flow through structures is handled using empirical equations.
7. Formulations for onshore sediment transport are still under development.
8. Sediment transport is calculated using the Lagrangian current velocities.
9. For a short term simulation, such as a hurricane timeframe, it is recommended to use a grid with less than 80,000 active cells.
10. It is recommended to have at least 10 computational cells in the surfzone in the cross-shore direction for nearshore circulation.
11. It is recommended to have at least 3 cells perpendicular to a channel or 10 cells across an inlet entrance.



## ***3.2 Input Data***

Fundamental data, such as bathymetry, background imagery, and meteorological data is required to run the model. Typically, a single bathymetry dataset does not contain all the details and important features. Therefore, a good bathymetry scatter set is needed to obtain accurate model results. Different data sets were merged into a final bathymetry (Figure 16). The data were collected from the sources described below.

### ***3.2.1 National Geophysical Data Center (NGDC)***

The first bathymetry data incorporated into the model was downloaded from the U.S. Coastal Relief Model (CRM) (NGDC 1999), which is supported by the National Oceanic and Atmospheric Administration (NOAA). The CRM database contains grids, known as Digital Elevation Models (DEMs), which integrate ocean bathymetry and land topography. These provide a resolution of 90 meters in the horizontal and 1 meter in the vertical. A custom DEM was delineated, which extends from Long Island to Cape May and includes 100 miles offshore.

### ***3.2.2 LiDAR***

New Jersey coast Light Detection and Ranging (LiDAR) data sets were used to enhance the beach resolution. This data is available in the NOAA Coastal Services Center website under the Digital Coast section. Two LiDAR data sets were used for this research work and each have a horizontal accuracy of 75 cm

and vertical accuracy of 20 cm. The data only includes topographic elevations since water turbidity in New Jersey do not allow LiDAR to penetrate through the water column. One of the data sets was collected in August 28, 2010 by the Joint Airborne Lidar Bathymetry Technical Center of eXpertise (JALBTCX) under the United States Army Corps of Engineers National Coastal Mapping Program (USACE 2010). The other data set was collected from the same source in November 16, 2012, after Hurricane Sandy, (USACE 2012) and was used to compare to the model results.

Because of the nature of how this data is collected, the file sizes are excessively large as they contain numerous data points. If used verbatim, the model computation time would be significantly extended without need, making it inefficient. Therefore, it is recommended to filter the data before incorporating it into the model. An alternative is to use SMS interface's grid filtering option for imported scatter sets.

### ***3.2.3 Dynamic Underwater and Coastal Kinematic Surveying***

#### ***(DUCKS) System***

The Coastal Group of The Center of Maritime System at Stevens Institute of Technology made use of the Dynamic Underwater and Coastal Kinematic Surveying (DUCKS) System (Miller et al. 2009) to gather elevation profiles of the groin field at the project site on September 22, 2011. Using a Real Time

Kinematics (RTK) GPS, the survey consisted of walking on the beach at low tide and driving a jet ski through the surfzone at high tide over a determinate set of grid lines, shown in Figure 15. The spacing of the profile lines was set to 76 meters in order to capture small scale changes in elevation of dunes, berms, and offshore bars. Both the GPS and an Odom Hydrographic single beam echo sounder were controlled via a computer, using the program HYPACK, to record coordinates and elevations in a single beam mode over the nearshore region. Then, based on the given ocean temperature and salinity, the data was post-processed by filtering the noise and adding tide correction files. The final product is a representation of the beach conditions before the storm.

Another survey was performed after the storm, in November 20, 2012, which is 4 days after the available LiDAR data. This survey only entailed the subaerial portion of the beach due to safety concerns regarding beach access and floating debris.

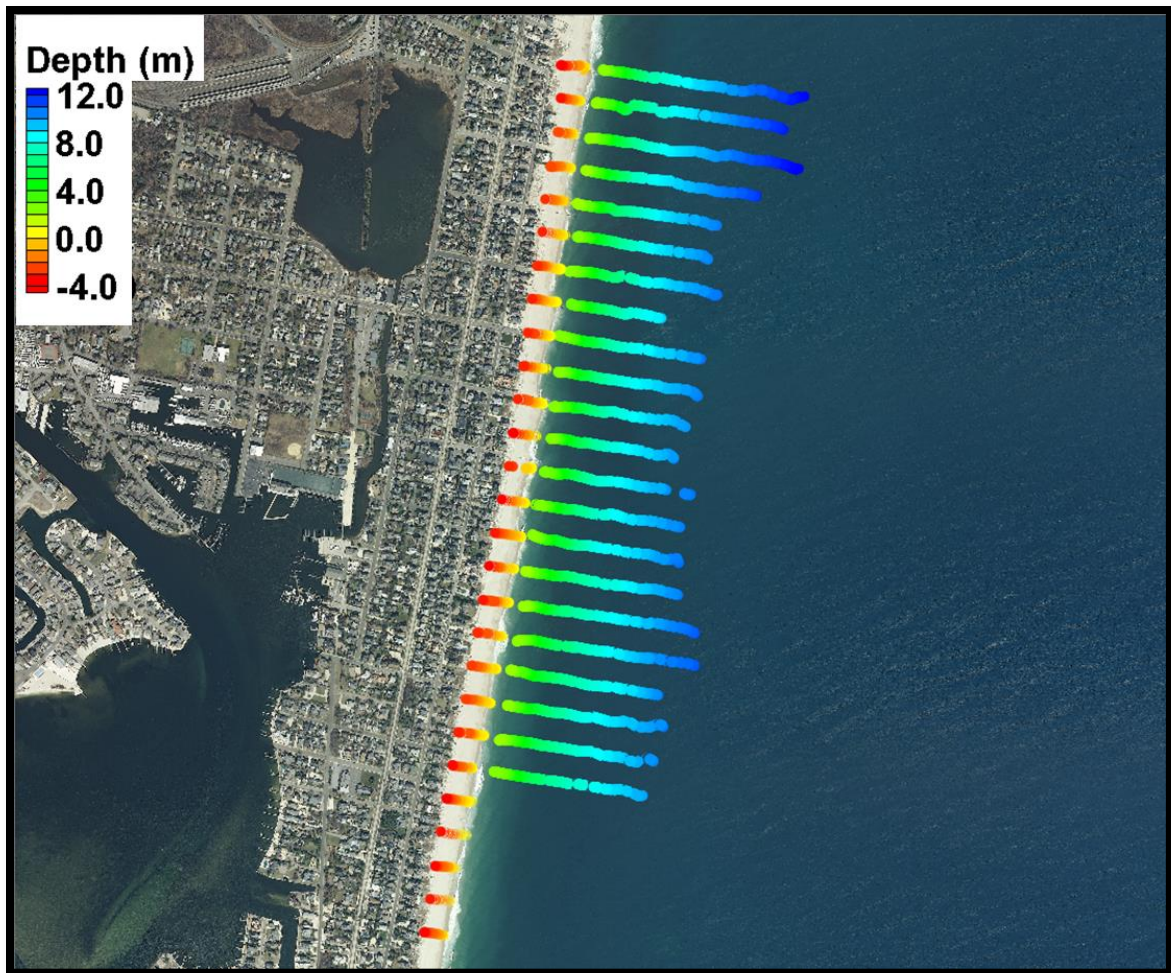


Figure 15: DUCKS System Survey (9/22/2011).

### **3.2.4 US Army Corp of Engineers**

Bathymetric data collected on February of 2012 by the US Army Corps of Engineers, Philadelphia District, was acquired. It includes hydrographic data of the Manasquan Inlet entrance, part of the main channel, and Point Pleasant Canal. This data depicts the channel shape in detail, which contributes to accurate sediment transport calculations.

The acquired data sources were incorporated into the model, they were all re-projected to State Plans Coordinates System and to the North American Vertical Datum of 1988 (NAVD 88) in meters. Aerial pictures were overlain on the bathymetry data to modify, refine, and smooth the contours in specific areas such as land-water boundary, channels, and coastal structures.

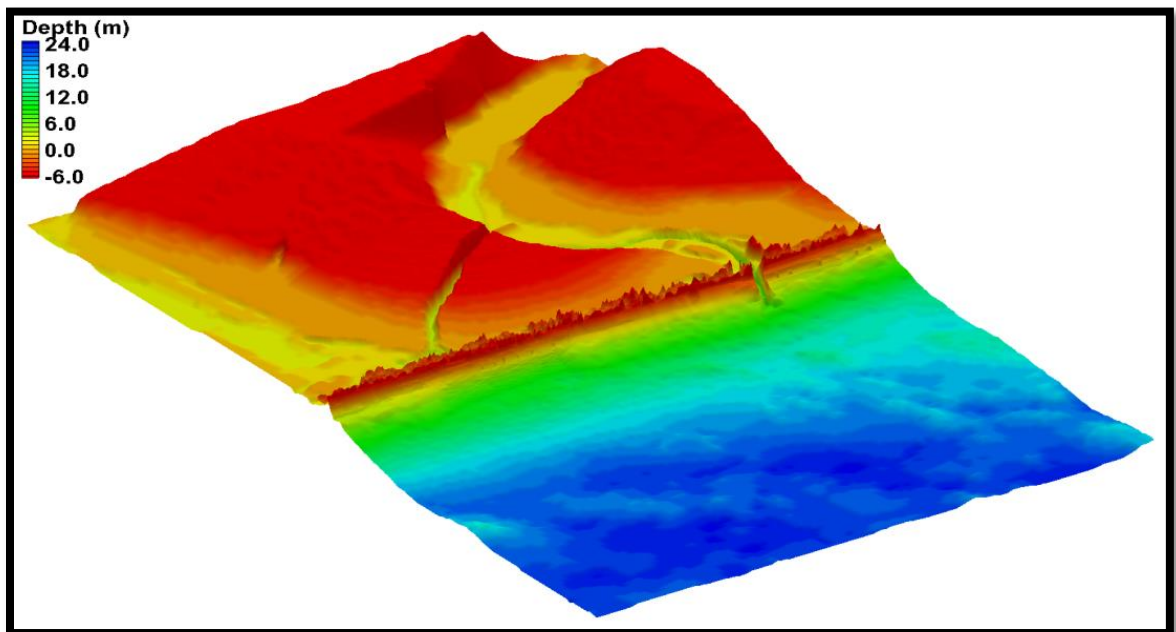


Figure 16: Final Bathymetry for High Resolution Model.

### **3.2.5 Orthoimagery**

The 2012 pre-storm New Jersey High Resolution Orthoimagery was obtained from the New Jersey Geographic Information Network (NJGIN), [https://njgin.state.nj.us/NJ\\_NJGINExplorer/index.jsp](https://njgin.state.nj.us/NJ_NJGINExplorer/index.jsp). The aerials help to set references and features within the bathymetry. The bathymetry was fixed by

hand to capture small scale changes from shoreline, beach, inlet, and channel features as accurately as possible (Figure 17). Visual inspection was also used for the most important features of the project which are the creation of the groins and jetties that barely were showed on the merged bathymetry data file. Groins were created and mapped as land points in the bathymetry file using the “Feature Points” command and they were assigned an elevation of 1 meter NAVD 88 datum which is approximately mean high water. Figure 18 shows one of the groins created in the model.



**Figure 17: Manasquan Inlet bathymetry.**



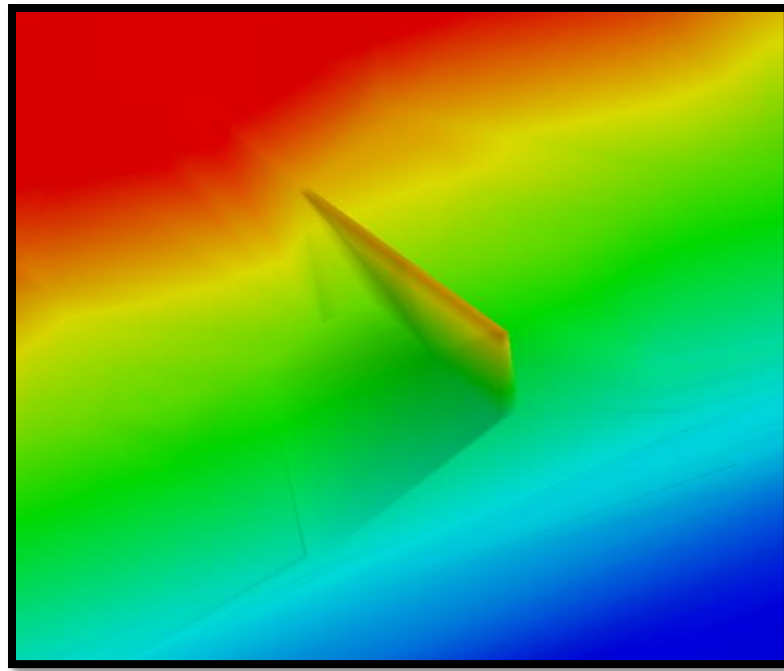


Figure 18: Karge groin recreated in the bathymetry.

### ***3.2.6 Meteorological data***

Wave and wind data during Hurricane Sandy was acquired from an offshore buoy, maintained by the National Ocean Atmospheric Administration's (NOAA) National Data Buoy Center (NDBC), (<http://www.ndbc.noaa.gov/>), and used as the offshore forcing of the CMS-Wave model. Buoy station number 44025, which is located approximately 40 nautical miles offshore of Bay Head, is the closest buoy to the site. Due to its offshore location, the buoy was fully exposed to over ocean wind and waves during the storm and recorded valuable data.

Tide data from the Atlantic City Steel Pier was used as the offshore forcing of the CMS-Flow model. The data can be found at the NOAA's website under Tides & Currents gauge number 8534720. Also, data from the Manasquan inlet tide gauge (USGS 01408050) during Hurricane Irene was used to calibrate the model.

Tropical storms are characterized by significant barometric pressure drop and, hence, intensified wind speed, in the system's eye. In addition, Hurricane Sandy was also characterized by the fact that the storm approached the coast of New Jersey along with the surge. Therefore, wind and pressure changes over time were expected at different locations in our domain. Since buoy data is collected at a fixed point it does not capture all of these changes. In order to account for this, two additional files, containing spatially variable wind and atmospheric pressure forcing throughout the storm, were provided by the CMS developer Dr. Lihwa Lin. However, this data was generated on a coarser regional grid.

### ***3.3 Grid Generation***

A regional scale (parent) grid with a resolution of 1000 meters (Figure 19) was used to incorporate the provided pressure and wind files. CMS-Flow model was run with these two files along with the Atlantic City water surface elevation as a forcing. Later, the output of this model was nested at the offshore boundary condition of a high resolution grid, shown in Figure 20. This is a non-uniform grid



with variable resolution ranging from 40 meters in the offshore to 5 meters in the surfzone and dry beach of the project. The grid is oriented parallel to the shore, a requirement of the CMS. The offshore boundary is located 3 nautical miles offshore and extends 1 mile north of the Manasquan Inlet and 1 mile south of the groin field. Relatively little rainfall was associated with Sandy allowing for the discharge from the Manasquan River to be neglected over the storm (5 days) simulation time span. The high resolution grid was used for both CMS-Wave and CMS-Flow models.

CMS-Flow transport and bed equations assume all cells have a movable bed in which sediment can be lifted and moved around. Hence, coastal structures and rocky bottoms were specified to have a hard bottom (non-erodible) so that only deposition occurs. There are three ways to define cells in the CMS-Flow model; active, inactive, and observation cells. The difference between the active and inactive cells is that active cells entail computation. In the model developed for this research work, active cells were specified up to approximately 50 meters inland of the seawall. Observation cells are used to save a time series of flow rate and transport rate output. In the model, observation cells were created in key locations such as the inlet ebb and flood shoals and in front of the Bay Head groin field at a water depth of about 3 meters. A bottom friction dataset of the entire domain was created using a Manning's coefficient of 0.025 to account for bottom roughness. This dataset was manually edited to account for the presence

of vertical piles under the bridges of the Manasquan River, gradually increasing the Manning's coefficient value up to 0.050.

CMS-Wave damping cells were selected to calculate the wave runup at the beach. Coastal structures such as groins, jetties, and bulkheads were defined as rubble-mound or wall breakwater structures. Therefore, the model calculates diffraction and reflection around the structures and, finally, damp on the shore. Monitoring stations were located at the same location as the observation cells of the CMS-Flow grid.

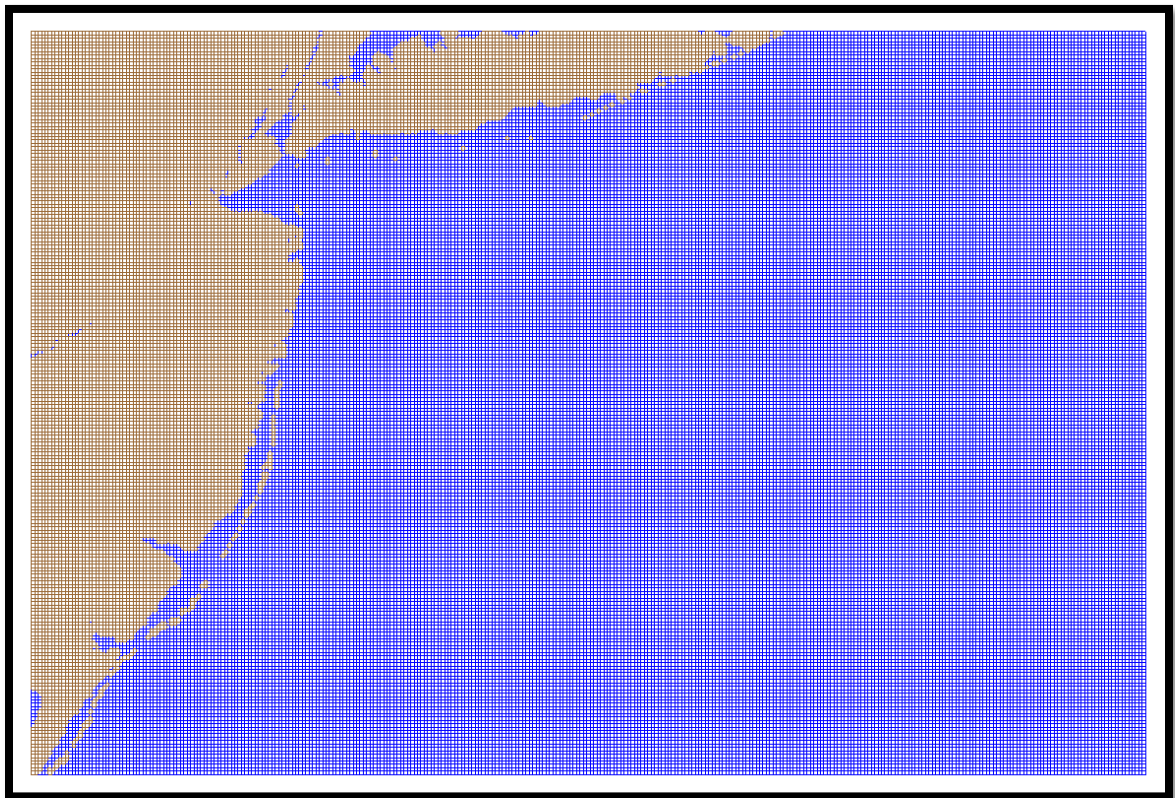


**Figure 19: Parent grid.**

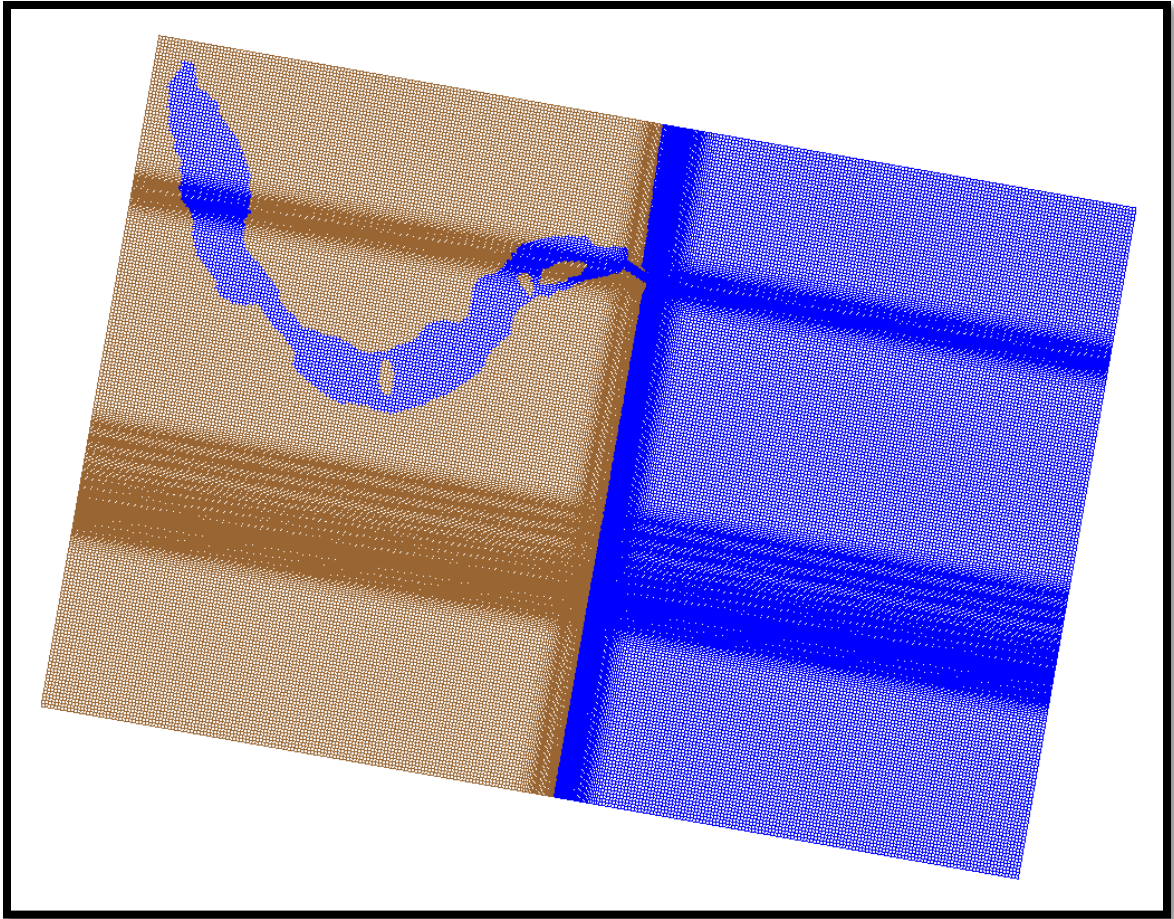


Figure 20: High resolution grid.

### **3.4 Calibration**

Hurricane Irene was the storm used to calibrate the model. It made landfall in New Jersey on August 28, 2011, approximately a year before Hurricane Sandy. Its trajectory followed a south to north direction along the coast of New Jersey and its wind intensity at the time of landfall was similar to that of Hurricane Sandy although with a smaller storm surge. CMS-Flow was run in the regional grid. The forcing at the offshore boundary condition were the water level data from the

Manasquan River tide gauge and the spatial wind and pressure files (atmospheric forcing) recorded during Hurricane Irene. Then, the calibration process was undertaken by comparing calculated water surface elevation results from the model against field measurements. Data from the USGS 01408050 tide gauge, located in the Manasquan River (Figure 21), was used and compared against model output at the same location. Figure 22 shows that the model slightly overestimated the observed water levels at high and low tide. In general, the model agrees with the values measured during the storm. The pressure and wind field files were key to improve the model and, hence, obtain accurate results. The root mean square error (RMS) between model and observations was 0.28. Once the model was calibrated, the Hurricane Sandy data was simulated.

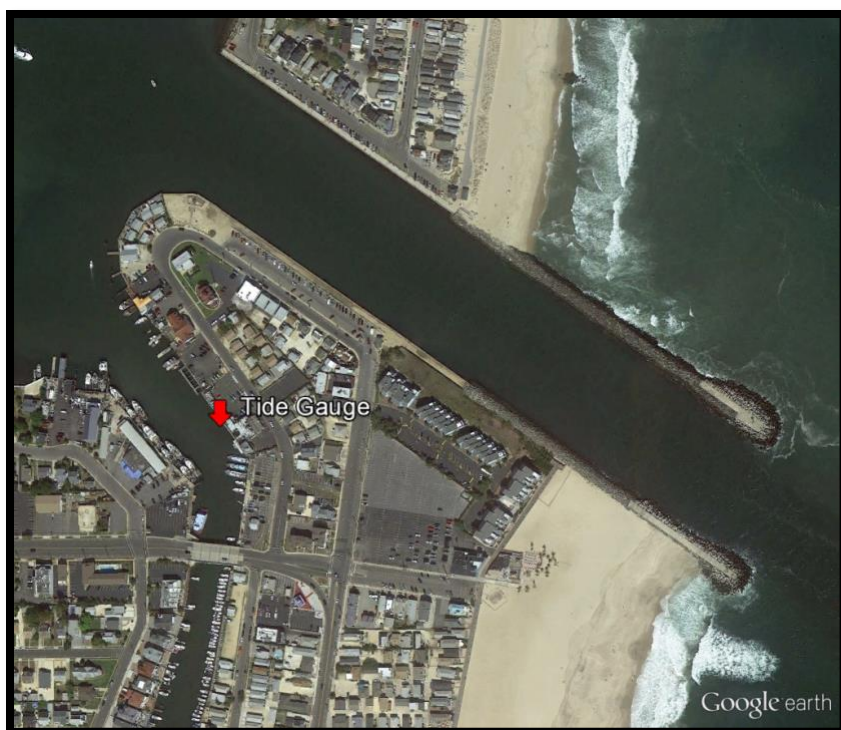


Figure 21: Manasquan River tide gauge location.

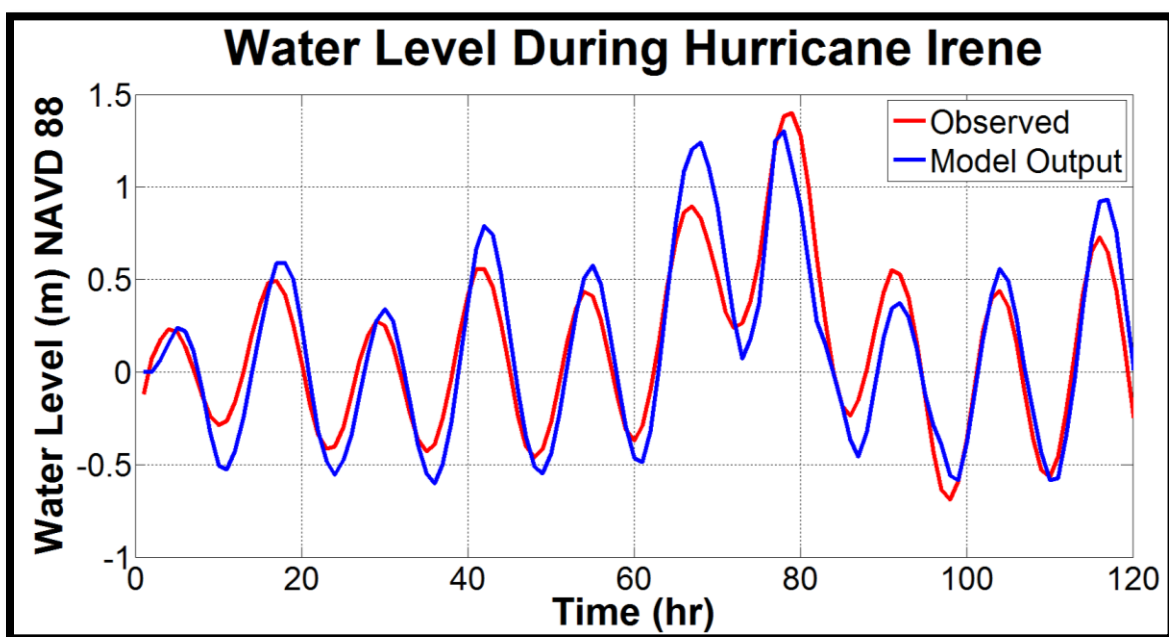


Figure 22: Water level comparison.

### ***3.5 Hurricane Sandy Simulation***

Hurricane Sandy was simulated following the same methodology used for the Irene simulation. The duration of the simulation was 132 hours, from October 26, 2012 12:00 AM (GMT) to October 31, 2012 12:00 PM (GMT). After the model was run in the parent grid, the output was nested on the offshore boundary of the child grid. The high resolution grid was then run, coupling CMS-Wave and CMS-Flow. Model parameters and sediment transport equations used are described below:

#### ***3.5.1 CMS-Flow Parameters***

- Water Parameters
  - Water temperature for the duration of the storm was obtained from the New York Harbor Observing and Prediction System (NYHOOPS) website ([hudson.dl.stevens-tech.edu/maritimeforecast](http://hudson.dl.stevens-tech.edu/maritimeforecast)). Water temperature is important as it modifies the water density affecting the submerged weight of the sediment. Subsequently will affect the velocity at which sediment is being transported. Water temperature and density values are shown in Table 2.

Water Temperature	15.5 °C
Water Density	1025 kg/m <sup>3</sup>
Hydrodynamic Time Step	0.25 sec

**Table 2: Water Parameters.**

- Hydrodynamic Time Step
  - The grid cell size for the surfzone area was set to 5 meters in order to capture detailed elevation changes. Hence, a hydrodynamic time step of 0.25 seconds was used to maintain a stable numerical scheme throughout the simulation.
  
- Others
  - The advective and mixing terms were included in the momentum equations.
  - Wall Friction was included.
  - Depth at which cells would start being dried was set to 0.05 meters.
  - The EXPLICIT solution scheme was used.

### ***3.5.2 Sediment Transport***

Sediment transport was calculated using the non-equilibrium total load transport approach, where the suspended load is not in equilibrium, and advection and diffusion are considered. It adopts a sediment transport adaptation concept and solves the advection-diffusion equations for total load concentration. There are two main advantages to the Non-equilibrium total load transport: 1) Accounts for temporal and spatial lags between flow and sediment transport (typically reduces transport) and 2) The model is more stable. The relationship relevant to this approach is as follows,

$$\frac{\partial}{\partial t} \left( \frac{hC_{tk}}{\beta_{tk}} \right) + \frac{\partial (U_j h C_{tk})}{\partial x_j} = \frac{\partial}{\partial x_j} \left[ v_s h \frac{\partial (r_{sk} C_{tk})}{\partial x_j} \right] + \alpha_t \omega_{sk} (C_{t* k} - C_{tk}) \quad (5)$$

where

$j = 1, 2, \dots, N$

$k = 1, 2, \dots, N$

$N$  = Number of sediment size classes.

$t$  = Time (sec).

$h$  = Total water depth (m).

$x_j$  = Cartesian coordinate in the  $j^{th}$  direction (m).

$U_j$  = Depth-averaged current velocity (m/s).

$C_{tk}$  = Depth-averaged total-load sediment concentration for size class  $k$ .

$\beta_{tk}$  = Total-load correction factor.

$r_{sk}$  = Fraction of suspended load in total load for size class  $k$ .

$v_s$  = Horizontal sediment mixing coefficient.

$\alpha_t$  = Total-load adaptation coefficient.

$\omega_{sk}$  = Sediment fall velocity.



The sediment balance equation for bed change is as follows,

$$\frac{1 - p'_m}{f_{morph}} \left( \frac{\partial z_b}{\partial t} \right) = \alpha_t \omega_{sk} (C_{tk} - C_{tk*}) + \frac{\partial}{\partial x_j} \left( D_s |q_{bk}| \frac{\partial z_b}{\partial x_j} \right) \quad (6)$$

where

$z_b$  = Bed elevation with respect to the vertical datum (m).

$p'_m$  = Bed porosity (-).

$D_s$  = the bed-slope coefficient (-).

$q_{bk} = hUC_{tk}(1-r_{sk})$  which is the bed load (m<sup>2</sup>/s).

$f_{morph}$  = Morphologic acceleration factor (-).

For more information about each of these variables and how the model calculates them, see the Coastal Modeling System User Manual. The model used for sediment transport capacity was the Lund-CIRP (Camenen and Larson 2007). This approach utilizes separate equations for suspended and bed loads and predicts well the sediment transport on the surfzone. Table 3 shows the sediment parameters used in the model.

Transport Rate Time Step	0.25 sec
Morphology Time Step	0.25 sec
Sediment Density ( $\rho_s$ )	2650 kg/m <sup>3</sup>
Bed Load Scaling Factor ( $f_b$ )	0.5
Suspended Load Scaling Factor ( $f_s$ )	0.5
Sediment Porosity ( $p$ )	0.4
Sediment Mean Size ( $D_{50}$ )	0.2 mm
Total Load Adaptation Length Method	Max (Bed & Suspended)
Bed Load Adaptation Length Method ( $L_b$ )	Depth Dependent
Bed Load Adaptation Factor	10
Suspended Load Adaptation Length Method ( $L_s$ )	Armanini and Silvio
Sediment Fall Velocity ( $\omega_s$ )	Soulsby-Whitehouse
Sediment Corey Shape Factor (CSF)	0.7

**Table 3: Sediment parameters used in the model.**

#### Notes

- Larger values of adaptation coefficient increase the local erosion or deposition and shorten the response time of the sediment concentration field to varying flow conditions.
- Larger values of transport scaling factors produce larger sediment loads.
- Larger values of bed-slope coefficient produce a smoothing of the morphology change.

### **3.5.3 Wind Velocity and Direction**

Wind data was obtained from NOAA buoy 44025, collected at a height of 5 meters above sea level during the storm. Wind velocity data is shown in Figure 23. The strongest winds reached the project area when the eye made landfall,

around hour 100 in the simulation. During this moment, the wind direction also significantly changed, as shown in Figure 24.

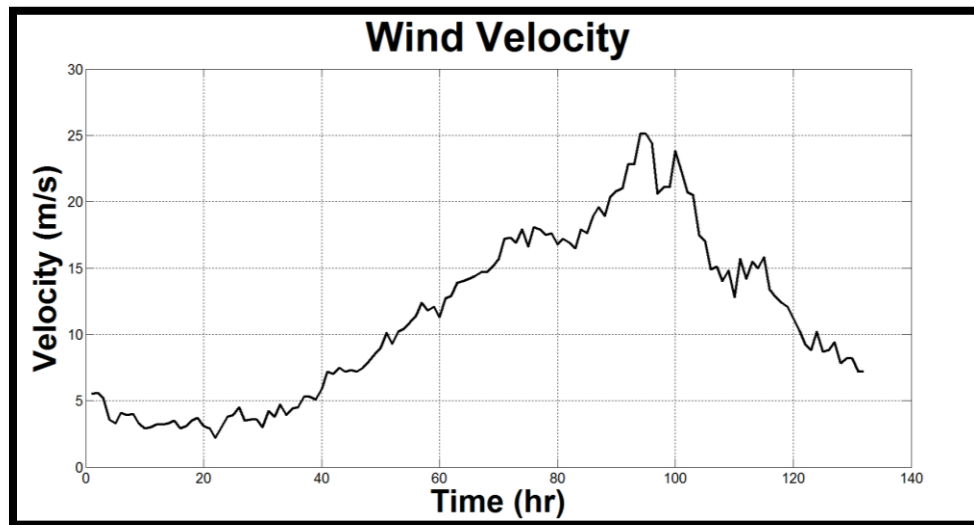


Figure 23: Wind velocity during Hurricane Sandy.

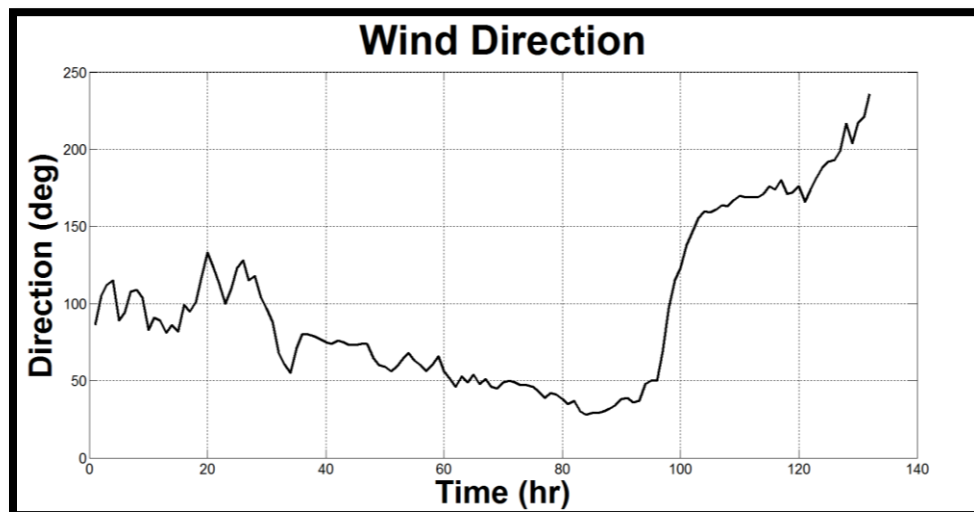


Figure 24: Wind direction during Hurricane Sandy.

### 3.5.4 CMS-Wave Parameters

A spectra grid was created using the Spectra Manager window within the SMS interface. Then, the directional wave spectra was created using wave height, angle, and peak period data recorded by buoy 44025 during the storm. Figure 25 shows the wave spectra density during the peak of the storm. The wave breaking formula used is an extended formulation of the Goda method (Sakai et al. 1989). For bed friction, a Darcy-Weisbach friction coefficient value of 0.005 was used (spatially constant). Non-linear wave effect was used and wetting and drying of cells was allowed.

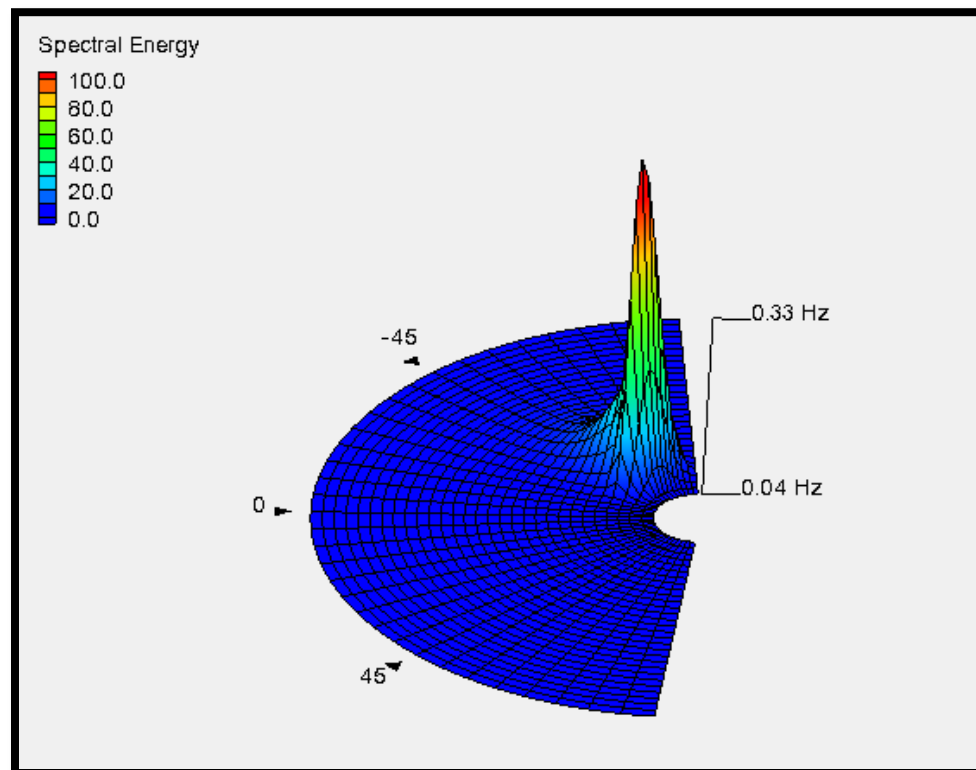


Figure 25: Wave spectra used in the model.

### **3.6 Validation**

To validate the model, beach profile data from post-storm surveys (subaerial) was compared to the final morphology dataset of the simulation. The sources were USACE National Coastal Mapping Program (JALBTCX) (Nov 16, 2012) and a RTK GPS survey performed by Stevens Institute of Technology Coastal Group (Nov 20, 2012) using the Dynamic Underwater and Coastal Kinematic Survey (DUCKS) System. Since a significant swell that could cause notable erosion/accretion did not occur between these two surveys, the model's sediment transport equations and parameters, such as bed load and suspended load scaling factors, were iterated until the model's post-storm elevation profile matched the survey data at the middle of the groin field. The beach profile in Figure 26 shows this comparison at the end of Howe St. Note the erosion in front of the seawall, depicted by the change in elevation within the first 5 meters away from the seawall location ( $x = 0$  meters). One must keep in mind that survey data has numerous elevation points whereas the model's coarser output provides an elevation point every 5 meters.

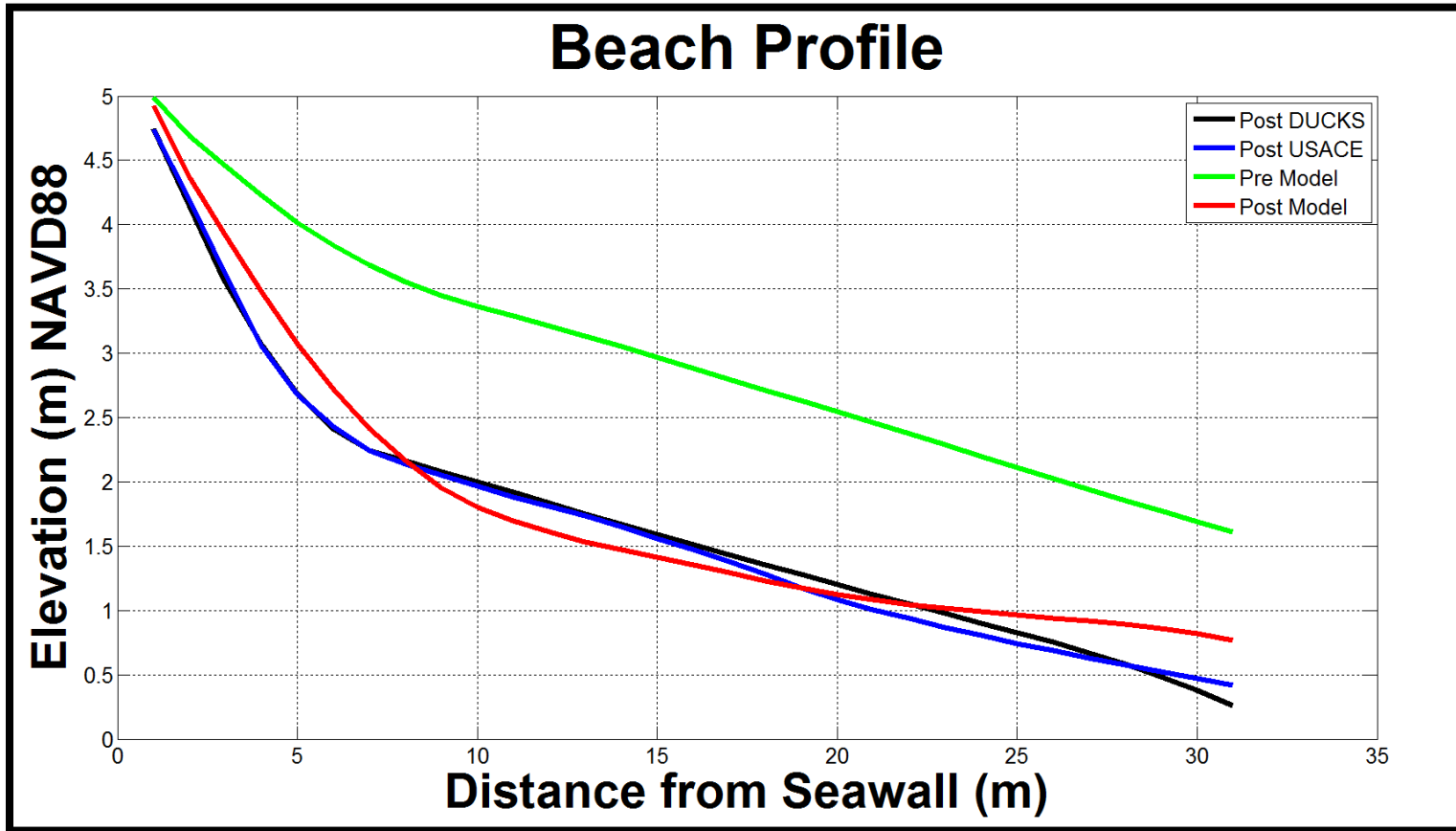


Figure 26: Beach profile comparison at Howe St.

# **CHAPTER 4**

## **MODEL RESULTS**

The model results discussed in this chapter correspond to a single time step of the simulation, which is the peak of the storm. In addition, the focus is the impact on the Bay Head groin field.

### ***4.1 Water Surface Elevation***

The water surface elevation in the model accounts for storm surge, which is responsible for how high into the beach the waves reach and accelerates erosion. In general, in coastal locations where dunes or a seawall are not present to dissipate wave energy, if the storm surge is high enough, waves can directly impact coastal structures and cause severe flooding.

#### ***4.1.1 Storm Surge***

The model shows a maximum storm surge of 3.9 meters NAVD 88 on October 30, 2012 at 8:00 pm EST (around the time of the storm's landfall). The left side of Figure 27 depicts the water surface elevation at the beginning of the simulation, note the groins are exposed. The right side of Figure 27 depicts the water surface elevation at the peak of the storm. Note the beach and groins are

underwater and the seawall was overtopped, flooding nearby houses. Seawater reached as far as 35 meters inland.

The Stevens Center for Maritime Systems' Coastal Group assessed the damages after the storm and found 74 watermarks at Bay Head. Most of them were found on the bay side and the maximum height recorded was 2.6 meters NAVD 88 located on Mount Street and Ocean Avenue. Every structure within the town was evaluated and 9 were found to be about to collapse. These were part of the first row structures located near the center of the groin field. Also, around 10 significant scour depressions were found due to the increase in flow velocity near structures foundations. Damage to the rest of the town was avoided by the seawall that significantly helped reduce incoming wave energy.

Another surge event happened 8 hours after landfall. This back-bay surge rapidly flooded the town on its bayside since no coastal protection was provided and low elevations are present. This second surge lasted the most because of the funnel effect created by the Barnegat Bay geometry. The back-bay surge was not modeled since it was not part of the scope of study.



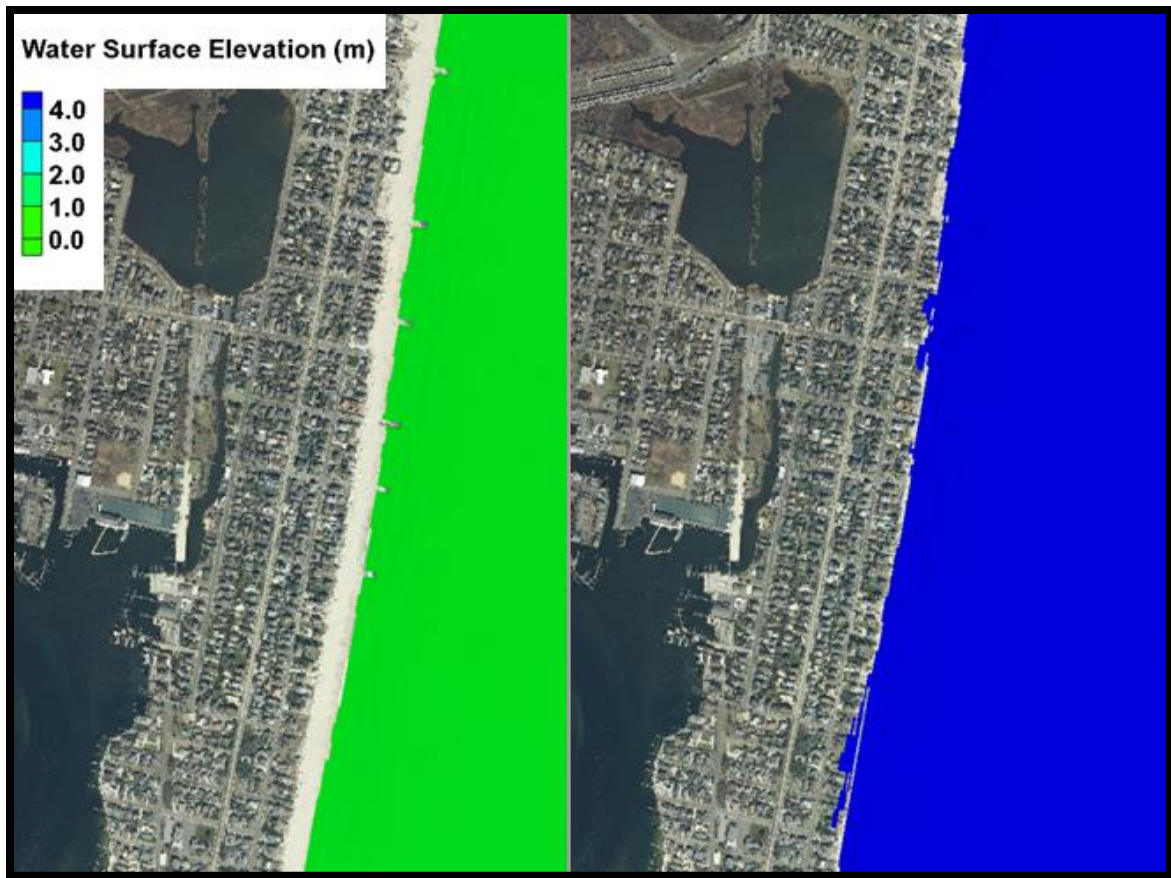


Figure 27: Hurricane Sandy surge left: at  $t=0$ ; right: max surge.

#### **4.1.2 Seawall Overtopping**

Wave runup is the maximum elevation waves will reach on the beach/structure face, measured from the still water elevation. It is one of the causes for beach erosion as well as wave structure overtopping and consists of two components: wave setup and runup of incident waves. CMS-Wave computes wave setup based on the horizontal momentum equations, neglecting current, surface wind drag, and bottom stresses.

Wave overtopping refers to the volumetric rate at which runup flows over the crest of a dune or structure. Figure 28 shows the volumetric discharges over the extent of the seawall where the southern end is represented by  $x = 0$ . An average volumetric flow of  $4.9 \text{ m}^3/\text{s}$  per meter of structure was found to take place at the peak of the storm. The total volume of water overtopping the seawall at this time step was  $6,000 \text{ m}^3/\text{s}$ . This is the equivalent of approximately 175 fuel tanker trucks dumping water over the seawall towards the houses. If desired, the total volume of water overtopped during the storm can be calculated integrating the water volume over all the time steps.

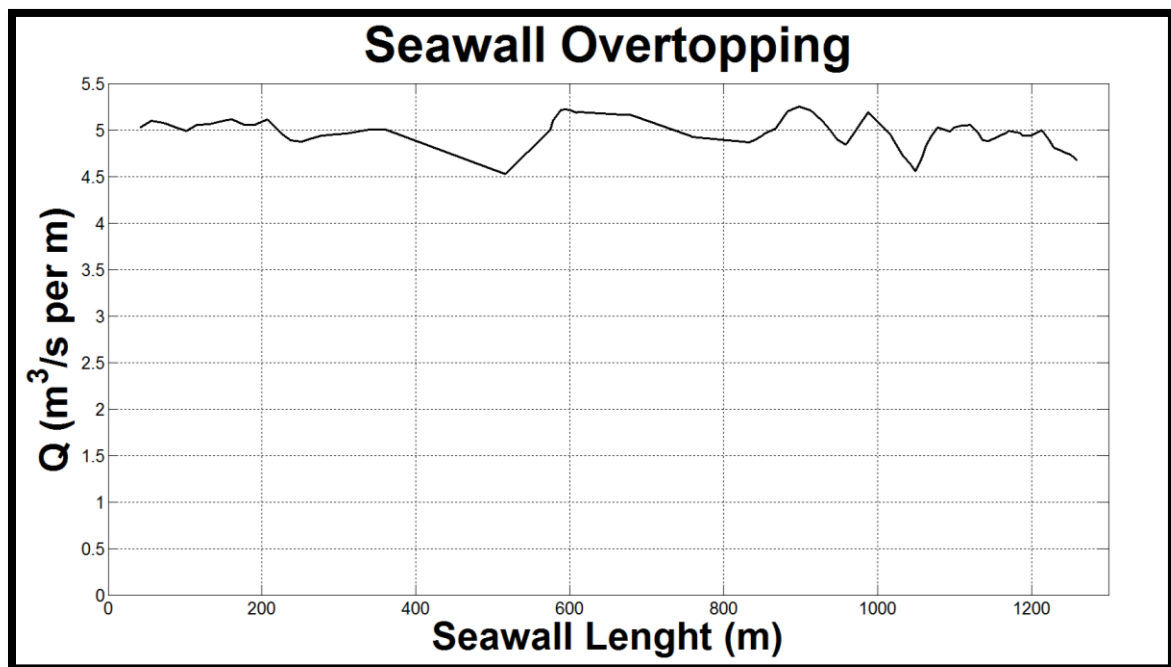


Figure 28: Seawall overtopping discharge.

## 4.2 Significant Wave Height

The largest wave height in the model's domain shoals to 12 meters. However, this wave broke several times as it progressed to the shoreline. By the time it reached the groin structures, its height was 6 meters, as shown by the green color in Figure 29).

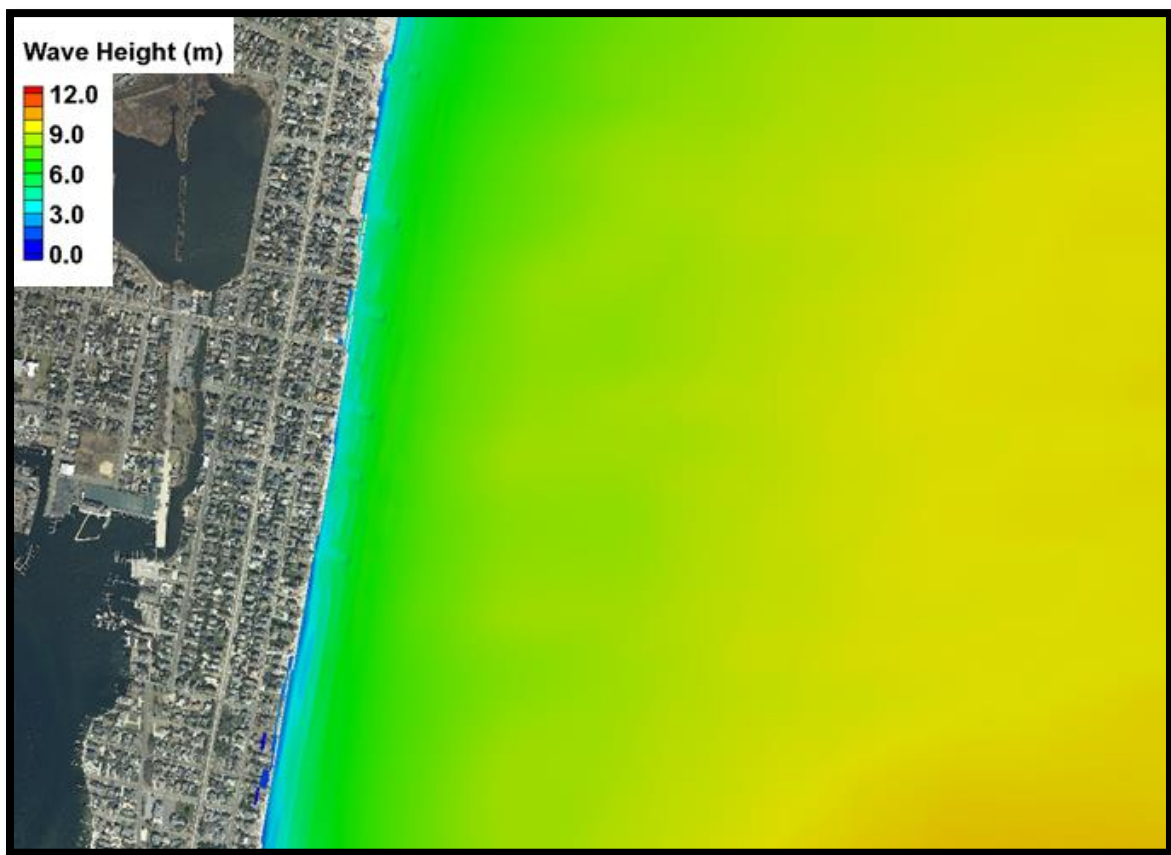


Figure 29: Significant wave height at the peak of the storm.

### 4.3 Wave-Induced Currents

Figure 30 shows the wave-induced currents around the groin field when storm surge arrive to the coast. The strongest nearshore currents measured on the model at this time step were 5 meters per second. All the groins, except for the Howe St. groin, were underwater due to the storm surge. Note the circulation that happened north and south of the Howe St. groin. This circulation was greatly influenced by the height and length of this particular groin. Also, at this time of the storm, cross-shore transport created sandbars that altered the nearshore hydrodynamics.

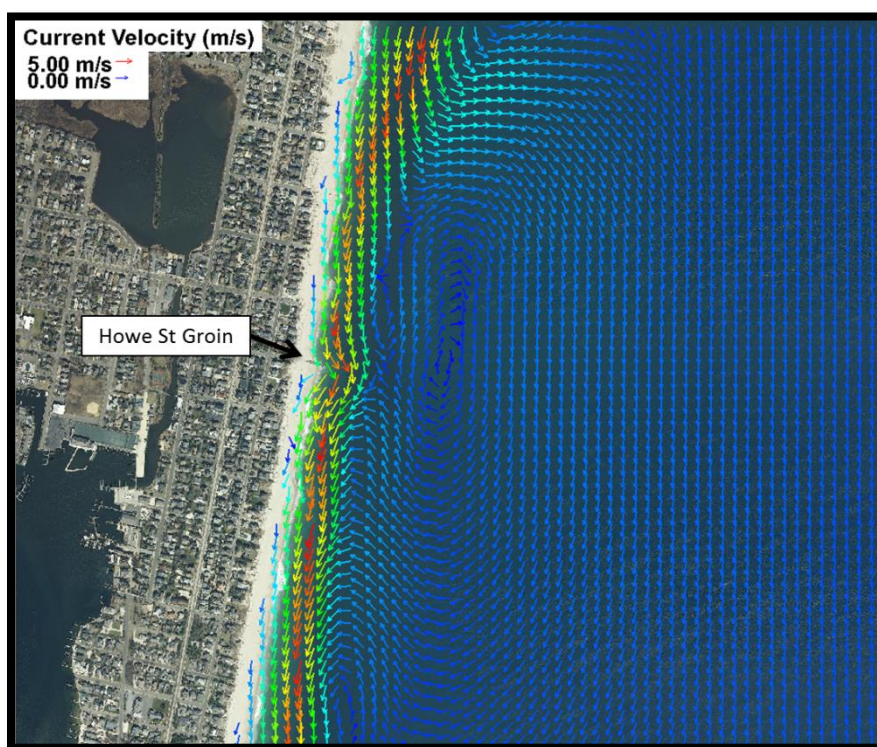


Figure 30: Wave-induced currents near the groin field.

#### ***4.4 Morphology Change***

Superstorm Sandy produced severe erosion in Bay Head and this was well captured by the model.

Figure 31 is a 3D view looking towards the shoreline and shows the morphology change for the Bay Head groin field produced by the storm. A positive elevation stands for accretion and negative elevation for erosion. The dune system over the seawall was completely washed away. The maximum beach erosion was 2 meters, located in front of the seawall, mostly because of the turbulence created by wave reflection. Approximately 1 meter of erosion took place in the groin cells (space between groins), leaving the structures completely exposed (Figure 32). A portion of the sand eroded from the dry beach was deposited offshore of the groins creating large bar systems (blue color in

Figure 31) located in 4 to 8 meters of water. The largest bar was formed at the northern side of the groin field, accreting as much as 1 meter of sand. It is known that sand deposited up to a depth of 8 meters will remain in the system and can return to the shore over time, during long period swell events. This process can be better captured in a beach profile plot.



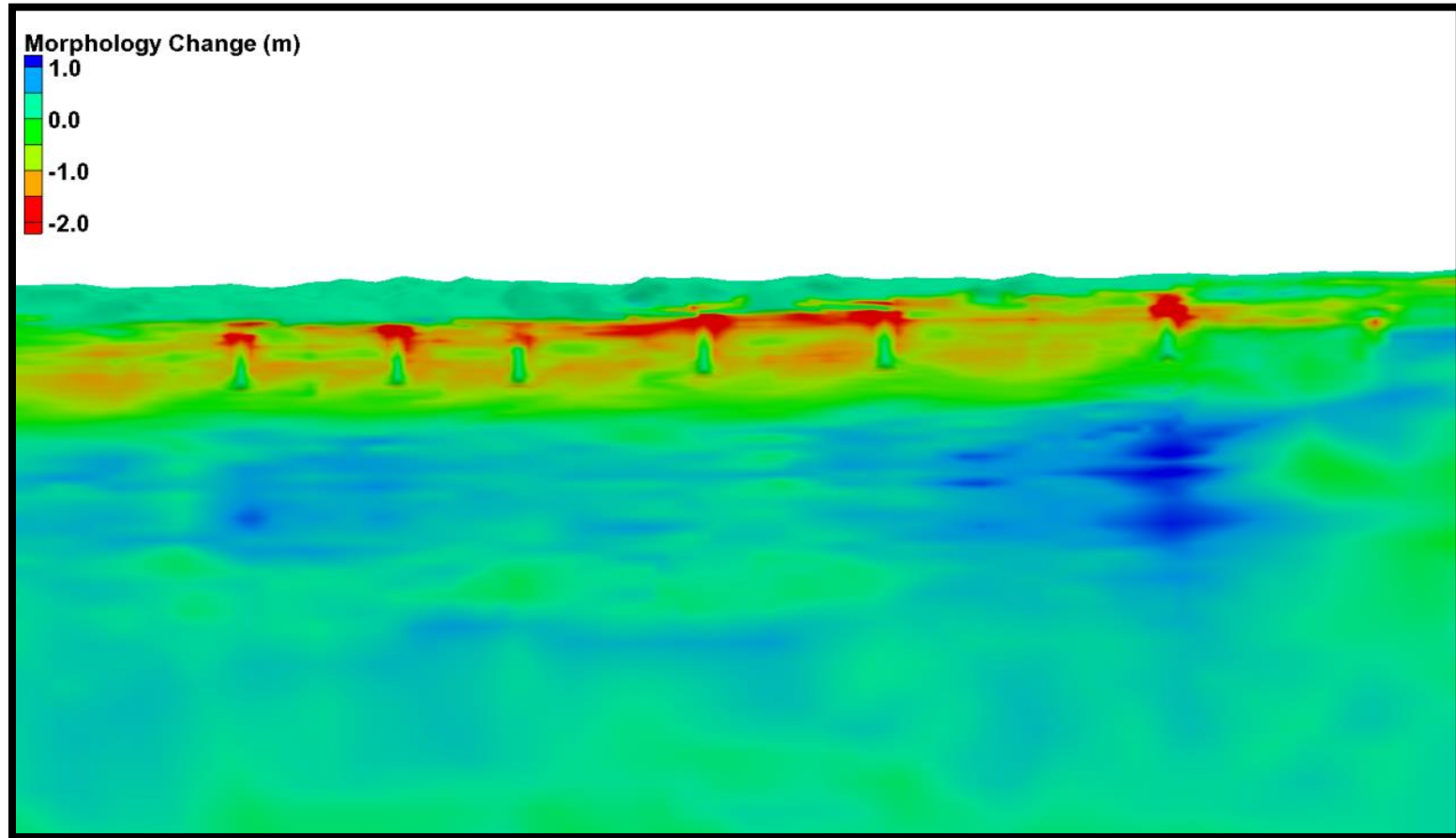


Figure 31: Morphology change at groin field.

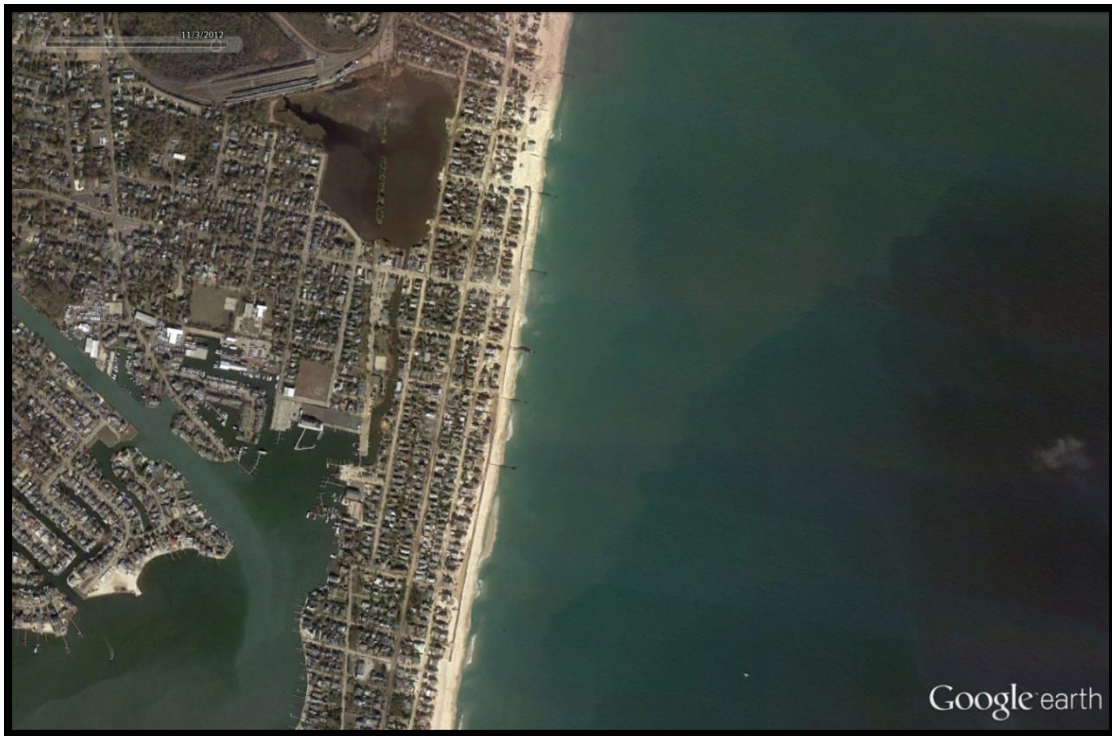


Figure 32: Bay Head aerial on Nov 3, 2012 (4 days after Hurricane Sandy).

#### ***4.5 Shoreline Position Change***

The amount of shoreline retreat along the Bay Head beach during the storm was well captured by the model. By definition, the shoreline location is defined by the mean high water (MHW) elevation. Figure 33 shows the change in shoreline position after Superstorm Sandy. Note that the shoreline retreat is larger near the groins than in the southern and northern ends of the groin field.



Figure 33: Shoreline position change.



## **4.6 Beach Profiles**

Post-storm beach profile data was collected using the DUCKS system described in Section 3.2.2. Also, LiDAR data was obtained to compare model results (Ref. Section 3.2.3). Beach profiles were created in the model, updrift and downdrift of each of the groins as well as north and south of the whole groin field, at the same locations of the survey lines (Figure 34). Figure 35 and Figure 36 show an example of the subaerial profiles since post-storm hydrographic survey was not available. On average, the profiles extracted from the model and those based on survey data differ by 36%. Part of this error is associated to the fact that the model's output resolution is 5 meters (coarser than the RTK survey). The root mean squared error (RMS) was calculated for each profiles (Table 4). It shows that the model better captured the erosion/accretion in the northern part of the groin field where the beach was not influenced directly by the seawall. All the beach profiles, from seawall to the shoreline, can be found in Appendix A. Three profiles, north, center and south of the groin field, were created and extended to the surfzone to show the formation of bars. These profiles are available in Appendix B.



Figure 34: Beach profile locations.

<b>Osborne St.</b>	Downdrift	37.4 %	0.35
	<b>Updrift</b>	<b>13.6 %</b>	<b>0.19</b>
<b>Karge St.</b>	<b>Downdrift</b>	<b>27.6 %</b>	<b>0.32</b>
	Updrift	41.1 %	0.46
<b>Harris St.</b>	Downdrift	37.9 %	0.45
	Updrift	33.7 %	0.34
<b>Howe St.</b>	<b>Downdrift</b>	<b>25.9 %</b>	<b>0.25</b>
	Updrift	42.0 %	0.36
<b>Mt St.</b>	Downdrift	42.5 %	0.63
	Updrift	32.8 %	0.42
<b>Chadwick St.</b>	Downdrift	55.5 %	0.45
	Updrift	50.4 %	0.58

Table 4: Average percent of error for each profile.

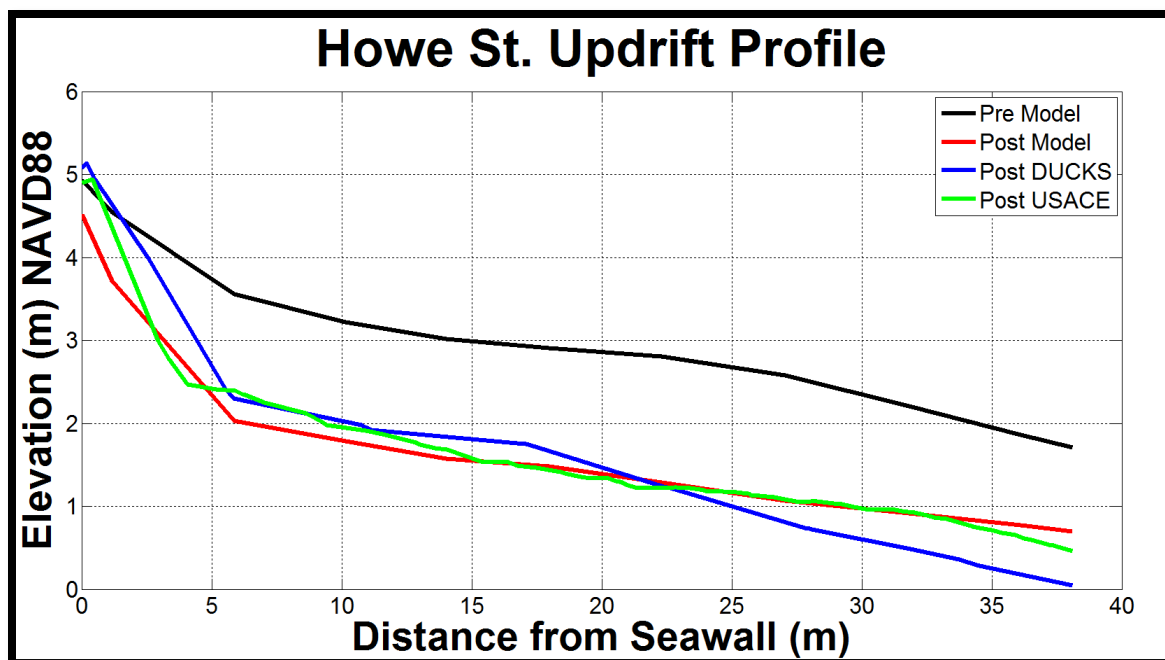


Figure 35: Updrift profile for the Howe St. groin.

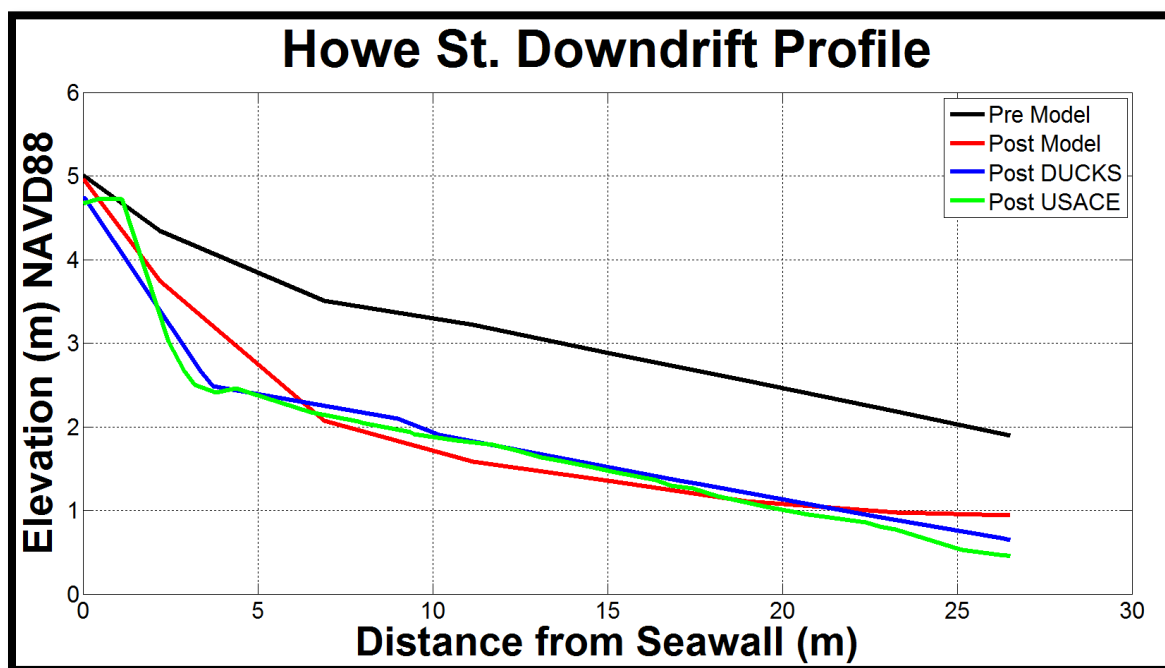


Figure 36: Downdrift profile for the Howe St. groin.

## ***4.7 Sediment Transport***

The sediment transport rate and volume loss during Superstorm Sandy were calculated using several approaches. First, the total sediment transport rate that bypassed the groins was determined by defining observation cells in front of each groin. Second, longshore sediment transport rate was calculated across three established feature arcs north, center and south of the groin field. Finally, a polygon was established around the study area to calculate volume loss during the storm.

### ***4.7.1 Observation Cells***

The total sediment transport rate that bypassed the groins was determined by defining a 3 meters deep observation cell in front of each groin. Figure 37 shows the location of these cells and Table 5 provides the model output for the net and gross longshore and cross-shore direction sediment transport rate. The sign convention is set so that positive is northward and offshore and negative is southward and shoreward. The net longshore shows that more sediment was bypassing the northern groins towards the north and all the cross-shore transport was directed onshore.



Figure 37: Observation cells location.

Groin	Net Longshore kg/m/s	Gross Longshore kg/m/s	Net Crossshore kg/m/s	Gross Crossshore kg/m/s
Orborne St.	0.0233	0.1354	-0.0014	0.012
Karge St.	0.0132	0.1473	-0.0065	0.0121
Harris St.	0.0066	0.1431	-0.0055	0.0119
Howe St.	0.0032	0.1473	-0.0096	0.0154
Mt St.	-0.0036	0.1402	-0.0112	0.0149
Chadwick St.	0.0006	0.1401	-0.0079	0.0141
Inlet Ebb	-0.0186	0.09	0.0484	0.0837
Inlet Flood	0.0005	0.0033	-0.0043	0.0141

Table 5: Sediment bypassing the groins.

#### **4.7.2 Feature Arc**

The longshore sediment transport rate in the groin field was estimated making use of the feature arc option which is based on spatial integration of the total load transport during the storm. The feature arc was located in the middle of the groin field and extends from the shoreline to the depth of closure (Figure 38). The groin field net sediment transport computed by this method was 61,540 m<sup>3</sup>/day northward. This is the equivalent of 338,400 m<sup>3</sup> of sediment that was moved during the storm under this arc. Note that the sediment transport rate calculated by this method corresponds to the groin field only and, therefore, does not represent the sediment transport in the entire established domain. Figure 39 shows the beach profile under this arc. Note that for this particular profile, the post storm profile shows no mass conservation or the typical equilibrium profile meaning sediment was lost from the system.

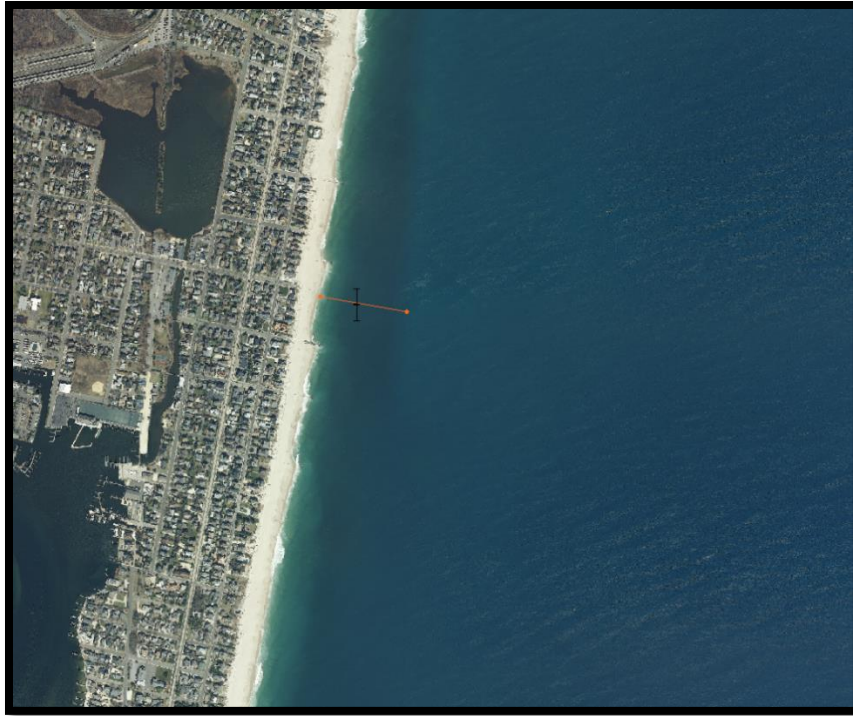


Figure 38: Feature Arc used to calculate sediment transport.

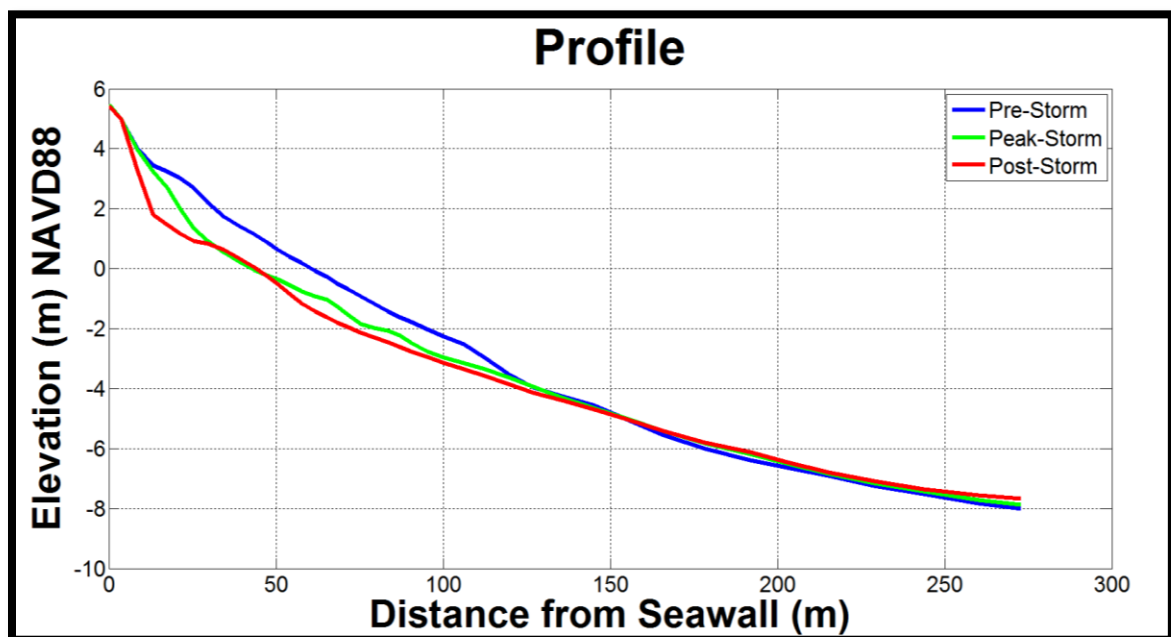
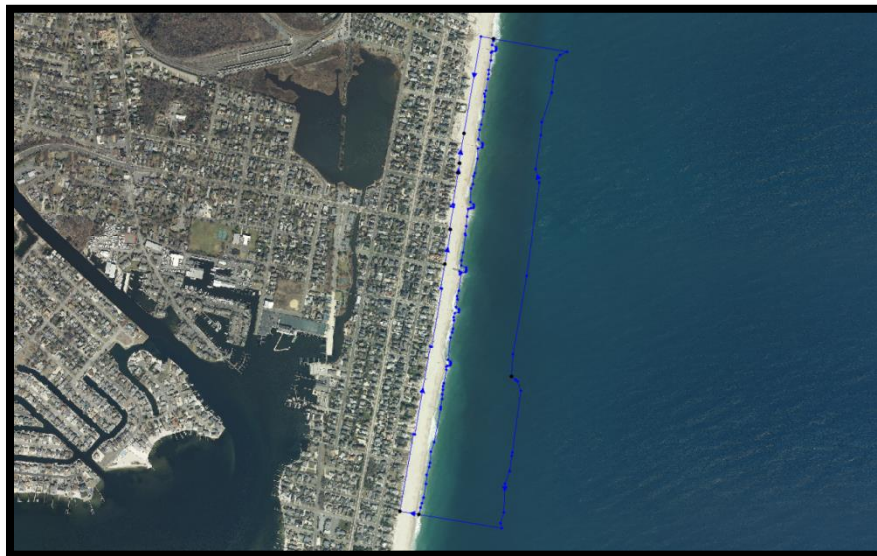


Figure 39: Beach Profile under Feature Arc.



### 4.7.3 Polygon

A polygon was established around the dry sand of the area of study in order to compare the storm induced beach erosion calculated by the computer model with that determined from the DUCKS pre and post-storm surveys. The beach erosion calculated by the computer model was  $107,930 \text{ m}^3$  while the erosion computed from the DUCKS surveys was  $93,910 \text{ m}^3$ . The volume calculation of this last one was based on beach profiles spaced at 76 meters and making use of AutoCAD. Then, a second polygon was established from the toe of the seawall to the depth of closure, which is approximately 8 meters for New Jersey. Figure 40 shows both polygons. Based on the computer model, the area of study lost a total of  $115,600 \text{ m}^3$  of sand during Hurricane Sandy.



**Figure 40: Polygons for sediment calculations.**



## CHAPTER 5

### Conclusions

#### ***5.1 Conclusion***

The computer model used in this study adequately represents the severe erosion suffered by the coast of Bay Head as a result of Superstorm Sandy. Post storm beach profiles are necessary to validate the sediment transport obtained from the model. The profiles extracted from the model are comparable to the survey data sources with an average maximum error of 36%. Beach erosion calculated by the computer model was  $107,930 \text{ m}^3$ , overpredicting the erosion calculated from DUCKS surveys by 15%. This discrepancy is influenced by factors such as sediment transport equations, grain size, and concentration profile used in the model. It is also affected by the difference in interpolation methods implemented by AutoCAD and the model, which has higher resolution between profiles. A total of  $115,600 \text{ m}^3$  of sand was lost. Based on the obtained results, it has been determined that the CMS model is a useful tool to calculate the sediment transport on complex coastal locations that experience large scale storms.

## ***5.2 Future Work***

The Coastal Modeling System provides extensive modeling possibilities. Hence, several things can be done in the future to improve the model results.

-The model domain was based on a single sediment size,  $D_{50}$ . Sediment samples can be obtained at different locations within the domain to perform a sieve analysis. Then, the respective mean sediment sizes can be used as input to the model in order to get a better sediment representation. Suggested key locations for sampling are the dry beach and surfzone at Bay Head, the bay side, and the inlet ebb and flood shoals.

-Use this model, which has been calibrated and validated, to study storm impacts on other coastal locations within the New Jersey Shore.

-Deploy various instruments during the next Hurricane to observe currents and better calibrate the model.

-The storm model XBEACH (Storm induced BEACH CHange Model) is suggested if a localized evaluation (groin field area only) of Hurricane Sandy's impact is to be performed.

## Vocabulary

### A

**Advection** – The process by which solutes are transported by the motion of flowing groundwater.

**Accretion** – The accumulation of sediment by natural forces or act of man.

**Aeolian Transport** – Sediment moved by the wind. As a result, ripples and dunes are created.

### B

**Bathymetry** – The measurement of depths in bodies of water.

**Barrier Island** – A long and narrow island that is parallel to the mainland and protects the coast from erosion.

**Bedforms** – Features on the seabed (e.g. ripples and sand waves) resulting from the movement of sediment over it.

**Breaching** – Opening created in a narrow landmass such as a barrier spit or barrier island that allows water to flow between the water bodies on each side of the landmass.

**Bulkhead** – A vertical retaining structure built for shore protection and harbor works.

**Bypassing Sand** – Hydraulic or mechanical movement of sand from the accreting updrift side to the eroding downdrift side of an inlet or harbor entrance.

## C

**Cross-shore** – Takes place perpendicular to the shoreline.

**Current** – A flow of water.

## D

**Datum** – Reference elevation used for several applications such as surveying, mapping, geology, and numerical modeling.

**Depth of Closure** – Offshore depth beyond which the bed elevation does not change with time.

**Downdrift** – Opposite side of the longshore drift of a structure that receives little or no sand.

**Dune** – A sand hill or sand ridge naturally formed by the wind, usually in desert regions and near lakes and oceans.

## **E**

**Ebb** – Time period when the tide level is falling and water flow comes out of the inlet; often referred to as the ebb current.

**Echo Sounder** - An electronic instrument used to determine the depth of water with respect to a datum by measuring the time interval between the emission of a sonic or ultrasonic signal and the reception of its echo after it reaches the bottom.

**Eddy** - Refers to the circular movement of water formed on the side of a main current.

**Erosion** – Process by which soil and rock are removed from their original position on the Earth's surface by action of wind, wave or water flow and then transported and deposited in other locations.

## **G**

**Groins** – A shore protection structure built perpendicular to the shoreline to trap littoral drift or retard erosion of the shore. Typically found in groups called groin fields.

**H**

**Hydrodynamics** – Entails the specific scientific principles that relate to the motion of fluids and the forces acting on solid bodies immersed in fluids, and in motion, relative to them.

**Hurricane** - An intense tropical cyclone in which winds tend to spiral inward toward a core of low pressure, with maximum surface wind velocities that equal or exceed 75 mph (65 knots).

**I**

**Inlet** – A short, narrow waterway connecting a bay, lagoon, or similar body of water with a large parent body of water.

**J**

**Jetty** – A structure built perpendicular to the shoreline with the intent of stabilizing an inlet and prevents the channel from being filled with sediment.

**L**

**Landfall** – The time at which a storm passes over shore.

**Longshore** – Parallel to, and near the shoreline.

## M

**Mean High Water** – The average of all the high water heights observed over the National Tidal Datum Epoch.

**Mean Low Water** – The average of all the low water heights observed over the National Tidal Datum Epoch.

**Mean Sea Level** – The arithmetic mean of hourly heights observed over the National Tidal Datum Epoch.

## N

**Nearshore** – Extending from or occurring along a shore. Extends from the depth of closure to the swash zone.

**Nodal Zone** – An area in which the predominant direction of the longshore transport changes.

**Non-cohesive sediments** – Sediment that do not contains the electromagnetic properties that causes the sediment to bind together.

## O

**Overwash** – Flow of water and sediment over the crest of a structure. It does not directly returns were it was originated after water level return to normal.

**P**

**Peninsula** – An area of land surrounded by water except for one side that is connected to the mainland.

**Permeability** – A measure of the ability of a material to transmit fluids.

**Porosity** – Percentage of the total volume of a soil sample not occupied by solid particles but by air (voids).

**R**

**Reflection of Water Waves** – The process by which the energy of the wave is returned seaward.

**Refraction of Water Waves** – The process by which the direction of a wave moving in shallow water at an angle to the contours is changed. The part of the wave advancing in shallower water moves more slowly than that part still advancing in deeper water, causing the wave crest to bend toward alignment with the underwater contours.

**Runup** – Height above the still water elevation (tide and surge) reached by the swash.



**S**

**Seawall** – Rock or concrete wall built parallel to the shore separating land and water areas to protect structures behind it from wave action during storm events.

**Sediment Budget** – Study of the amount of sand available in the system versus the amount of sand that leaves the system. It is a useful tool to predict morphological change over time in a particular coastline.

**Sandbars** – A long mass or low ridge of submerged or partially exposed sand built up in the water along a shore or beach by the action of waves or currents.

**Shoreline** – The location where shore and water meet.

**Seabed** – Bottom of the ocean; also known as seafloor.

**Sediment Transport** – The movement of sediment in the fluid along the coast due to the motion of the waves and currents.

**Setup** – Increase in mean water level after wave breaking due to onshore mass transport of the water by wave action.

**Setdown** – Drop in water level outside of the breaker zone to conserve momentum as wave particle velocities and pressures change prior to wave breaking.

**Shear Stress** – The external force acting on an object or surface parallel to the slope or plane in which it lies. It is the responsible for initiation of motion of the sediment.

**Shoals** – An area of relatively shallower water.

**Spring Tide** – Strong tides (large rise and fall of the tide) that occur when the Earth, the Sun, and the Moon align. They occur during the full moon and the new moon.

**Surfzone** – The area where waves break and energy is dissipated. This area is defined between the outermost wave breaking point to the limit of wave uprush.

**Surge** – An abnormal offshore rise of sea level associated with a low pressure weather system, typically tropical cyclones and strong extratropical cyclones, where strong wind pushes the ocean's surface onshore.

**Swash** – Location where waves rush up and down the dry sand.

**T**

**Tidal Inlet** – A narrow channel that connects the open sea with a bay. They are subjected to tidal changes creating ebb and flood shoals and complicated flow velocity patterns and eddies.

**Tidal Prism** – Volume of water in an estuary or inlet between mean high tide and mean low tide.

**Transport Rate** – Rate at which sediment is moved along the nearshore due to waves and currents.

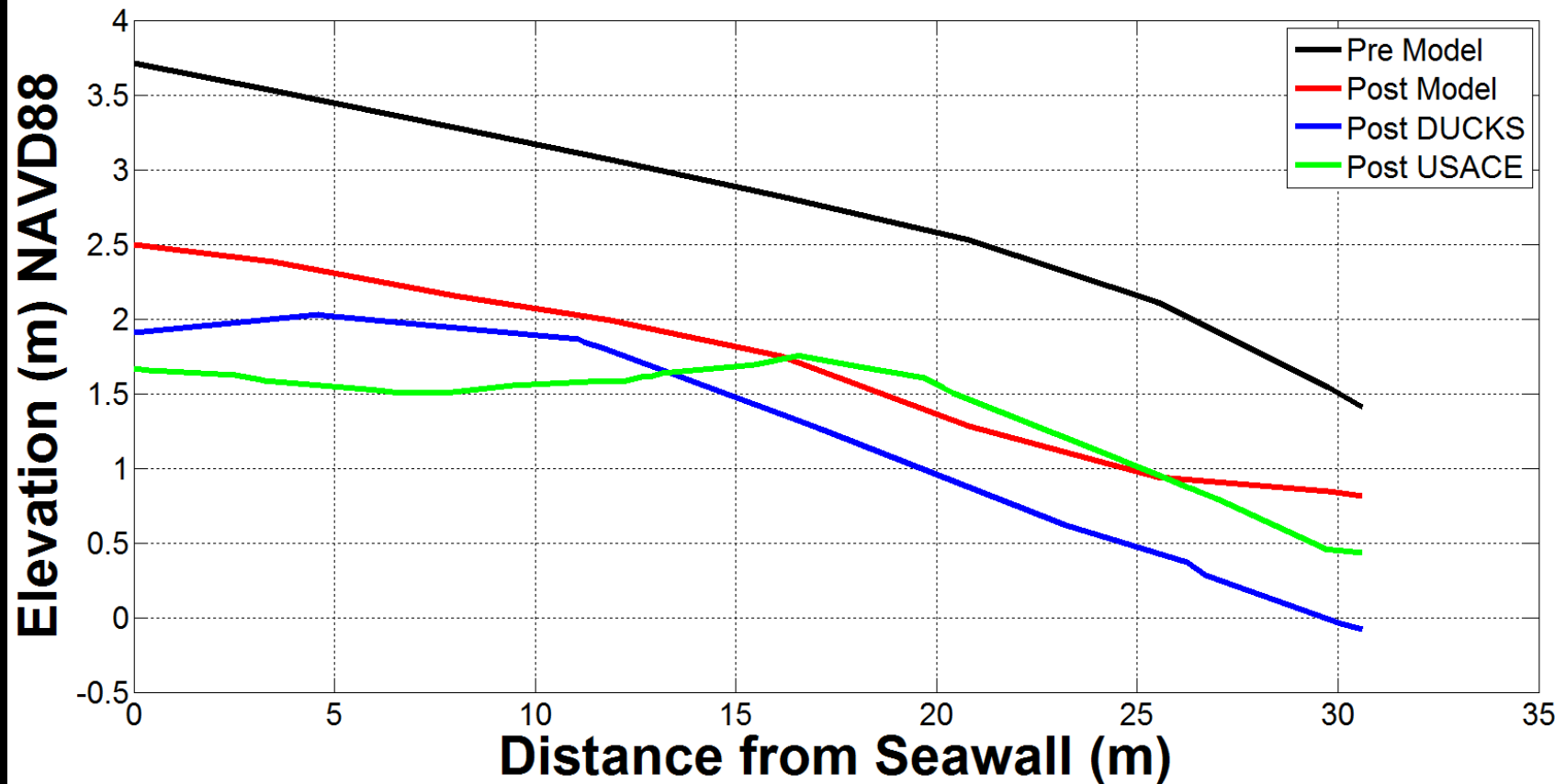
**U**

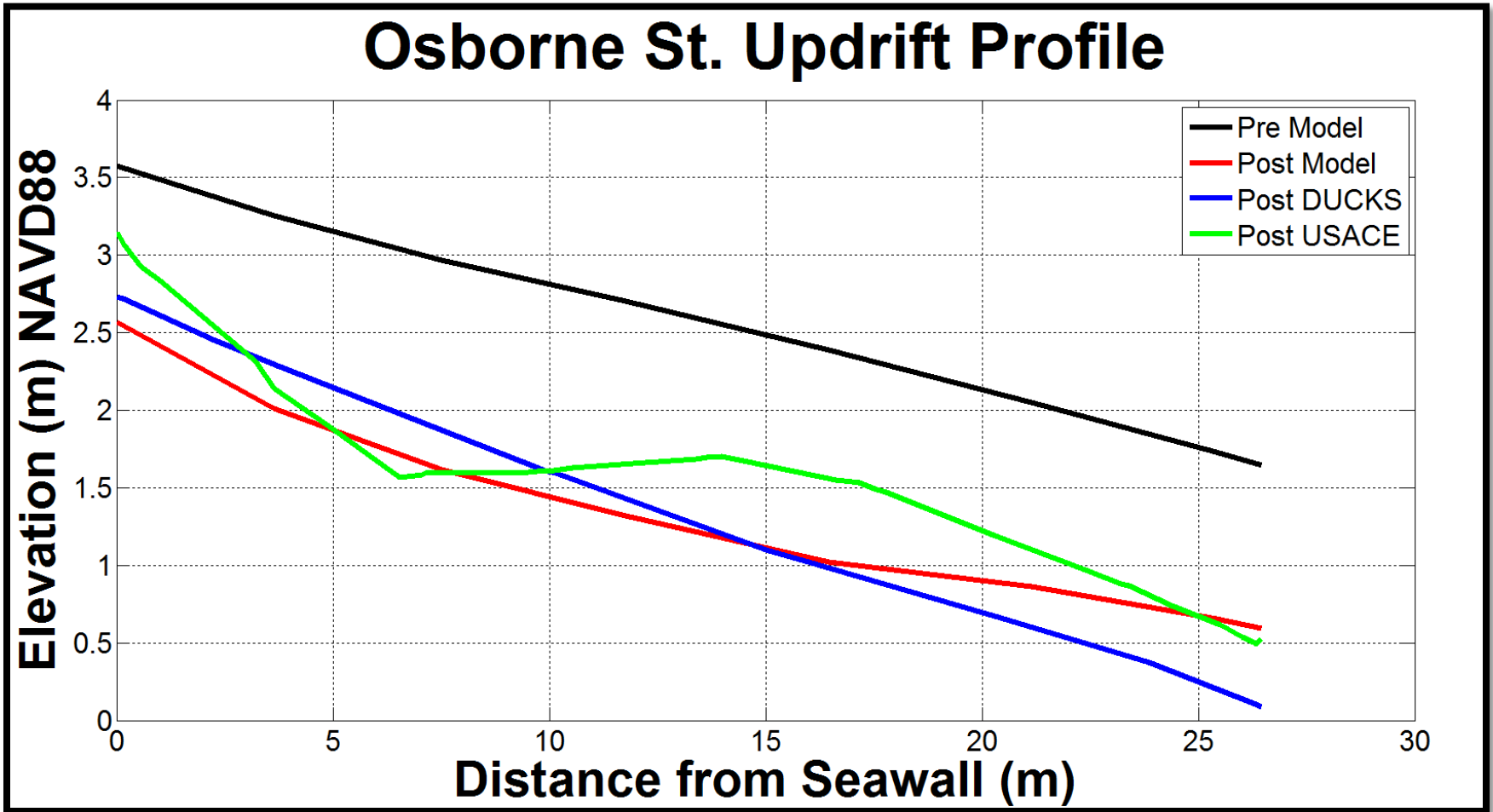
**Updrift** – Side of the groin that directly captures the sand from the longshore drift.

## **Appendix A**

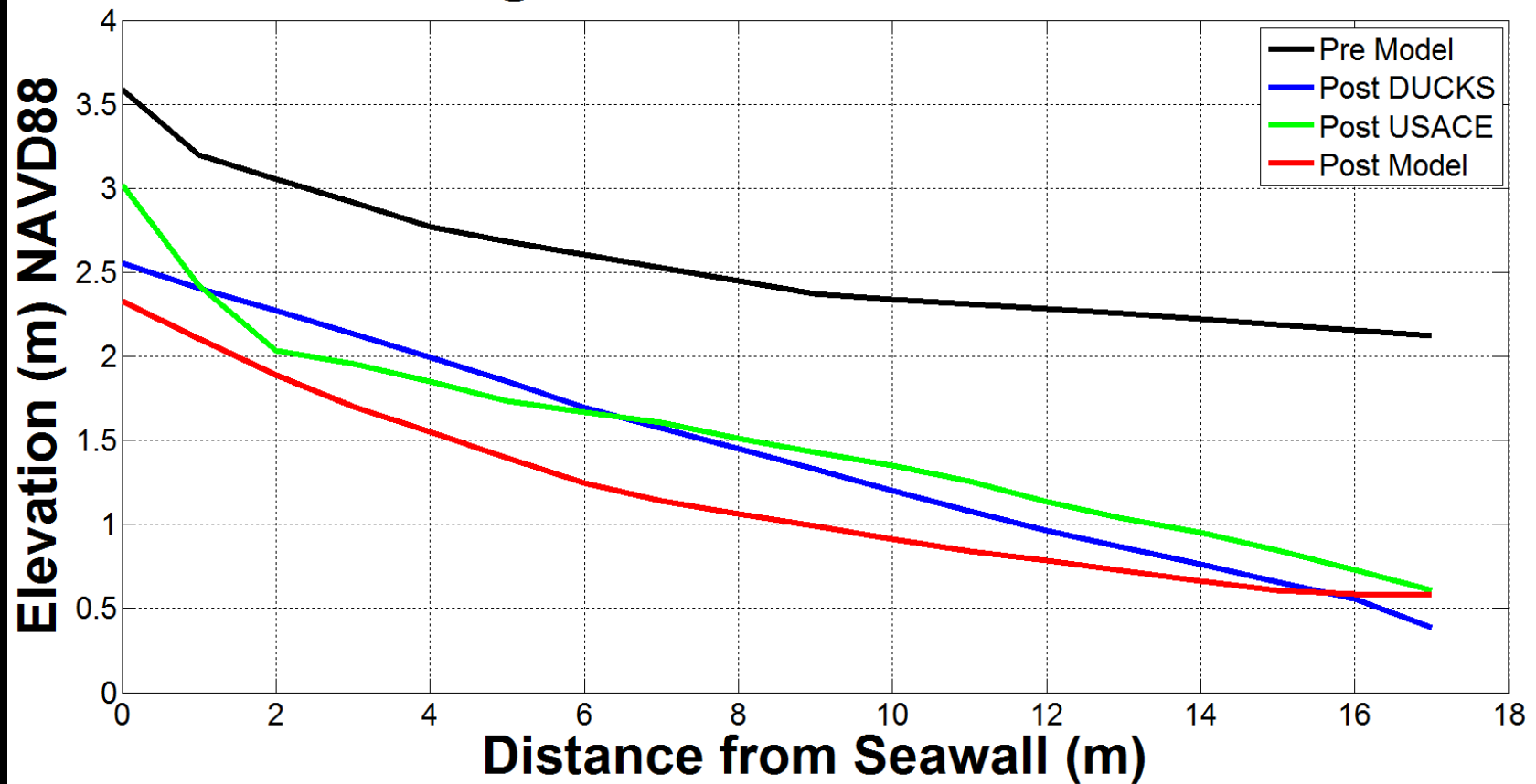
Beach profiles updrift and downdrift each groin.

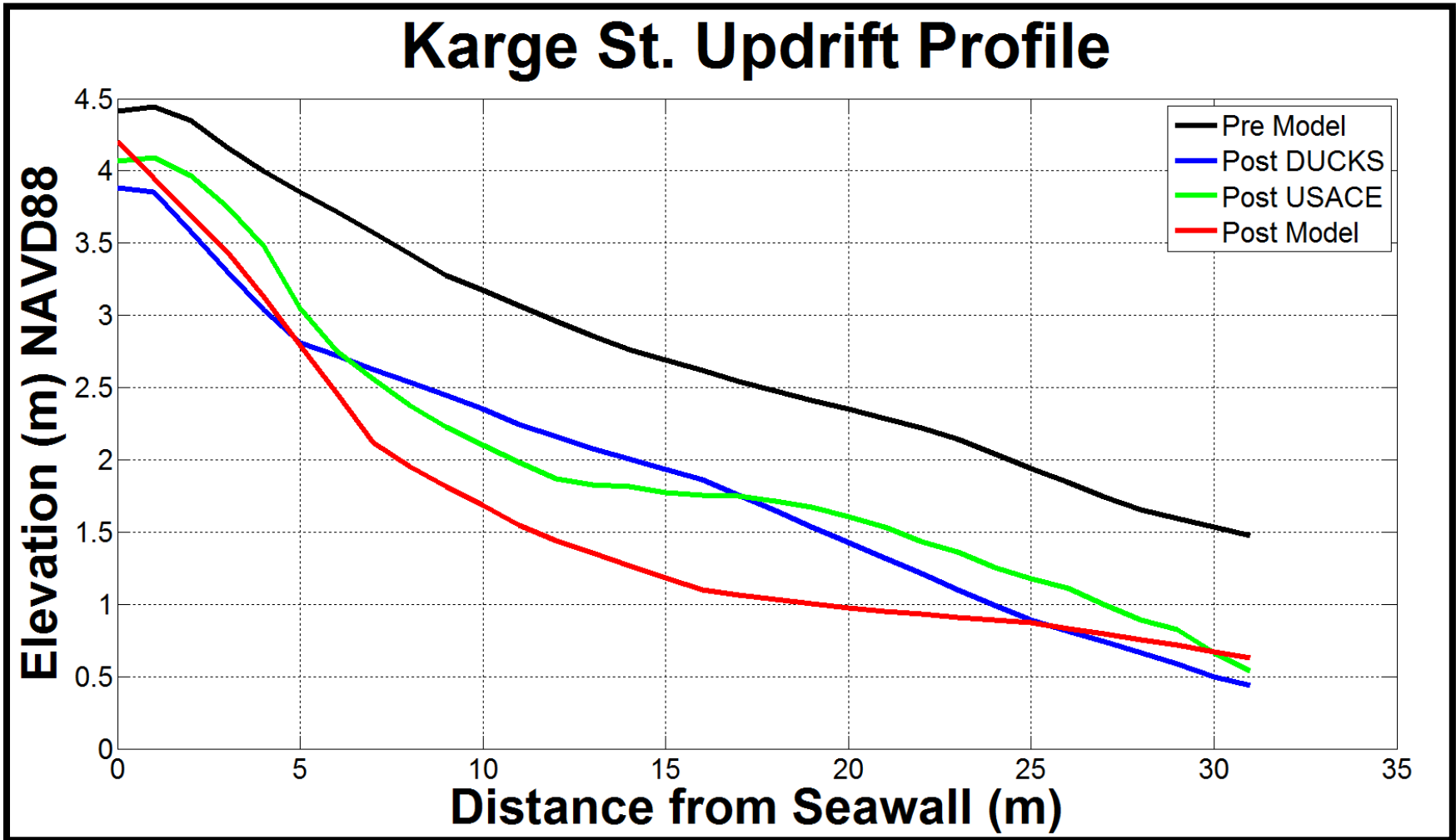
## Osborne St. Downdrift Profile





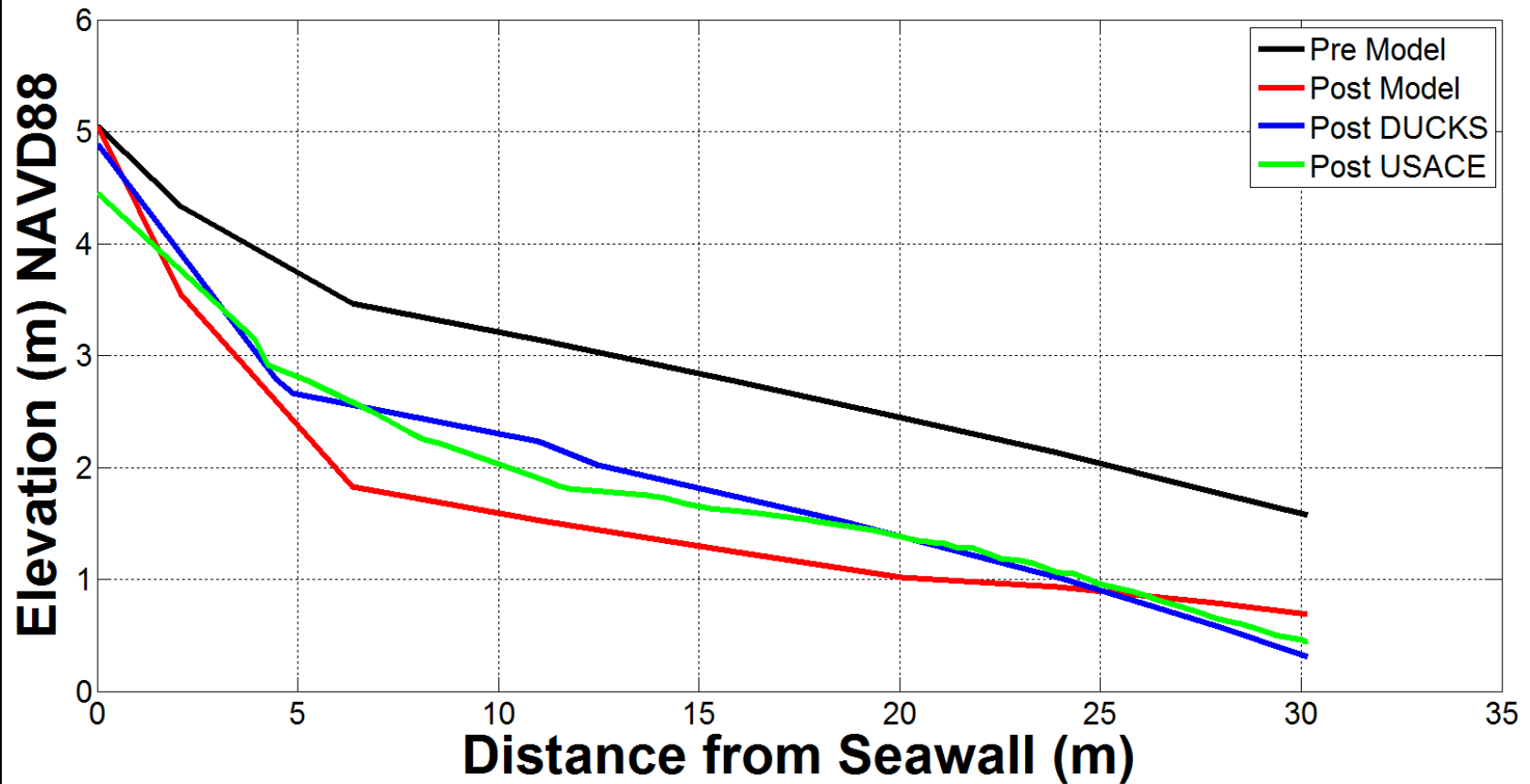
## Karge St. Downdrift Profile



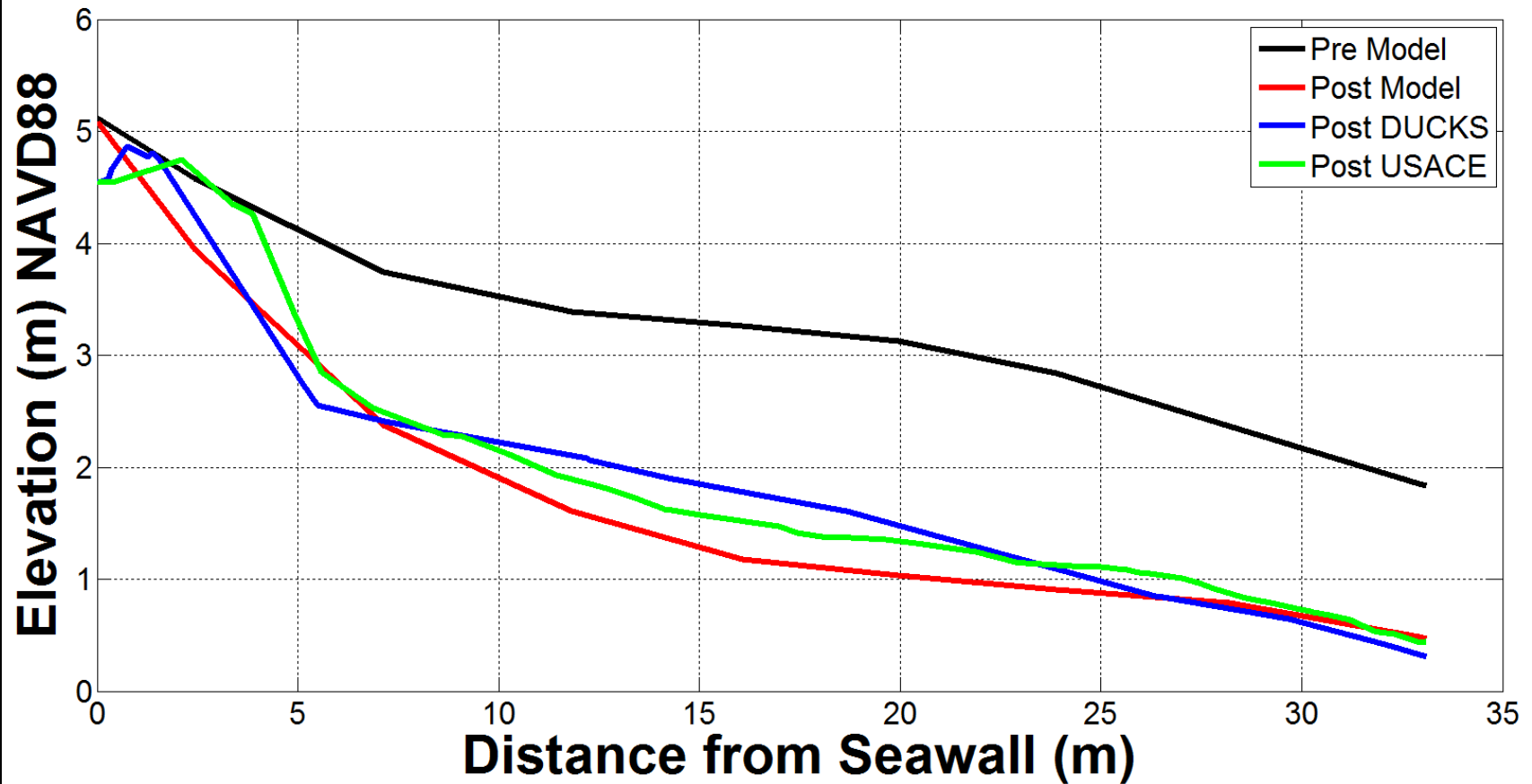


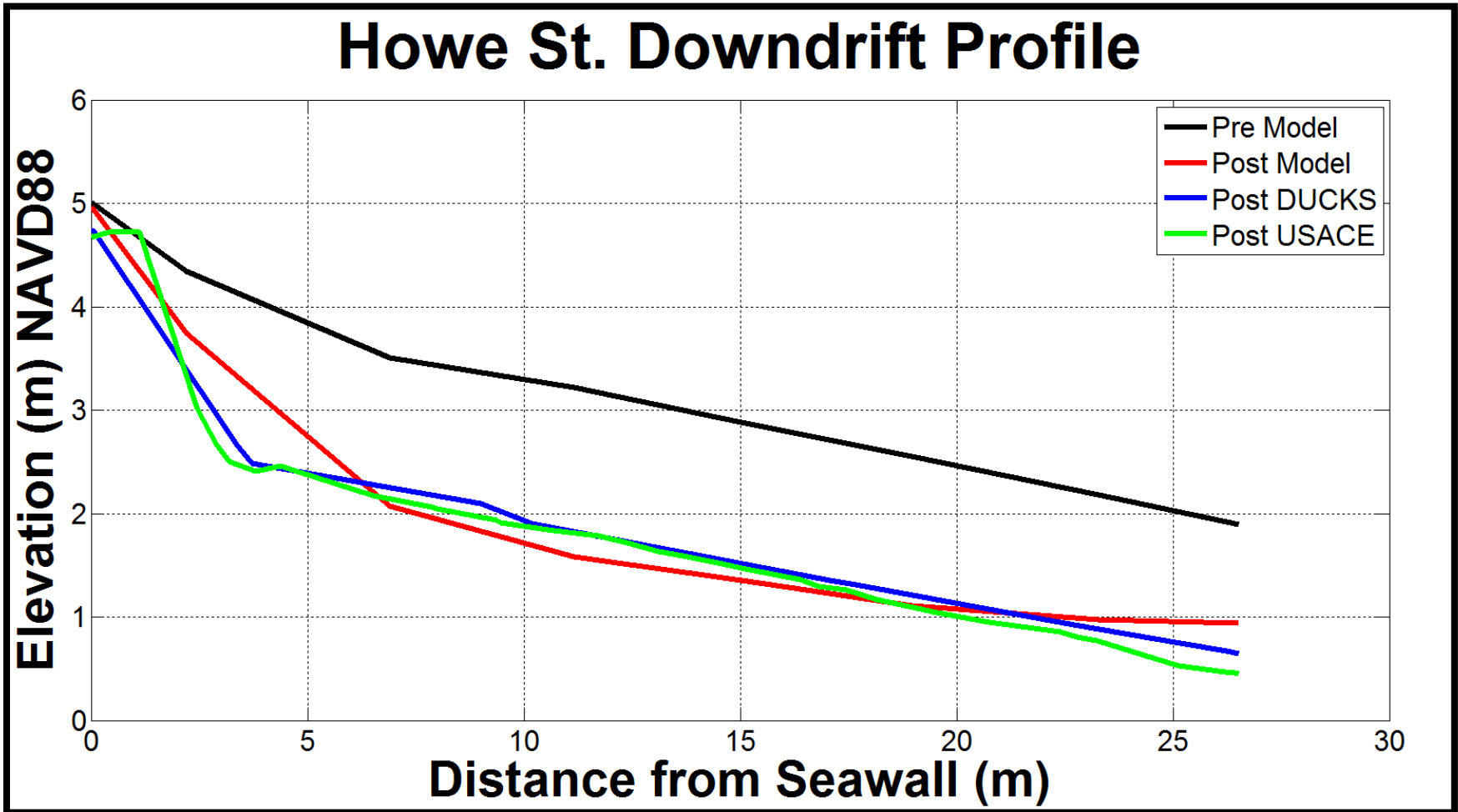


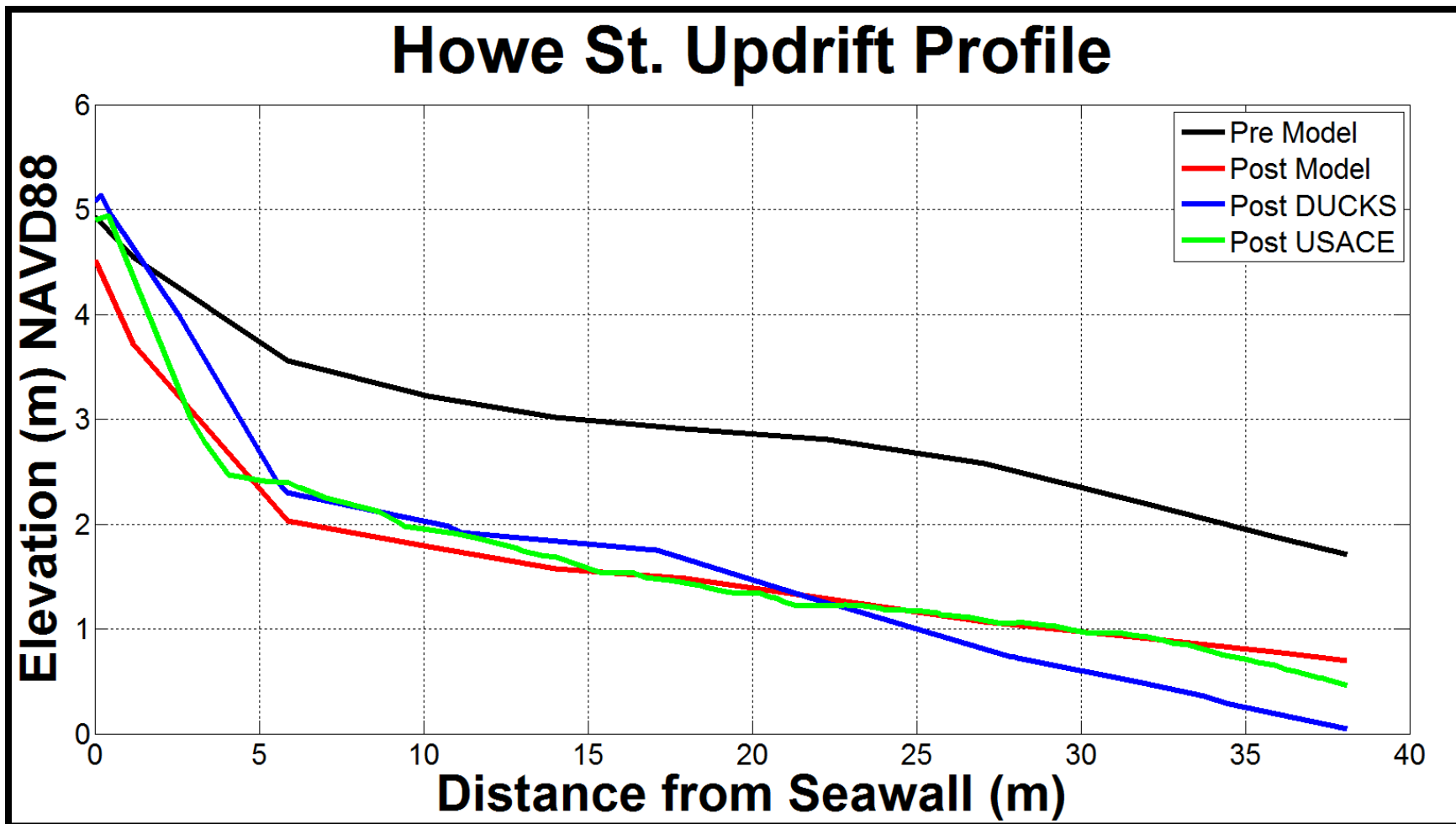
## Harris St. Downdrift Profile

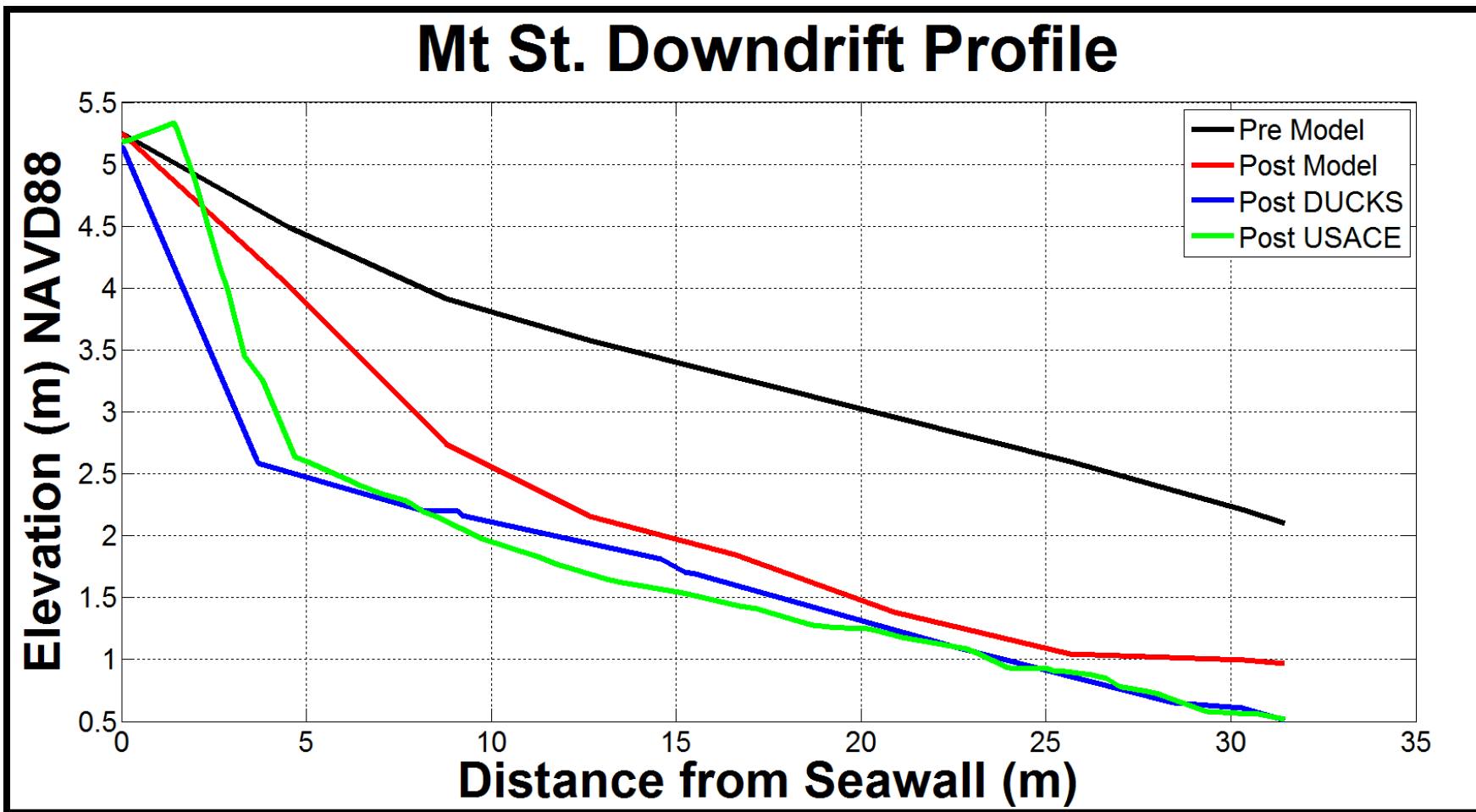


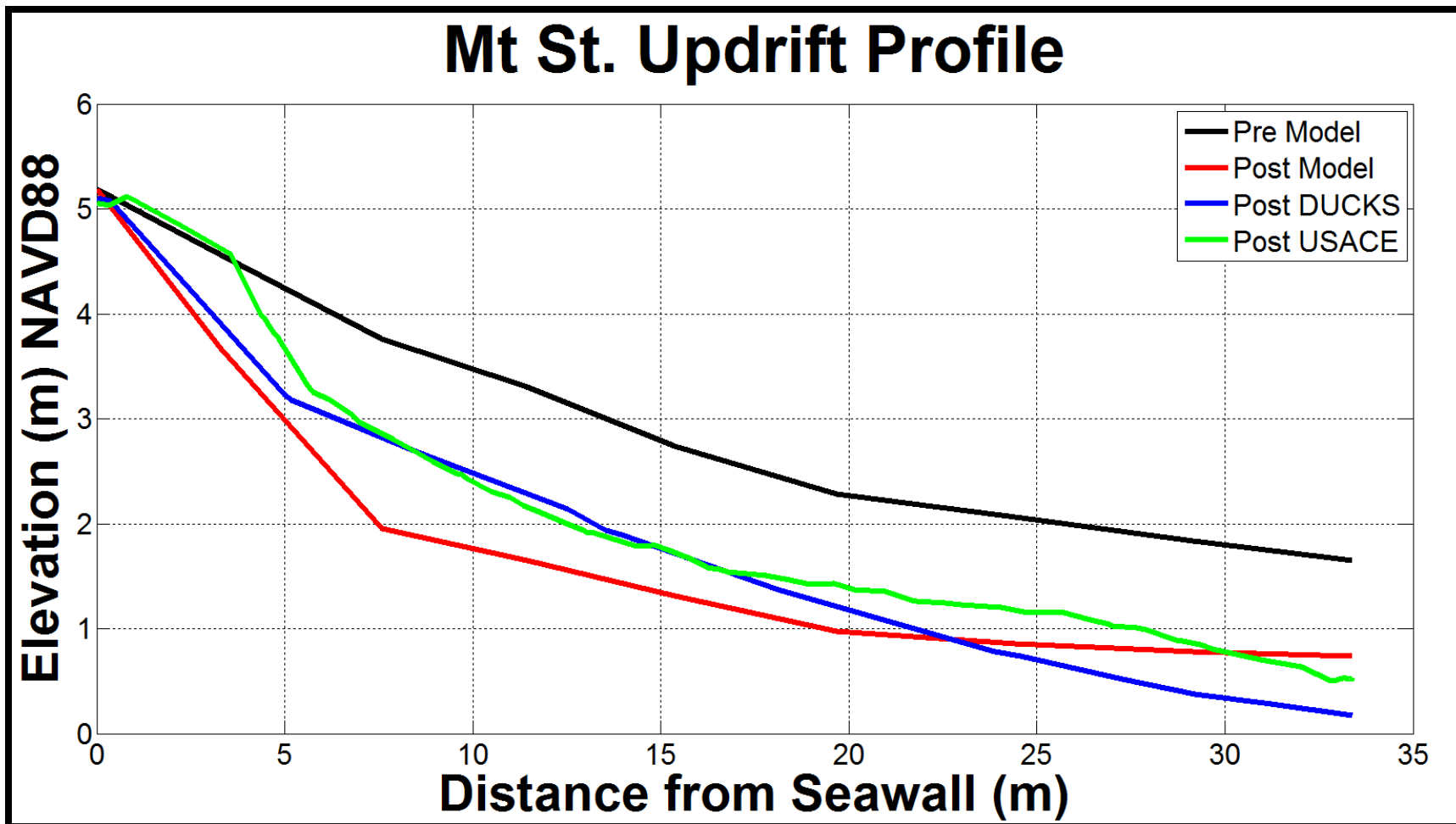
## Harris St. Updrift Profile



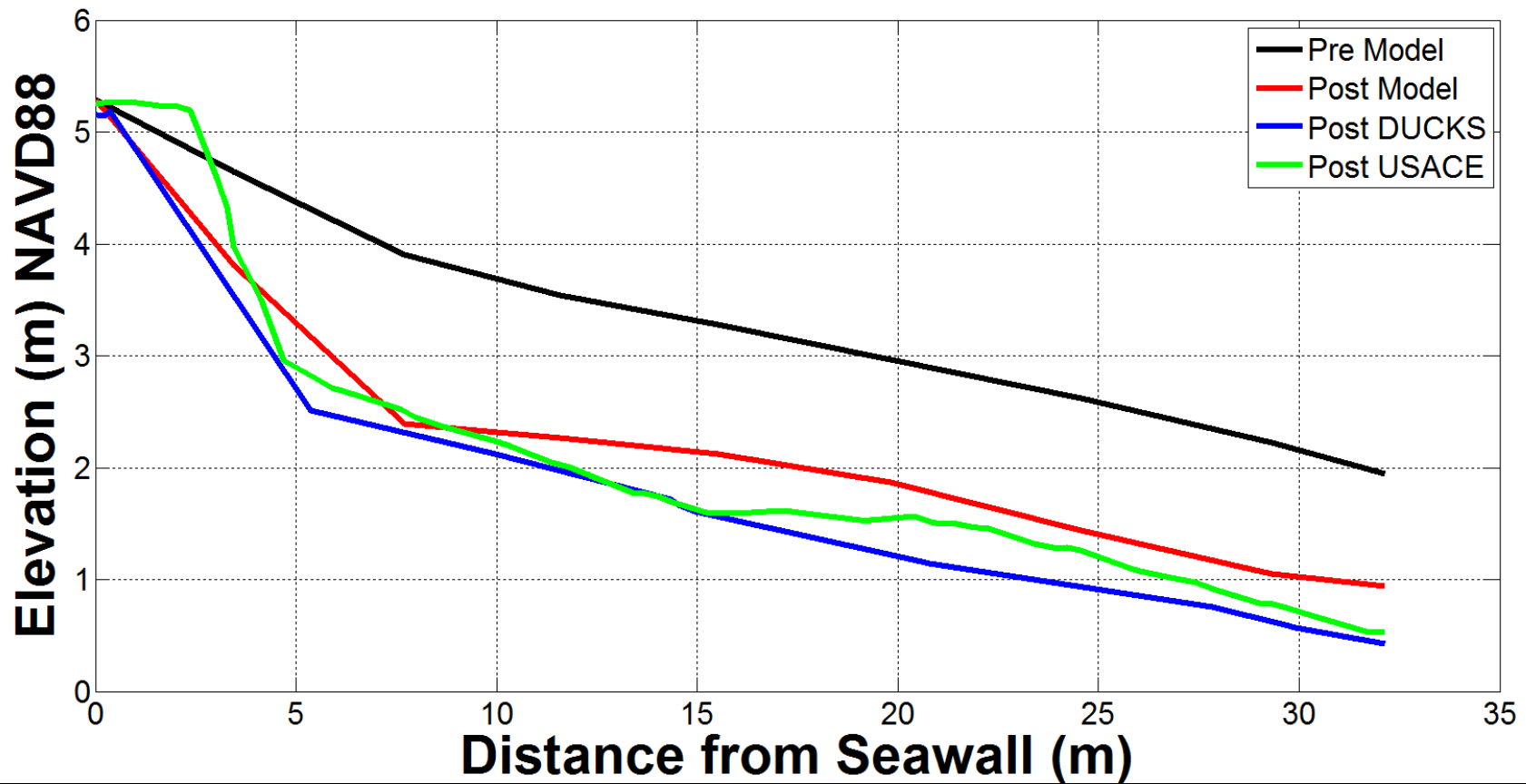




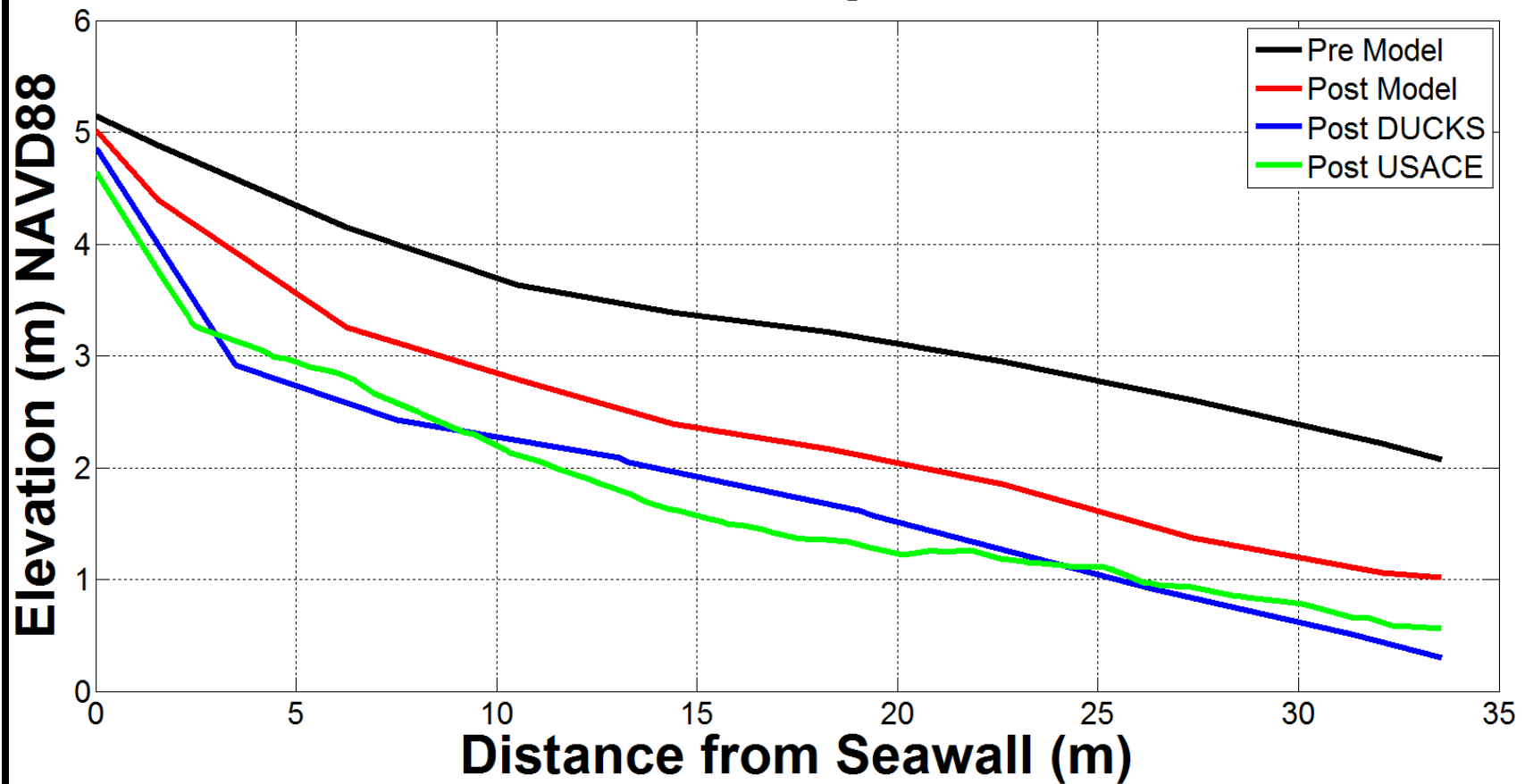




## Chadwick St. Downdrift Profile



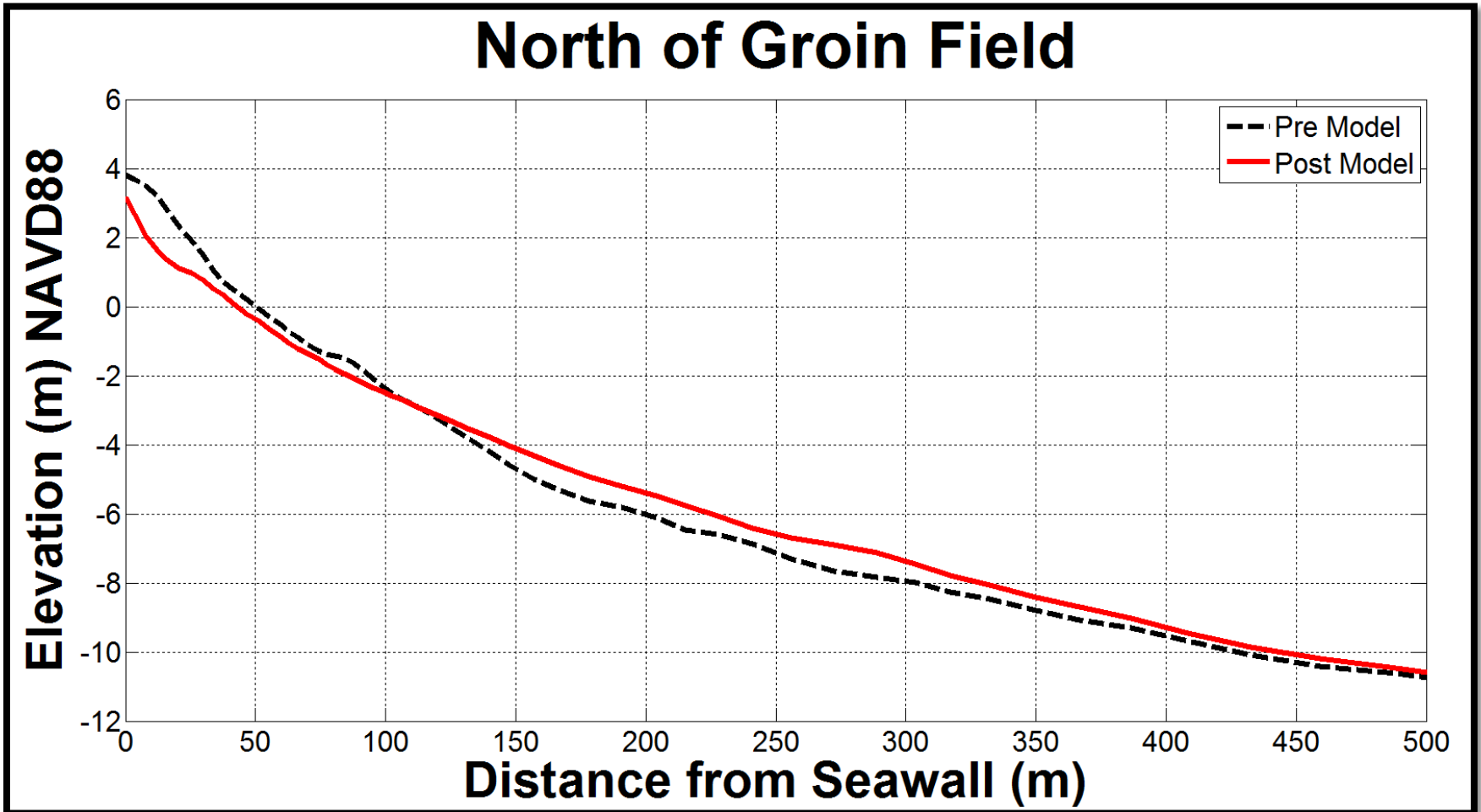
## Chadwick St. Updrift Profile

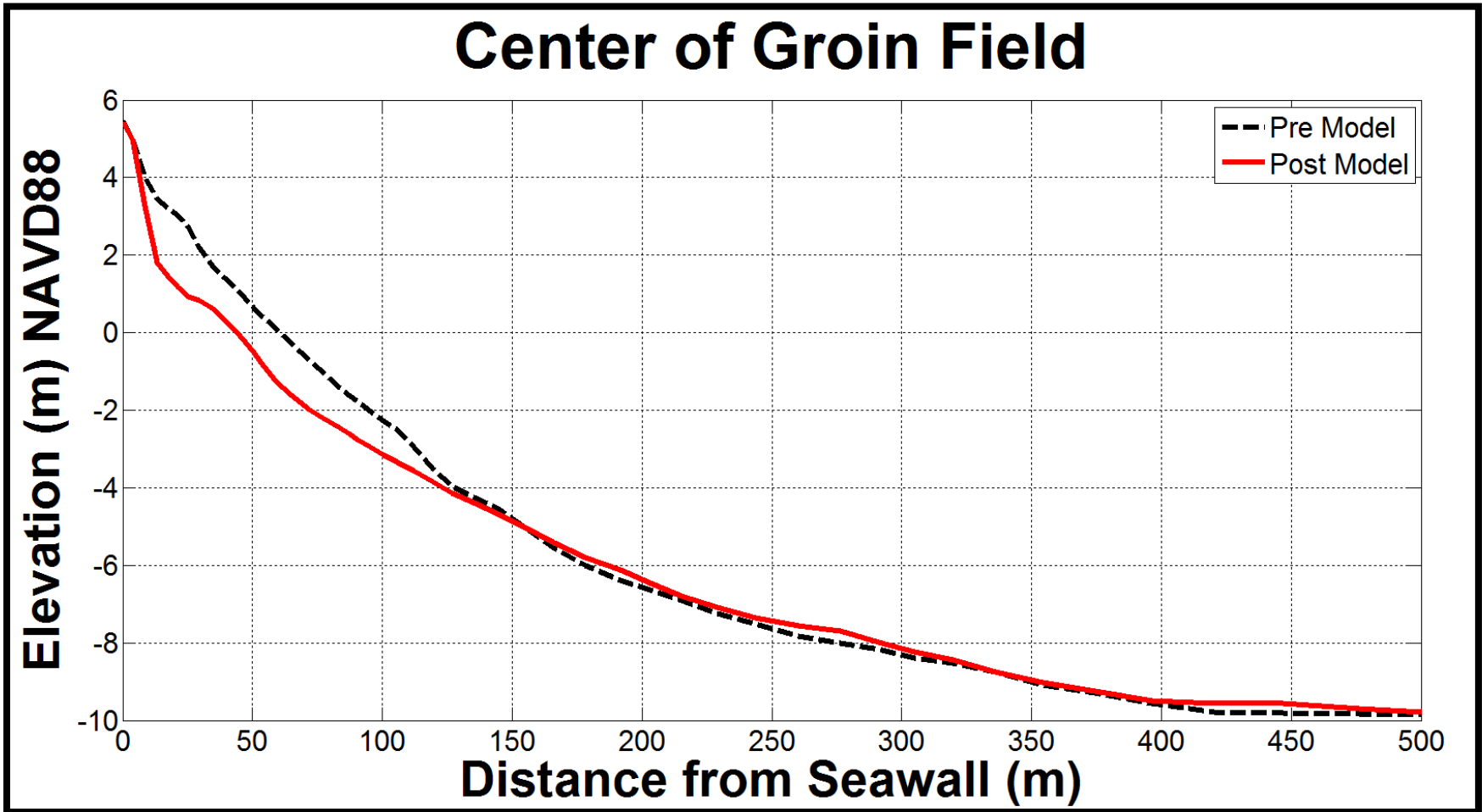


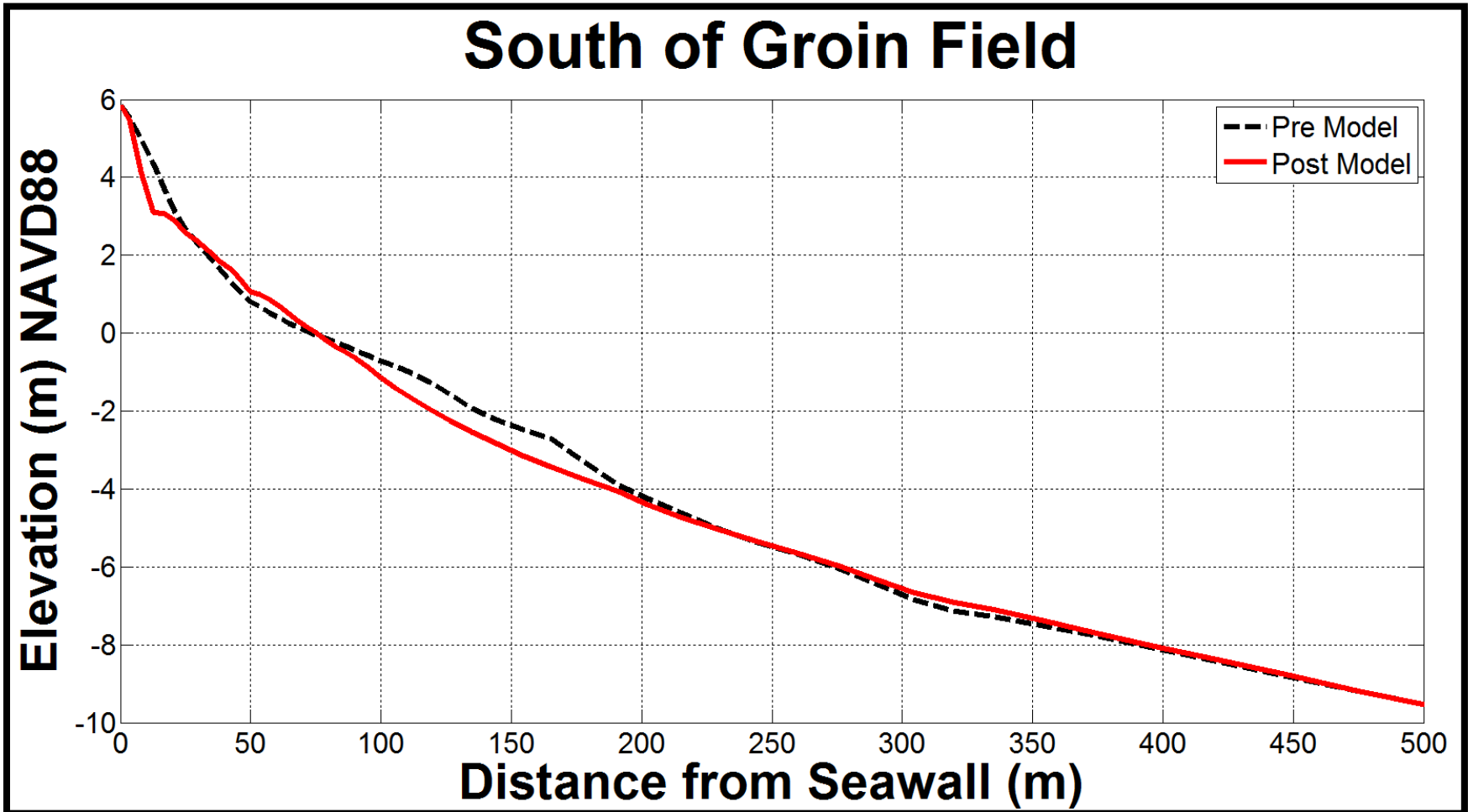


## **Appendix B**

Beach profiles around the groin field.







## References

Camenen, B., and Larson M., (2007). *A unified sediment transport formulation for coastal inlet application*, Technical Report ERDC-CHL CR-07-01, Coastal and Hydraulics Laboratory, ERDC, US Army Corps of Engineers, Vicksburg, MS, USA.

Beck, T., and Kraus, N.C., (2010). Ebb-Tidal Delta Development Where Before There Was None, Shark River Inlet, New Jersey. Report 2.

Bruno M.S., (1988). *A Study of the Feasibility of Sand Bypassing for the Alleviation of Erosion at Manasquan and Shark River Inlets, New Jersey*: Report Submitted to Div. of Coastal Resources, New Jersey.

Bruun, P., (1954). "Coastal erosion and development of beach profiles," U.S. Army Beach Erosion Board Technical Memorandum No. 44, Beach Erosion Board, U.S. Army Corps of Engineers, Washington, DC.

Buttolph, A.M., Reed, C.W., Kraus, N.C., Ono, N., Larson, M., Camenen, B., Hanson, H., Wamsley, T., and Zundel, A. K., (2006). Two-dimensional depth-averaged circulation model CMS-M2D: Version 3.0, Report 2: Sediment transport and morphology change. *Tech. Rep. ERDC/CHL TR-06-9*, U.S. Army Engineer Research and Development Center, Coastal and Hydraulic Engineering, Vicksburg, MS.

Caldwell, J.W., (1966). Coastal Processes and Beach Erosion: *Journal of the Society of Civil Engineers*, Vol. 53, No. 2, 142-157.

Dean, R.G., (1977). "Equilibrium beach profiles: U.S. Atlantic and Gulf Coasts," Department of Civil Engineering, Ocean Engineering Report No. 12, University of Delaware, Newark.

Dean, R.G., and Dalrymple, R.A., (2002). *Coastal Processes with Engineering Applications*, Cambridge University Press, Cambridge, 147-149 pp.

Farrell, S.C., (1980). *An Evaluation of Longshore Sand Transport at Manasquan Inlet*, New Jersey: Report Submitted to Philadelphia District, U.S. Army Corps of Engineers.

FitzGerald, D.M., Kraus, N.C., & Hands, E.B., (2000). Natural mechanisms of sediment bypassing at tidal inlets. Vicksburg, MS: US Army Corps of Engineers.

Hanson, H., (1989). "Genesis: A Generalized Shoreline Change Numerical Model." *Journal of Coastal Research*, Vol5, No. 1, pp. 1-27.

Larson, M., and Kraus, N.C., (1989). "SBEACH: Numerical Model for Simulating Storm-Induced Beach Change. Report 1: Empirical Foundation and Model Development," Technical Report CERC-89-9, Coastal Engineering Research Center, U.S. Army Corps of Engineers, Vicksburg, Miss.

Lin, L., Demirbilek, Z., Mase, H., Zheng, J., and Yamada, F., (2008). CMS-Wave: a nearshore spectral wave processes model for coastal inlets and navigation projects. *Tech. Report ERDC/CHL TR-08-13*. Vicksburg, MS: U.S. Army Engineer Research and Development Center.

Mase, H., Oki, K., Hedges, T.S., and Li, H.J., (2005). "Extended energy-balance-equation wave model for multidirectional random wave transformation." *Ocean Engineering*, 32(8-9), 961-985.

Miller, J.K., Mahon, A., Herrington, T.O., (2009). "Development of the Stevens Dynamic Underwater and Coastal Kinematic Surveying (DUCKS) System", *Coastal Protection Technical Assistance Service, Davidson Laboratory TR-2878*.

Poff, M.T., Stephen, M.F., Dean, R. G., Mulcahy, S., (2004). "Permeable Wood Groins: Case Study on their Impact on the Coastal System" *Journal of Coastal Research*, SI(33), 131-144.

Militello, A., Reed, C.W., Zundel, A.K., and Kraus, N.C., (2004). Two-dimensional depth-averaged circulation model CMS-M2D: Version 2.0, Report 1, Technical documentation and user's guide. Coastal and Hydraulics Laboratory Technical Report ERDC/CHL TR-04-02. Vicksburg, MS: U.S. Army Engineer Research and Development Center.

National Geophysical Data Center, (1999). Coastal DEM Metadata Record U.S. Coastal Relief Model - Northeast Atlantic First Edition, NESDIS, NOAA, U.S. Department of Commerce <http://www.ngdc.noaa.gov/dem/metadata/viewer/713>

Reed, C.W., Brown, M.E., Sánchez, A., Wu, W., and Buttolph, A.M., (2011). "The Coastal Modeling System Flow Model (CMS-Flow): Past and Present," *Journal of Coastal Research*, Special Edition, 59, 1-6.

Shields, A. (1936). Anwendung der Aehnlichkeitsmechanik und der Turbulenzforschung auf die Geschiebebewegung[Application of similarity mechanics and turbulence research on shear flow]

Sakai, S., N. Kobayashi, and K. Koike., (1989). "Wave breaking criterion with opposing current on sloping bottom: an extension of Goda's breaker index." *Annual Journal of Coastal Engineering* 36:56-59, JSCE (in Japanese).

USACE, (2010). "2010 US Army Corps of Engineers (USACE) Joint Airborne Lidar Bathymetry Technical Center of eXpertise (JALBTCX) Lidar: New Jersey (Topo)", *NOAA's Ocean Service, Coastal Services Center (CSC)*, Charleston, SC

USACE, (2012). "2012 US Army Corps of Engineers (USACE) Joint Airborne Lidar Bathymetry Technical Center of Expertise (JALBTCX) Topobathy Lidar: Post Super Storm Sandy - Coastal New Jersey and New York", *NOAA's Ocean Service, Coastal Services Center (CSC)*, Charleston, SC

Shore Protection Manual, (1884). Fourth Edition, 2 vols. U.S. Army Engineer Waterways Experiment Station, Coastal Engineering Research Center, U.S. Government Printing Office, Washington D.C.

Wu, W., Sánchez, A., and Mingliang, Z., (2011). An implicit 2-D shallow water flow model on an unstructured quad tree rectangular grid," *Journal of Coastal Research*, [In Press]